The Spatial Variability of Elemental and Isotopic Compositions of Carbon and Nitrogen Within Sediments in a Subtropical Mangrove Forest

A thesis submitted in fulfilment

of the requirements for the degree

of

Master of Science (Research) in Earth Science

at

The University of Waikato

by

YULIANA RAMIREZ MATIZ

THE UNIVERSITY OF
WAIKATO
Te Whare Wānanga o Waikato

2020

Abstract

Mangrove forests are coastal habitats, which provide numerous ecosystem services in tropical and temperate regions, including burial and storage of Carbon and Nitrogen in the sediments. In New Zealand mangrove coverage is rapidly expanding throughout muddy coastlines and estuaries, in direct contrast to the current global trend of declining mangrove coverage. In this thesis, we explore the spatial distribution of Carbon and Nitrogen content and isotopic compositions in the sediments of a mangrove forest in New Zealand.

The field site is the Firth of Thames mangrove forest, which has rapidly expanded since around 1950, and now reaches 1 km in width over the southern Firth. Sediment cores with lengths ranging from 34 to 40 cm were collected from twelve across-shore transects and two along-shore transects. At each location, samples were taken from the surface and at depth, resulting in a total of 175 samples, providing substantial spatial coverage across the forest. A number of samples of mangrove vegetation were also collected. Elemental and isotopic analyses were performed on the sediment and vegetation samples. Additionally, grain size, fluorometric determination of Chlorophyll-a pigments and loss on ignition analyses were made on a selected subset of sediment samples. The elemental analyses in sediments showed mean concentrations of 2.09%, 1.59%, and 0.23% of total carbon, organic carbon and nitrogen, respectively, with generally larger concentrations at the surface. The C:N ratios were much larger from tree tissue samples (mean 38.01) relative to sediments (mean of 6.83). The mean $\delta^{13}C$ and $\delta^{15}N$ values in sediments were -23.04‰ and 8.20‰, respectively, while the mangrove samples were ^{13}C-depleted (mean of -26.89‰) and exhibited a wide range in the Nitrogen isotope composition (values from 4.89-11.94‰).

Surface sediment samples showed a progressive increase of N, C and OC towards the interior of the mangrove forest, a decrease in $\delta^{13}C$ values, but no clear spatial pattern was discerned in the depth samples. Despite some scatter, $\delta^{15}N$ values were relatively constant in the across-shore direction. The elemental and isotopic concentration in the sediments did not appear to be affected on a large scale by the freshwater discharge, which locally influenced only the concentrations within the sediments on the adjacent riverbanks. Relatively high $\delta^{13}C$ values and low C: N ratios indicate the predominance of an allochthonous marine source for carbon in

FoT mangrove sediments. Neither algal biomass nor grain size were found to be correlated with OC content in the Firth of Thames sediments. A gross estimate (integrated over the top 10 cm) of C and N stocks was 13.26 t C ha^{-1} and 1.47 t N ha^{-1}, respectively, thus adding to the recognition of these forests as efficient carbon and nitrogen sinks.

This research contributes to the knowledge of C and N content, sources and burial patterns in subtropical mangrove sediments. Such information is required to underpin environmental management decisions, for example prior to undertaking restoration or removal projects.

Acknowledgements

I thank first and mostly to my Supervisor Dr. Julia Mullarney. This project was a great personal challenge for me; from the beginning in a foreign country, she brought support to all my doubts. Was her dedication and courage through the field experiment what allowed us to continue. She always kept faith in me despite the laboratory issues, and I counted on her support in writing the thesis even in times of pandemic. Her leadership combined with joy will guide my path to become a better professional.

I want to give special thanks to Waikato Regional Council for financially sponsoring this project. To Colfuturo, the Colombian foundation who gave me their financial support for the Master's degree, to the University of Waikato for offering me the Research & Enterprise Study Award and the American Chemical Society Petroleum Research Fund for partial support of this research.

My husband, Edward, must know that without his support and care, I would not have had the opportunity to study once again. His every way effort made possible to complete this stage of my life. My son, Mateo, who is a small machine which impulses me every day, many thanks for your joyful, love and patience. He made this adventure more rewarding. Many thanks to my family and friends in Colombia, they encouraged me from the beginning, being aware of my well-being and supported me when I need it.

The support provided in logistics and physical effort by Dean Sandwell was indispensable for this investigation. In the same way, many thanks to Morgan Harvey, Tiago Dutra, Hemanth Vundavilli, and Erik Horstman for their unconditional collaboration on the field stage. The company of Bérengère Dejeans and Peter de Ruiter in the whole process is memorable. I would also like to thank Anjana Rajendram and Judith Hoult, for their immeasurable patience and dedication to the samples at Waikato Stable Isotope Unit. Noel Bates, thank you very much for your enormous help in the soil laboratory. Cheryl Ward, thank you very much for your cooperation with the thesis edition. Last but not least, Dr. Merilyn Manley-Harris thanks for helping us to solve the chemical problem that stopped our progress for a moment, your help was invaluable.

Table of Contents

List of Figures

List of Tables

1. Introduction

1.1 Background

Mangroves are flowering trees adapted to coastal and estuarine conditions, including seawater, tidal influence, surges, periodic inundation and runoff currents (Duke, 2017). Mangrove forests grow in intertidal zones in tropical and subtropical regions between latitudes 30°N and 30°S (Giri *et al.*, 2011), limited by major ocean currents and the winter 20 ° C seawater isotherm (Alongi, 2002). Mangroves are considered to be a foundation species controlling food webs and biodiversity (Polidoro *et al.*, 2010; Huxham *et al.*, 2017). These trees provide numerous ecosystem services such as coastal protection (Mazda *et al.*, 1997; Alongi, 2008; Vo-Luong & Massel, 2008), habitat for diverse fauna (Kandasamy & Bingham, 2001) and carbon sequestration (Daniel *et al.*, 2011; Twilley *et al.*, 2017). These ecosystem services have been estimated to have a value of greater than US$1.5 billion per year (Costanza *et al.*, 1997; Polidoro *et al.*, 2010). Nevertheless, the increasing population around coastlines worldwide has dramatically increased the clearing of mangroves. These forests are globally disappearing at a rate of approximately 1% per year, due to coastal development, conversion of land to aquaculture areas, and fuel and timber production (Polidoro *et al.*, 2010).

1.2 Mangroves in New Zealand

On the north island of New Zealand, mangroves cover an area 26,050 ha and are found from 34°27'S in the far north to 38°50'S on the west coast at Kawhia Harbor (Horstman *et al.*, 2018). The New Zealand mangroves belong to a single species, *Avicennia marina var. australasica*, or 'grey mangrove' (Figure 1.1). This species tolerates a wide range of environmental conditions such as changes in water and air temperature, salinity and daylight. These trees have aerial roots, or pneumatophores, which extend radially from the trunk, and emerge from the soil (Horstman *et al.*, 2018). Mangrove forests occupy areas where mudflats have reached an adequate elevation in the intertidal (Swales *et al.*, 2015).

Figure 1.1. *Avicennia marina var. australasica* trees in the forest fringe at the Firth of Thames, New Zealand.

In contrast to the global trend, New Zealand mangroves are expanding, at a rate of ~4.1% per annum (Bulmer *et al.*, 2017). Following European settlement, extensive deforestation intensified erosion, thus increasing sediment loads into New Zealand estuaries (Swales *et al.*, 2007). The estuarine sediment input, along with larger nutrient inputs, has favoured the habitat for the areal expansion of mangroves during the last 50-70 years (Horstman *et al.*, 2018).

In order to counteract the expansion of mangroves, communities in the four regions where mangroves thrive in New Zealand have practised legal and illegal removals in an attempt to return estuaries to previous sandflat ecosystems; however, such attempts are often not successful (Lundquist *et al.*, 2014; Bulmer *et al.*, 2017; Horstman *et al.*, 2018). Moreover, mangrove clearances can lead to an excess of carbon (C) and nitrogen (N) in coastal systems, and subsequent eutrophication and hypoxia, with negative consequences for ecosystem function. Bulmer *et al.* (2016) estimated that the removal of one hectare of New Zealand mangroves can result in the loss of 79 tons of Carbon and 8.3 tons of Nitrogen per hectare.

1.3 Carbon cycling in mangrove ecosystems

Carbon is the common element in all life forms and is the 15th most abundant element in the Earth's crust (Reece *et al.*, 2014). The increase in carbon dioxide emissions worldwide and the respective environmental consequences have increased interest in ecosystems with the capacity to act as blue carbon stocks (Bulmer *et al.*, 2016). Mangroves are highly productive ecosystems (Bouillon *et al.*, 2008; Alongi, 2018) and about 14% of carbon sequestration by the global ocean is due to these forests (Alongi, 2014). Twilley *et al.* (2017) suggest that about 40% of the organic carbon generated in these ecosystems is exported to coastal waters and around 10% is captured and retained in sediments.

Mangroves are among the most C-rich forests in tropical areas; however, a global burial rate estimation is ambiguous given it is difficult to account for the diversity of environmental settings where mangroves thrive and the proportions of CO_2 emitted due to removal of these forests (Twilley *et al.*, 2017). Additionally, the structure (height and the base area of the tree) and the function, that is, how much Carbon a mangrove tree sets, are conditioned by factors at different scales: The geographical position determines the temperature, precipitation and evapotranspiration; environmental setting (lagoon, estuary, river mouth) controls the area and distribution of the forest; hydrodynamics such as tides, waves and river discharge, control sediment and nutrient supply, and affect the attributes of trees from the outermost area in the fringe to inner mangroves (Twilley *et al.*, 2017). The key components of the carbon cycle within mangrove ecosystems are summarised in Figure 1.2 and Table **1.1**.

Table 1.1. Summary of the components of the carbon cycle in a mangrove ecosystem.

Abbreviation	*Component*
GPP	Gross Primary Production.
R_a	Respiration by autotrophs or primary producers
R_h	Respiration of heterotrophs
NPP	Net Primary Production. The storage of chemical energy defined as NPP= GPP-R
POC	Particulate Organic Carbon
DOC	Dissolved Organic Carbon
DIC	Dissolved Inorganic Carbon
NTEm	DIC+DOC+POC. Net exchange of tidal inflow-outflow
NTEo	DIC+DOC+POC. Exchange with coastal ocean
I_t	DIC+DOC+POC. River inflow
NEPm	GPP- (Ra+Rh) ± NTEm. Net productivity of Mangroves.
NEPo	GPP+ I_t -(Ra+Rh) ± NTEm ± NTEo. Net productivity of estuary.

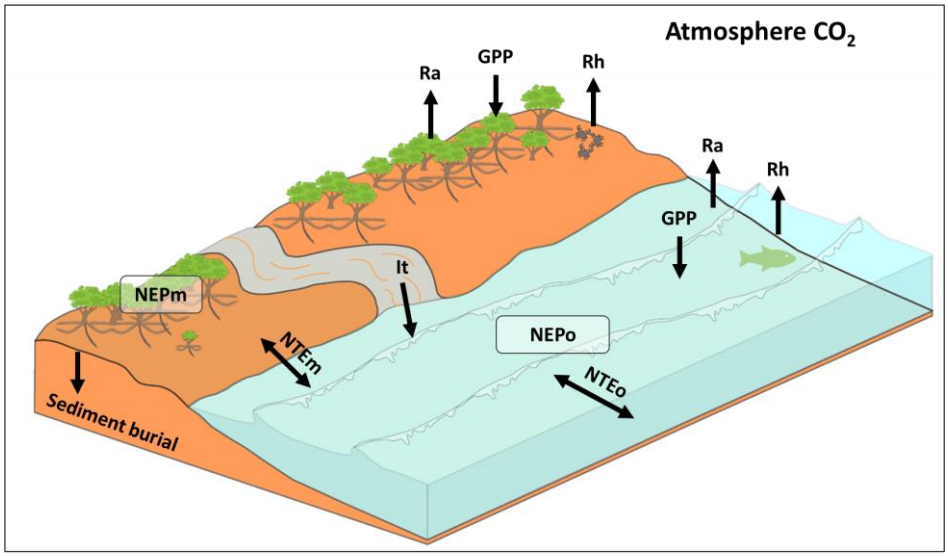

Figure 1.2. Summary of the main elements of Carbon cycling within a mangrove ecosystem. Taken and modified from Twilley *et al.* (2017). See Table 1 for definition of abbreviations.

The interaction of mangroves with tidal flow and waves affects the capacity of the forest to capture organic allochthonous material and retain autochthonous material. Norris *et al.* (2017) reveal that high turbulence generated in areas with dense vegetation (as within fringe zone) restricts the deposition of sediments, while less intense turbulence landwards allows the deposition of fine sediments; thus, the accretion of the shoreline occurs from the interior outwards.

Despite the many difficulties in calculating the carbon budget of the coastal zone, Bouillon *et al.* (2008) nonetheless estimated a global net primary production of 218 Tg C a^{-1}, assuming a total area of 160,000 km^2 of mangrove forests. Likewise, according to a synthesis of current literature, Carbon derived from mangroves globally has the following fate: carbon burial with a rate of 18.4 Tg C a^{-1}, a CO_2 efflux from mangroves systems in the order of 42 ± 31 Tg C a^{-1}, and export as DOC (24 ± 21 Tg C a^{-1}) and POC (22 ± 27 Tg a^{-1}). However, these values only approach 45% of the global NPP and ~ 112 ± 85 Tg C a^{-1} has not been accounted for in current budgets.

1.4 Nitrogen cycle

Nitrogen comprises most of the Earth's atmospheric air (~ 78%) and is the fourth most abundant element in cellular biomass. nitrogen (N) is found in various compounds that circulate in the air, soil, animals and bodies of water. The nitrogen cycle (Figure 1.3) is composed of 5 fundamental processes:

1. Nitrogen fixation, where the N in the atmosphere (N_2) is converted to NH_4^+ / NH_3 due to the action of diazotrophs and rhizobium bacteria (present in the roots of leguminous plants) or by lightning strikes.

2. Nitrogen uptake or assimilation is a process in which organisms uptake the fixation compounds.

3. When organisms die and decompose, bacteria or fungi return nitrogen to NH_4^+. This step is called mineralization.

4. Nitrification, also processed by bacteria, is when Ammonium (NH_4^+) is converted to Nitrate (NO_3^-). Nitrate is easily leached from the soil due to its high solubility.

5. Finally, NO_3^- is converted to nitrite (NO_2^-) and reduced in other compounds such as N_2O, NO, and N_2 thus completing the cycle (Stein & Klotz, 2016; Manley *et al.*, 2019).

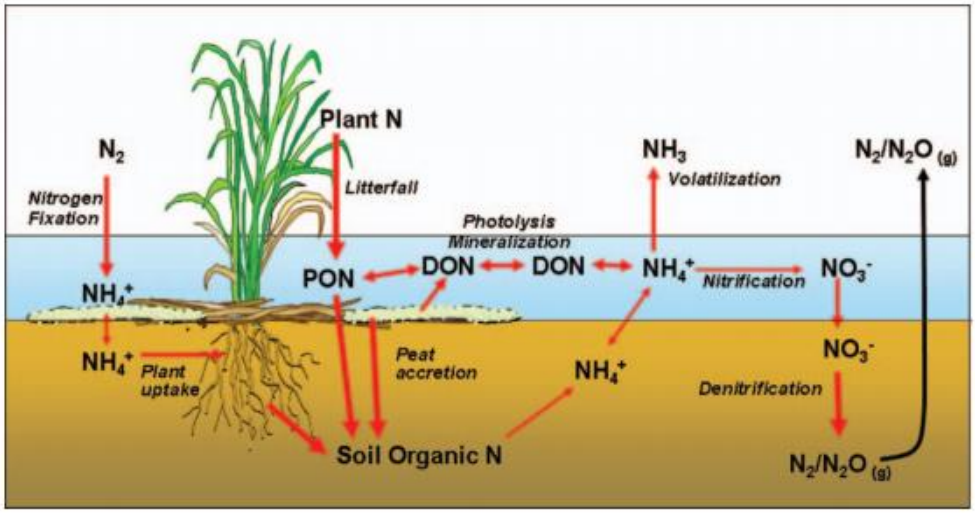

Figure 1.3. Summary of the main processes in Nitrogen cycle in wetland systems. From Inglett *et al.* (2011). PON: particulate organic Nitrogen, DON: dissolved organic Nitrogen.

1.5 Isotopic compositions: $\delta^{13}C$, $\delta^{15}N$ and C/N ratios

There are two types of stable isotopes ^{12}C and ^{13}C of carbon and the ^{14}C is a radioactive isotope broadly used in radiometric dating (Stute, 2006). The ratio of ^{13}C: ^{12}C is normally expressed as per mille deviation (‰ $\delta^{13}C$):

$$\delta^{13}C = \left(\frac{\left(\frac{^{13}C}{^{12}C}\right)\text{Sample}}{\left(\frac{^{13}C}{^{12}C}\right)Standard} - 1 \right) \times 1000,$$

where Pee Dee Belemnite is used as the standard (Lamb *et al.*, 2006). Carbon sources and transport pathways within an estuary environment can be assessed through the elemental analysis of carbon and nitrogen in conjunction with the $\delta^{13}C$ values (Thimdee *et al.*, 2003; Tue *et al.*, 2018). The greatest ranges of variability in ^{13}C: ^{12}C ratio occur in biological material compared to geological samples (Figure 1.4). Terrestrial plants, in comparison with marine vegetation show the most significant differences in $\delta^{13}C$; likewise, plants with different photosynthetic pathways (C3, C4, or Crassulacean Acid Metabolism-CAM) have different

fractionation ranges (Dawson *et al.*, 2007). Plants adapted to very saline environments, as mangroves, are commonly of C4 or CAM type (Lamb *et al.*, 2006)

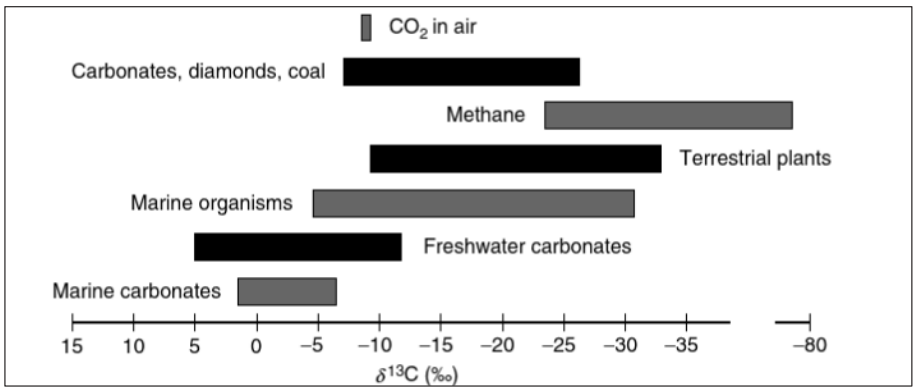

Figure 1.4. Observed ranges of $\delta^{13}C$ in some materials present on earth. Taken from Dawson *et al.* (2007).

^{15}N is a stable isotope of Nitrogen that constitutes 0.365 of the total percentage of Nitrogen in the Earth. As with the stable carbon isotope, ^{15}N is quantified about a reference standard $\delta^{15}N$ represented in the "per mille" (‰) difference between the isotope and atmospheric N_2. In marine environments, this isotope varies between -2‰ and -30‰ (Montoya, 2008). Isotopic studies of ^{15}N are useful tools for making connections in changes in marine production due to exogenous nutrient inputs, for example, the entry of anthropogenic Nitrogen into the food web.

The sediments in the land-ocean limit, where mangrove forests thrive, receive organic material from autochthonous (derived from plants and animals in-situ) and allochthonous (imported from elsewhere, e.g. via river input and exchange of tidal inflow-outflow) sources (Lamb *et al.*, 2006). Terrestrial vegetation has C/N ratios of greater than 12, while bacteria and marine algae have C/N values lower than 10. In intra-tidal areas, the presence of algae may introduce N to the sediments and decrease the C / N ratio (Figure 1.5). The $\delta^{13}C$ values in terrestrial C4 plants vary between -17‰ to -9‰, whereas CAM (Crassulacean acid metabolism) photo synthesisers have a more extensive range between -11‰ to -28‰ (Lamb *et al.*, 2006).

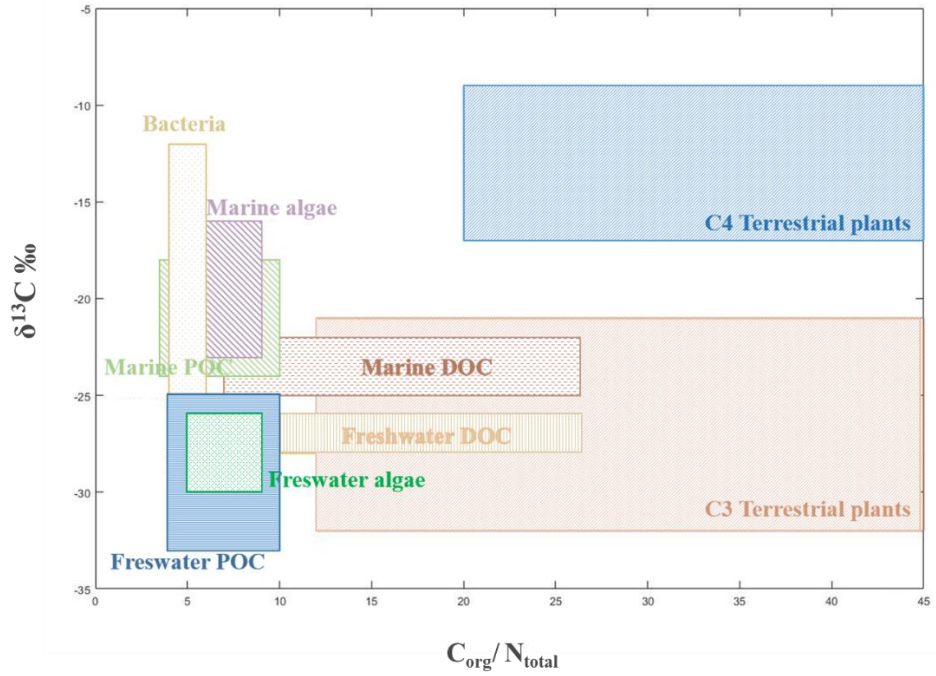

Figure 1.5. Typical value ranges of $\delta^{13}C$ and C/N ratio for organic matter in coastal environments. Figure made following Lamb *et al.* (2006) and references therein.

1.6 The study site: Background

The Firth of Thames (FoT) is a shallow marine embayment structurally demarcated by the Hauraki Rift on the North Island of New Zealand. The Firth is confined between horsts where basement rocks emerge: the Hunua Range to the west and the Coromandel Peninsula in the east (Naish *et al.*, 1993). The FoT receives freshwater and sediments from three rivers (Swales *et al.*, 2015): Suspended sediment loads of the Waihou and Piako Rivers are estimated to be 160,000 $t.yr^{-1}$ and 30,000 $t\ yr^{-1}$, respectively (Hicks *et al.*, 2011). No estimates were available for the much smaller Waitakaruru River. The sediments in the Firth are smectite-rich muds which are derived from the alteration of detrital volcanic glass (Naish *et al.*, 1993). The ambient temperature fluctuates between 13 and 22 °C with mean annual rainfall of 1.4 $m.y^{-1}$ (Lovelock *et al.*, 2010). The FoT is mesotidal, with tidal ranges between 2.9 m (spring) and 2.2 m (neap). Above the intertidal flats mean tidal currents can reach speeds of 0.2 $m.s^{-1}$ (Swales *et al.*, 2015).

The proximity to sediment source areas from the large rivers, combined with the broad tidal range, currents within the estuary, and shallow bed slope, favoured the construction of approximately 70 km^2 of intertidal mudflats in the southern FoT (Lovelock *et al.*, 2010; Swales *et al.*, 2015). Since European settlement in New

Zealand, large-scale deforestation of river catchments increased the land erosion and accelerated the infilling of river valley estuaries and the accretion of tidal flats. These new areas with larger nutrient inputs favoured the expansion of New Zealand mangroves (Horstman *et al.*, 2018), and in the FoT, mangrove trees have colonised more than 11 km^2 of mudflat since the early 1960s (Swales *et al.*, 2015). Mangroves occupy the intertidal flat from 1 m above mean sea level (MSL) to the north and 2 m above MSL towards the land in the south edge. A stop-bank was constructed on this landward edge to prevent seawater incursion into the lower farmland adjacent to the mangrove forest (Lovelock *et al.*, 2010). The expansion of the mangrove forest in FoT occur in recruitment periods, which appear to be a response to periods of unusually calm conditions or a decline of external forcing (as sea level rise, changing weather, salt-marshes establishment) known as "windows of opportunity" (Balke *et al.*, 2015).

1.7 Knowledge gaps

Despite the importance of mangroves as blue carbons pools, research on storage of carbon as belowground matter in sediment and wood production is limited (Bouillon *et al.*, 2008). Alongi and Mukhopadhyay (2015) estimate that mangroves contribute between 10 and 15% of carbon storage in coastal sediments, but suggest that further research is needed on the origin of carbon buried in mangrove forest and its role in peat formation. The functioning of mangroves as C and N storage pools has been previously established in New Zealand (Lovelock *et al.*, 2010; Bulmer *et al.*, 2016; Bulmer *et al.*, 2017; Horstman *et al.*, 2018); however, the majority of studies have focused on quantifying the C and N stock in trees and root biomass with less work done on storage within the sediments themselves. Similarly, research on the sources, spatial distribution and variability of C and N within forests is limited. One exception is a previous study of New Zealand mangroves in the Waitemata Harbour, which revealed that the carbon retained in the fringe zone is primarily allochthonous and in the forest interior, carbon is mangrove-derived (Yang *et al.*, 2013). However, this previous investigation did not evaluate the spatial variation in carbon within the estuary, and nitrogen content was also not measured.

1.8 Aim of this thesis and research questions

The present research aims to understand the controls on the spatial distribution of elemental and isotopic distribution of carbon and nitrogen within the muddy sediments of a subtropical mangrove forest. We address the follow sub-questions:

1. Is there a difference in elemental concentrations and sources, and the isotopic signatures of sediments between vegetated and non-vegetated areas?

2. How spatially variable are carbon and nitrogen, $\delta^{13}C$, and $\delta^{15}N$ within the mangrove forest and adjacent river and mudflat systems?

3. Do rivers provide a spatial control on the distributions of elements and isotopic compositions? Are there other potential dependencies of spatial patterns on factors such as sediment texture or algal biomass?

To achieve the objectives of this study, extensive sampling and laboratory analyses were carried out on samples taken in the mangrove forest and mudflat zone of the Firth of Thames.

1.9 Structure of this thesis

Chapter 2 describes the field and laboratory experiments, including the methodology followed and our modification of the method of sample preparation for the estimates of organic carbon (OC). Results are presented in Chapter 3, while our findings and implications are discussed in Chapter 4, which also includes a comparison of our results with previous research from around the globe. Finally, Chapter 5 summarises the most relevant research findings and outlines avenues for future work.

2. Field and Laboratory Measurements

In this chapter, a description of the field measurements and the laboratory methodology is provided. This study necessitated a slight modification of existing methodology for removing the inorganic material from the sediment samples. The reasons for this change in procedure are detailed in section 2.3.2.

2.1 Study site

The field site was the mangrove forest, and intertidal mudflat at the southern end of the Firth of Thames (FoT) on the North Island of New Zealand (Figure 2.1). The mangrove forest encompasses the mouths of the Waihou, Piako and Waitakaruru rivers (Figure 2.2).

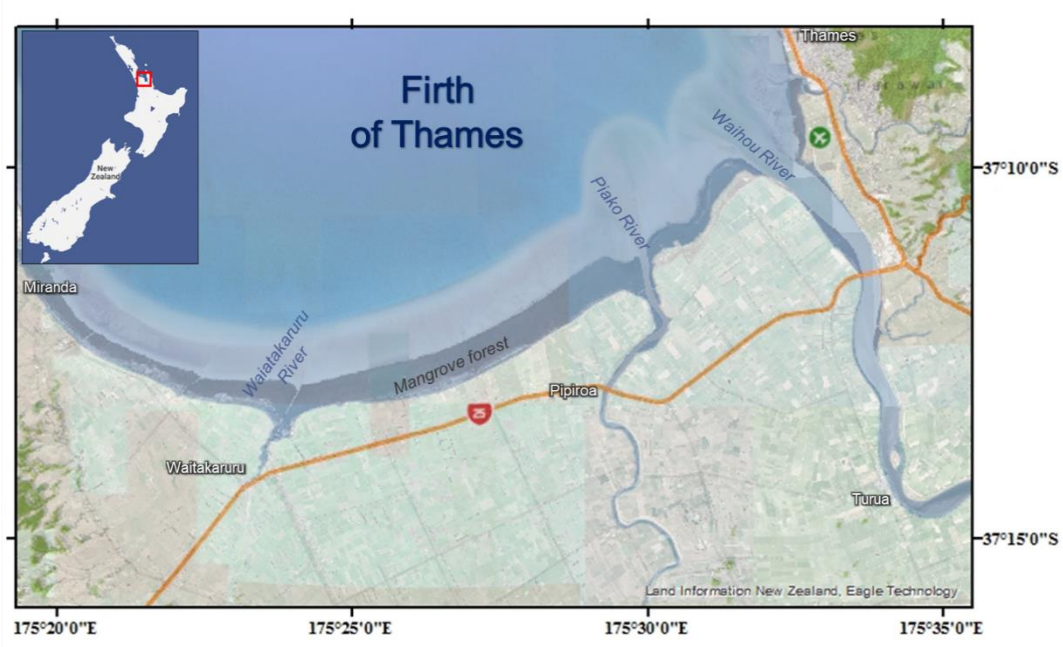

Figure 2.1. Field site location. The red box demarcates the position of the Firth of Thames within the North Island of New Zealand. Source map: Land Information New Zealand.

Samples were taken across a number of transects throughout the domain (Figure 2.2a): Twelve across-shore transects were sampled in the summer of 2019 (11-16 February). These transects have been denoted transect A (in the west, near Miranda) to L (east side of the Firth close to the town of Thames). Over the same time period, 11 additional locations along the river banks were sampled: 7 within the Waihou

River (two on the river east side near Turua and two on the west side near Kopu and the remaining three stations were 2.5 km downstream), two within the Piako (near Pipiroa) and two within the Waitakaruru (near Canal East Road). Similarly, two approximately shore-parallel transects (Y and Z) were sampled from a boat on August 27th of 2019 (Figure 2.2a).

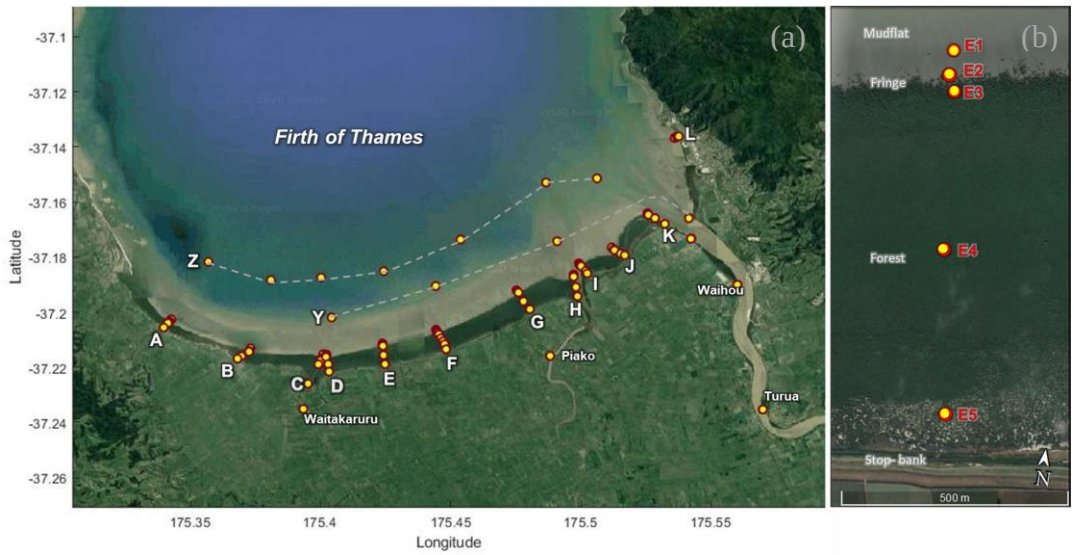

Figure 2.2. a) Location of transects and stations in the rivers that flow into the Firth of Thames. b) General stations position within the transect.

Each cross-shore transect consisted of 5 sample locations, with the exception of the F transect, where 9 stations were employed. Those locations denominated with the number 0 or 1 were on the bare mudflat in front of the mangrove forest, locations 2 and 3 were in the thin 'fringe' zone between forest and mudflat, and the other samples were distributed along the across-forest transect (Figure 2.2b). For most transects, the forest samples consisted of sample 4 half-way into the width of the forest and sample 5 close to the back of the forest. Shore-parallel transects Y and Z comprised 4 and 7 sampling stations, respectively. Additionally, samples of vegetation were taken at a few locations (details below in section 2.2). In total, 193 sediment samples and 35 vegetation samples were obtained. A summary of sample locations is given in Table 2.1.

Figure 2.3. Firth of Thames a) in mudflat and b) fringe zone

Table 2.1. Summary of samples within each transect for this research. Generally, depth samples were taken from 34 to 37 cm, but for a few shorter cores, samples were taken from a shallower depth.

Table of samples and analysis in Firth of Thames								
Transect	**Stations**	**Surface samples (0-2 cm)**	**Depth samples (34-37 cm)**	**Vegetation samples**	**Core Samples**	**Grain Size Samples**	**Chlorophyll *a* samples**	**Loss on Ignition Samples**
A	5	5	5	-	-	4	6	10
B	5	5	5	7	-	-	-	-
C	6	6	6	-	-	4	-	12
D	5	5	5	-	-	4	-	10
E	5	5	5	-	-	-	-	-
F	9	10	9	25	18	6	7	18
G	5	5	5	-	-	-	-	-
H	5	5	5	-	-	4	-	10
I	5	5	5	-	-	4	-	10
J	5	5	5	-	-	-	-	-
K	5	5	5	-	-	4	6	10
L	5	5	5	-	-	4	6	10
Y	4	4	4	-	-	4	4	8
Z	7	7	7	-	-	6	6	14
Turua	2	2	2	-	-	4	4	4
Waihou	5	5	5	-	-	4	-	-
Piako	2	2	2	3		4	4	4
Waitakaruru	2	2	2	-	-	4	4	4
Total samples	87	88	87	35	18	60	41	124

2.2 Sediment and vegetation sampling

Sediment samples were collected using two metallic push cores for samples collected on foot. A gravity core was used in the offshore sampling (transects Y and Z). The push corers were designed at the University of Waikato (Figure 2.4a). The corers were of length 40 cm, with a diameter of 10 cm, and a top lid was used during extraction in order not to contaminate the sample (Figure 2.4b & c). The gravity corer was a fibreglass tube of 7 cm diameter (Figure 2.4 d & e); the open bottom allows the sample collection as the corer penetrates the seabed.

Figure 2.4. Corers used in field sampling. a) Push corer with handle to generate pressure and torsion. b) Push corer in a mudflat station. c) Land core extraction. d) Boat sampling. e) Core extraction from the gravity corer

Cores were extruded in-situ and sectioned. Surface samples (S) were taken from the top 2 cm. Depth samples (D) were generally taken from 34-37 cm depth. In a few cases, when the full length of cores was not obtained, the depth sample was taken from closer to the surface. Similarly, for the centre (F) transect, two cores were split into 9 sections to provide a higher-resolution vertical profile throughout the depth of the core.

Additionally, samples of mangrove vegetation were taken from transect F, and station 2 of the Piako River. Sections of leaves, trunk and roots (pneumatophores) were taken and stored separately. All samples were frozen within 5 hours of collection. Subsequently, samples were stored at ~ -20 ℃ in the Science School freezer at the University of Waikato for proper preservation before analysis.

2.3 Sample preparation for analyses

Laboratory analyses of sediment samples were undertaken to provide elemental and isotopic concentrations of carbon (C) and nitrogen (N), grain size, Chlorophyll *a* concentrations and bulk estimates of organic matter content. The methods are described below.

2.3.1 Elemental and isotopic analysis

To prepare for analysis, sediment samples were defrosted for 48 hours in a refrigerator at a temperature between 3 and 4°C and sieved through a sieve of 500 μm to remove the remains of vegetation, shells and organic material. Sieving used ultrapure water (Milli-Q water, 18.2 MΩ cm-1) to avoid contaminating the sample (Figure 2.5a). The sieved sediment was placed in foil containers and then dried in a oven for 48 hours at 50°C (Figure 2.5b). The samples were not centrifuged since a percentage of solved organic matter (SOM) or clay can be suspended in the water column and affect the results. Samples were allowed to cool in a desiccator for one hour and preserved in pre-labelled containers of 50 ml. Samples were ground into a ~ 5 μm powder using a mixer ball mill at 27.5 Hz for 1 minute. Each ground sample was split into two halves – with one half left untreated, while the other half underwent treatment to remove carbonates.

Following the procedure of (Yu *et al.*, 2018), the untreated samples were weighed into two tin containers for use in the elemental analyser in the Waikato Stable Isotope Unit (WSIU). The untreated samples ($N_{samples}$ = 193) were used to provide measurements of total carbon (%TC), total nitrogen (%N) and $\delta^{15}N$ (‰).

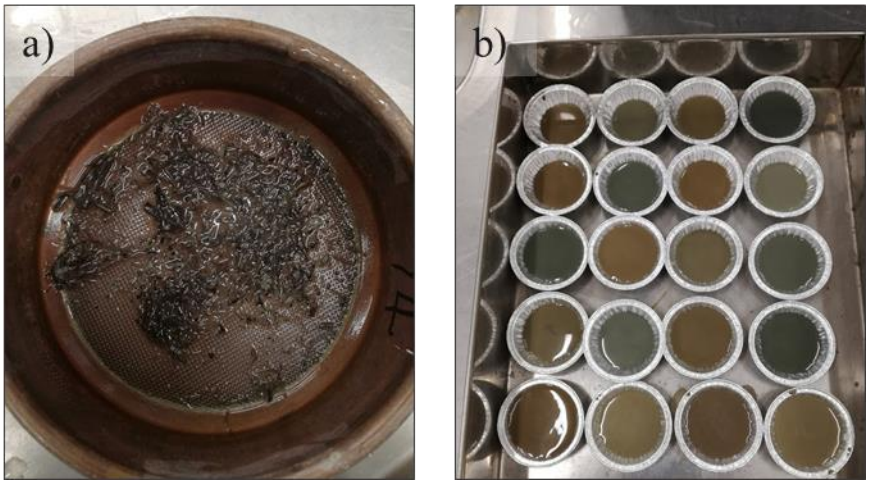

Figure 2.5. Process of sieving. a) organic remains after sieving a sample. b) Foil containers with sieved samples to be placed in the oven.

The other half of each sediment sample ($N_{samples}$ = 193) was treated with acid to remove carbonates from the sample, to provide measurements of organic carbon (% OC) and $\delta^{13}C$ (‰). Procedures were slightly modified versions of those given in Yu *et al.* (2018). Details of the motivation for the modification are provided in section 2.3.2. Throughout the procedure gloves were won to prevent contamination. 1 g of ground sediment sample was placed into a pre-weighed heat-resistant glass container (Figure 2.6a), and 10 ml of 4M Hydrochloric acid (HCl) was added to dissolve carbonates and stirred to distribute the sediment evenly. After an hour, 10 ml of ultra-pure water (Milli-Q water, 18.2 MΩ cm-1) was added at room temperature, and the mixture heated on a heating plate (within a fumehood) at a constant temperature of 110 ° C (measured inside the beaker) (Figure 2.6b). Heating occurred for between 20 and 30 minutes to evaporate water and acid (Figure 2.6c). Samples were removed from heat at this point to avoid carbon loss. To eliminate any remaining water, samples were placed in the oven for 24 hours at 50 °C. To prevent damage to the isotope analyser, samples need to have a pH of at least 4, so 10 ml of ultrapure water was added and stirred to homogenise the sample and pH measured using a previously calibrated pH-meter. If pH <4, the heating, drying and rinsing steps were repeated. After this procedure, an increase in weight of the samples was recorded around 8% possibly due to the integration of hydrogen free radicals in the structure of the clays. Once the pH was acceptable, the sample was dried once more for 48 hours at 50 ° C, then removed from the oven, left to cool down in the desiccator for one hour and subsequently ground for one-minute.

Lastly, the treated samples were weighed into tin containers for TOC and $\delta^{13}C$ analysis (Figure 2.7).

Figure 2.6. Acid treatment to sediment samples. a) Acidification of ground samples. B) Heating and evaporating process. c) desiccation cracks in a sample correctly dried.

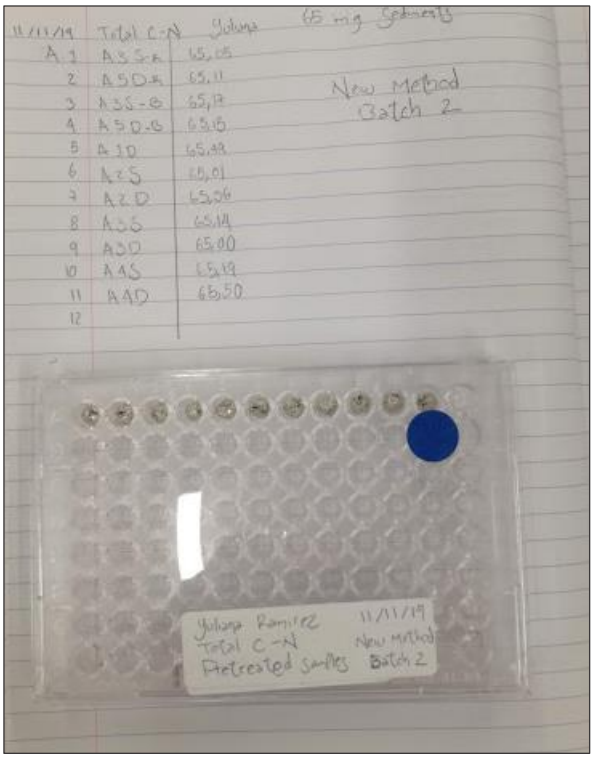

Figure 2.7. Samples inside tin capsules

The vegetation samples (n = 35) were defrosted for 24 hours and rinsed with ultrapure water to remove remains of sediments and exogenous organic remains. The samples were subsequently dissected at 50°C for 48 hours, ground at 27.5 Hz

for 2 minutes in the mixer ball mill, weighed and preserved in tin containers for elemental and isotopic analysis.

Total C and N concentrations in the samples were detected using a CHNOS Elemental Analyzer with an accuracy of 0.1% abs. Isotopes ^{13}C and ^{15}N were measured using a Dumas elemental analyser (Europa Scientific ANCA-SL) interfaced to an isotope mass spectrometer (Europa Scientific 20-20 Stable Isotope Analyser) with a measurement precision of ±0.5% for ^{13}C and ±0.1% for ^{15}N . The isotope analyses results are expressed as $\delta^{13}C$ and $\delta^{15}N$, where

$$\delta^{13}\mathrm{C} = \left(\frac{\left(\frac{^{13}\mathrm{C}}{^{12}\mathrm{C}}\right)\mathrm{Sample}}{\left(\frac{^{13}\mathrm{C}}{^{12}\mathrm{C}}\right)Standard} - 1 \right) \times 1000, \text{ and}$$

$$\delta^{15}\mathrm{N} = \left(\frac{\left(\frac{^{15}\mathrm{N}}{^{14}\mathrm{N}}\right)\mathrm{Sample}}{\left(\frac{^{15}\mathrm{N}}{^{14}\mathrm{N}}\right)Standard} - 1 \right) \times 1000.$$

The $\delta^{13}C$ samples are compared to precalibrated C_4 sucrose which is cross-referenced to Pee Dee Belemnite (-10.8‰), and the $\delta^{15}N$ samples to a urea standard, which is referenced to atmospheric nitrogen (-0.45‰). Thus, the results of the analyses correspond to values of total carbon (% TC), nitrogen (% TN), organic carbon (% TOC), and deviations (measured in parts per thousand, ‰) of $\delta^{13}C$ and $\delta^{15}N$. The procedures are summarized in Figure 2.8.

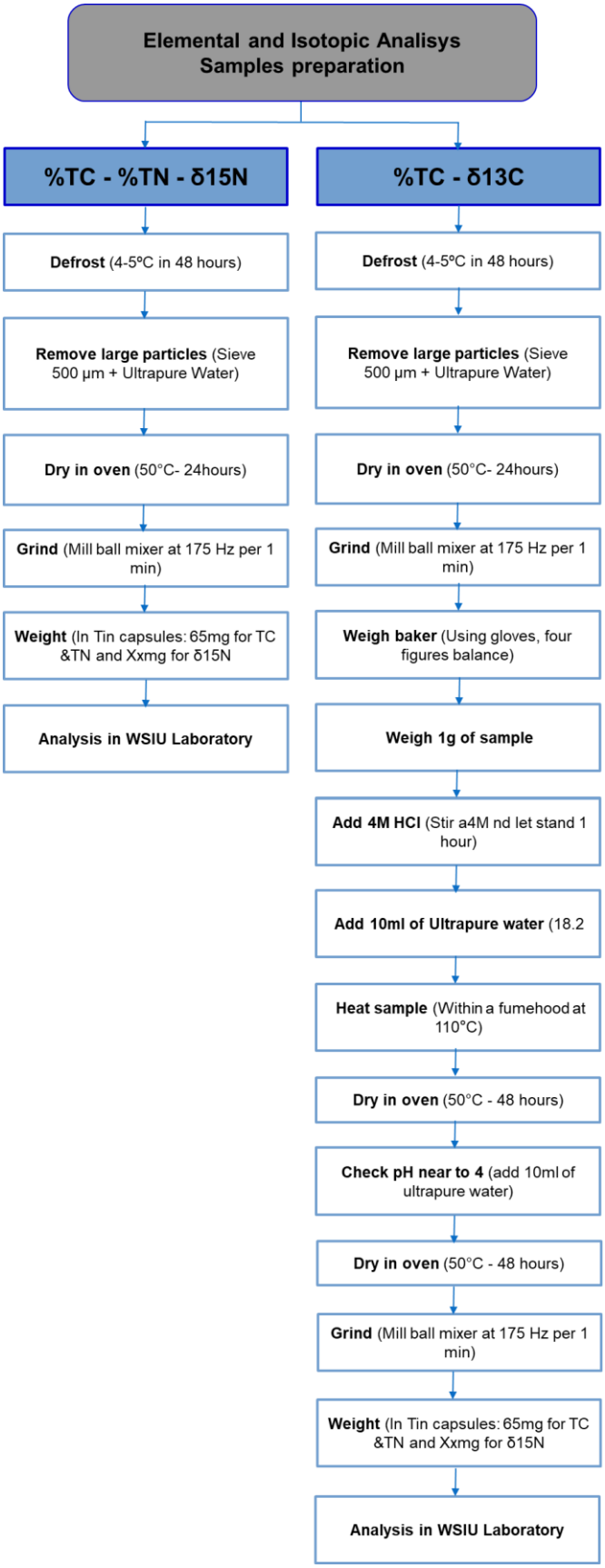

Figure 2.8. Flowchart for the sample preparation of isotopic and elemental analysis.

2.3.2 Motivation for modification of sediment treatment procedure

Numerous previous studies have described many procedures to prepare sediment samples to analyse organic carbon (OC) content and $\delta^{13}C$ values (Tue *et al.*, 2011; Yu *et al.*, 2018), in which the samples are pre-treated with acid, rinsed and centrifuged to remove excess acid. However, when trying to follow such a procedure during our research, the results repeatedly yielded larger values for organic carbon than the total carbon value. To rule out possible instrumentation errors in the WSIU laboratory, six samples were sent to an external laboratory; and results registered the same error (differences ranging from 1.80 to 0.01% of OC> TC). The source of the errors was identified as occurring the during implementation of the 'Rinse method' through two possible mechanisms: 1) to bring the sediments to a pH of 4 after acidification, the sample was rinsed and centrifuged six times. In the last centrifugation cycles the un-flocculated clay remained in suspension, and when the water was discarded, an unknown percentage of clay was inadvertently also removed from the original sample. 2) Once they had been treated, the samples retain part of the acid as it was not possible to reach he initial pH (~ 7) despite being rinsed numerous times.

Difficulties with the rinsing methodology have previously been identified by Brodie *et al.* (2011), who examined the most common methods of acid treatment: rinse method, acidification in silver capsule and acidification by acid vapour (Figure 2.9) and found inconsistent results. Their research showed that during the rinse method an organic carbon loss is observed that does not translate into a lower percentage in the results of CHN analysis, on the contrary, an increase in the percentage of organic carbon was found (~ 4%). This error is likely due to a loss of inorganic material such as fine colloids which is recorded as an artificial % OC elevation (Froelich, 1980; Harris *et al.*, 2001).

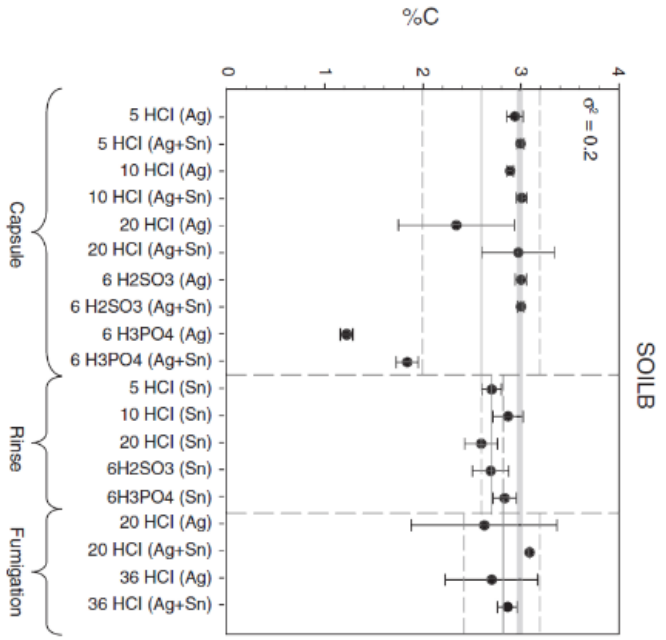

Figure 2.9. Comparison of the methods used by Brodie *et al.* (2011) to obtain the percentage of OC in a sediment sample with different acids and concentrations. The solid grey box indicates the value of the sample without treatment (SOILB, International Soil Standard from LECO corporation with C = 3.00 ± 0.05%). Grey lines are mean value for each method and dashed grey lines standard deviation (1σ). Figure source: Brodie *et al.* (2011).

Given these drawbacks, we consulted with the Department of Chemistry at the University of Waikato who suggested a new method in which post-acidification water is not discarded (thus preventing accidental loss of fine sediments) but evaporated. Therefore, the sample is acidified, rinsed with ultrapure water, evaporated and dried in the same container. This change in procedure allowed colloidal material to be retained and showed consistent results after three trials on multiple samples, thus it was deemed appropriate for this research.

2.3.3 Grain size analysis

A subset of 61 samples was selected for grain size analysis (Figure 2.10). The sites were chosen according to a probable granulometry change along the FoT such as riversides and estuary limits (Figure 2.10). The original sample was sieved (500 um) and organic matter and carbonates removed using 50 ml 10% hydrogen peroxide (H_2O_2) and 10–15 ml of 10% HCl at 60–80 °C. After standing for 72 hr, samples were washed with pure water, centrifuged for 3 min at 1500 rpm, and dispersed

with Sodium hexametaphosphate 0.05 M $(NaPO_3)_6$. Samples were then analysed using the Malvern Mastersizer 2000 laser particle sizer.

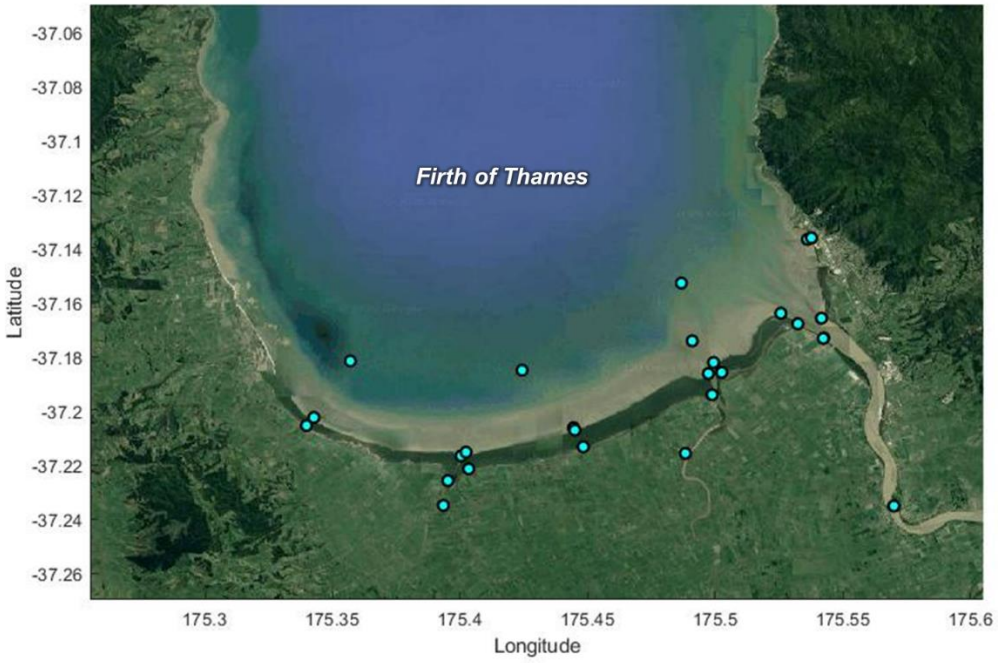

Figure 2.10. Subset of samples for which grain size analysis was performed.

2.3.4 Fluorometric determination of Chlorophyll *a* pigments.

The amount of algal biomass was estimated in a subset of 47 sediment samples of sediments (Figure 2.11), using standard fluorometric methods (Table 2.2). Briefly, the (previously acetone treated) sample is excited with a fluorometer with broadband blue light and the algae pigments are detected by fluorescence in the red waveband. Pigments derived from the degradation of algal chlorophyll (Phaeopigments) are corrected by acidifying the sample.

Figure 2.11. Area in the mudflat of Firth of Thames covered by green algae

Table 2.2. Procedures adopted to estimate the algal biomass in sediments

Procedure	**Elements and equipment**
Homogenize a subsample and preserve at -20°C	50 ml lid container
Freeze dry subsamples in the Thermophile and Microbial Biochemistry and Biotechnology Unit (Figure 2.12)	Dewar with liquid nitrogen
Weigh 0.15g of sample into clean tubes	15 ml Centrifuge tubes
Prepare 90% buffered acetone	Add 100 ml of saturated $MgCO_3$ to 900 ml pf analytical-grade acetone into a lid glass bottle
Add 10ml of buffered acetone and shake	Buffered acetone
Leave samples stand in a fridge in the dark for 24 hours shaking them at least once.	Fridge at 4-5°C
Gather clean glass cuvettes for each sample to analyse	
Shake vigorously each sample and centrifuge for 10 minutes at 3300 rpm	Centrifuge
Stand samples in room temperature in the dark for 30 minutes	
Calibrate Fluorometer and warm up it for 15 minutes (Figure 2.13)	Follow instructions in protocol/ Fluorometer
Take a blank reading of 5ml of the 90% buffered acetone into a cuvette	Buffered acetone
Take a second reading after adding 150 µl of HCl (let stand 90 seconds before)	0.1N HCl
Measure 5ml of sample and place the cuvette into fluorometer (if reading says Over dilute sample with buffered acetone).	Sample or supernatant, buffered acetone
Add 150 µl of HCl to the sample and let stand 90 seconds, take a second reading in the fluorometer	0.1N HCl

Figure 2.12. Samples are treated with liquid Nitrogen prior to freeze dry treatment.

Figure 2.13. Fluorometer used for the green algae estimations

The weights and fluorometer readings are recorded on a data sheet; then the calculation of the sediment chlorophyll *a* content is estimated as:

Chla a (µg/ g dw) = Fs((r/r-1)(Rb-Ra)(volume extracted/sample weight)(df)))/1000

Phaeo (µg/ g dw) = Fs((r/r-1)(sRa-Rb)(volume extracted/sample weight)(df)))/1000,

where the volume extracted is 10 ml buffered acetone, Fs is the response factor for sensitivity setting from fluorometer calibration, Ra is the reading before acidification minus the blank reading, Rb is the reading after acidification minus blank reading, r is an acidification coefficient, and df is a dilution factor.

2.3.5 Loss on Ignition (LOI) methodology

The elemental Carbon content measurements were also supplemented by bulk estimates of organic matter content for 124 samples using loss-on-ignition method. In this analysis, 1 g of the previously defrosted, sieved, dried and ground sample was placed in a pre-weighed container and dried for 3 hr at 50°C, followed by 4-hours heating at 500°C in a muffle furnace (Figure 2.14). After 1-hr of cooling in a desiccator, samples were weighed, and content of organic matter estimated as:

$$SOM(\%) = \frac{DW - AFDW}{DW} * 100,$$

where SOM is the Soil Organic Matter, DW is the dry sample weight (g), and AFDW is the ash free sample weight (g).

Figure 2.14. Comparison of sediment before and after being taken to the muffle furnace

3. Results

3.1 Introduction

This chapter presents the results of the different laboratory analyses. The findings of elemental analyses for sediment and vegetation samples will be shown first, then the isotope data. Results from fluorometric analysis of chlorophyll a, grain size analyses, and loss on ignition are described at the end of this section.

3.2 Elemental analysis

3.2.1 Summary statistics

The data for total concentration of nitrogen (N), carbon (TC), organic carbon (OC) and inorganic carbon (IC=TC-OC) in sediments are presented here. At each sampling station, the preserved sediments were sectioned and categorised as 'surface' for the sample at the top of the core (first 2 cm) and 'depth' at core bottom (typically at a depth of 34 to 37 cm, but shallower in a few cases where long cores were not obtained).

Table 3.1 shows the summary statistics for the elemental analysis results. The mean concentrations of N, TC, OC and IC are larger on the surface than in depth samples. Among the measured elements, surface samples have a greater variance compared to depth samples. Skewness is an asymmetry measure in the distribution, measurements close to 0 show a normal and symmetric distribution; positive values indicate a bias to the left and negative values a leaning to the right. The most biased data are the IC concentration and the C/N ratio (OC/N) in both surface and depth samples. The N in depth samples are skewed towards higher values, and the C values are biased skewed towards lower concentrations. One sample of OC gave a clearly inaccurate value in the laboratory analysis, likely owing to contamination in the sample; thus, the number of total samples varies between 86 and 87. Table 3.2 shows the average values of the difference between the surface and depth samples. The TN values are most consistent, but the carbon values and the differences between surface and depth C/N ratios are highly variable, as variances are often much larger than the mean.

Table 3.1. Main descriptive statistics are shown for Nitrogen (N), Total Carbon (TC), Organic Carbon (OC), Inorganic Carbon (IC) and C/N ratio in surface and depth samples.

	N (%) Surface	N (%) Depth	TC (%) Surface	TC (%) Depth	OC (%) Surface	OC (%) Depth	IC (%) Surface	IC (%) Depth	C/N Surface	C/N Depth
Mean	0.25	0.21	2.23	1.88	1.69	1.43	0.54	0.46	6.69	6.90
Variance	0.0042	0.0023	0.43	0.26	0.29	0.15	0.05	0.029	0.90	1.65
Skewness	-0.58	-1.29	0.60	1.29	0.25	0.64	5.35	2.83	3.16	4.41
C. level (95%)	0.01	0.01	0.14	0.11	0.12	0.08	0.05	0.04	0.20	0.27
Min	0.05	0.04	0.64	0.39	0.35	0.24	0.22	0.09	4.08	4.84
Max	0.43	0.32	4.38	4.61	3.24	3.33	2.29	1.33	12.68	14.15
n	87	87	87	87	86	87	86	87	86	87

Table 3.2. Mean difference in surface and depth samples of the results in Nitrogen (N), Carbon (C), Organic Carbon (OC), Inorganic Carbon (IC) and C/N.

	N (%)	C (%)	OC (%)	IC (%)	C/N
Mean Diference	0.043	0.35	0.27	0.070	-0.21
Variance	0.0059	0.51	0.30	0.086	0.93

The box plots shown in Figure 3.1 show the distributions of concentrations of C, N and OC, in addition to the calculated values of inorganic carbon and C/N Ratio (C/N = OC/N). In all cases, median values are similar to the mean values (Table 3.1) indicating influence of outliers was limited. For surface samples, the median values of N, C and OC are 0.25%, 2.15% and 1.65%, respectively, while the median concentrations of the depth samples are smaller for each variable: 0.21%, 1.91% and 1.48% in N, C and OC, respectively. The median IC values are 0.49% in surface samples and 0.44% in depth samples. Finally, the C/N ratio is similar at both depths: 6.5% in surface and 6.6 in depth.

The concentration values in mangrove tissues are displayed in the Figure 3.2 (n = 35); these values include samples of leaves, branches, trunks and pneumatophores. Nitrogen values are generally low but nonetheless show larger concentrations than for the sediment samples (median value 1.07%), carbon concentrations are large (median is 43.25%), while the median C/N ratio for these mangrove samples is 39.93.

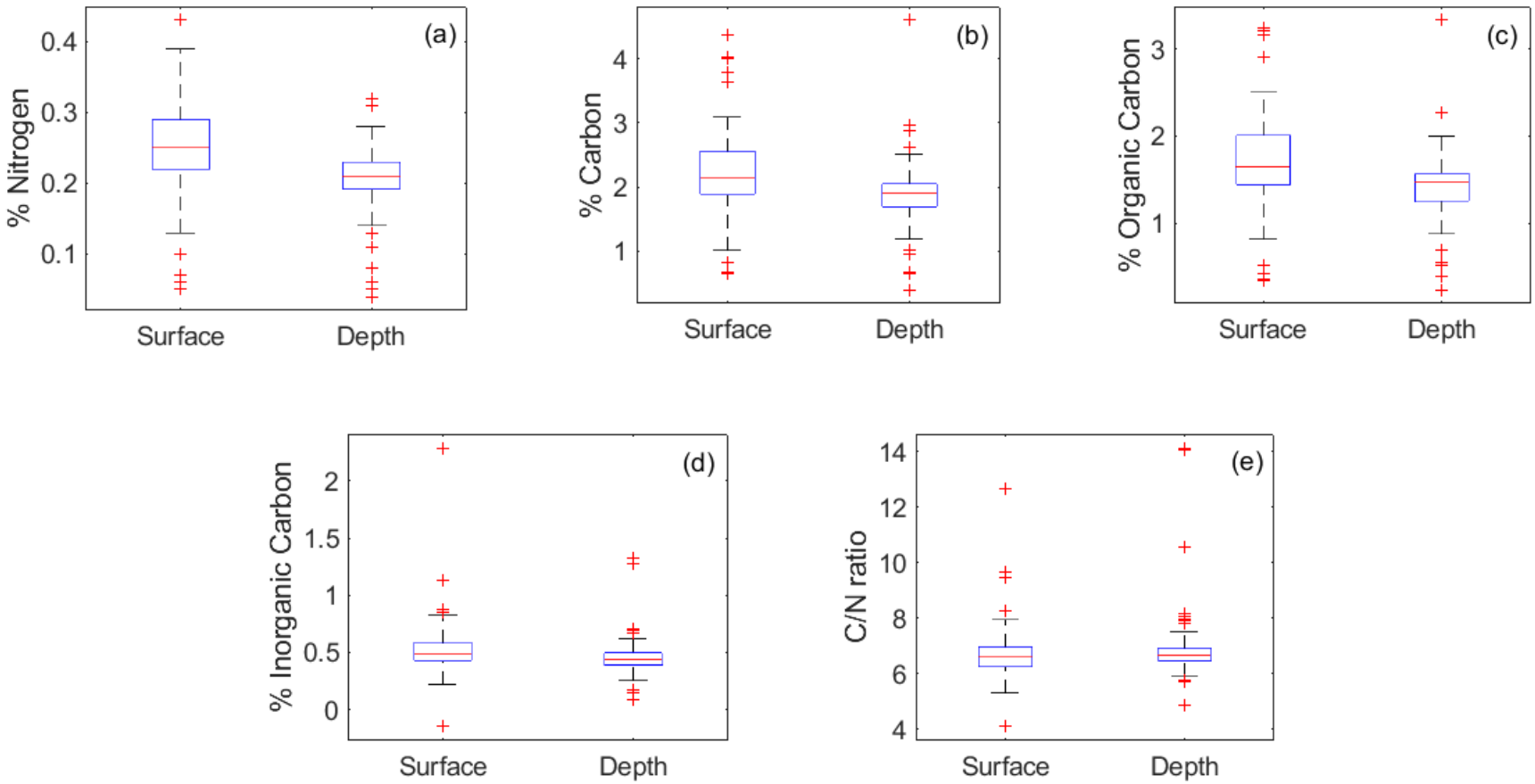

Figure 3.1. Box plots of Nitrogen (a), Carbon (b), Organic Carbon (c) and Total Inorganic Carbon (d) concentration plus C/N ratio (e) in sediment samples of the Firth of Thames. The boxes edges represent 25th and 75th percentiles and the horizontal red line indicates the median value. Whiskers show the full range of the data (excluding outliers, which are plotted as red crosses).

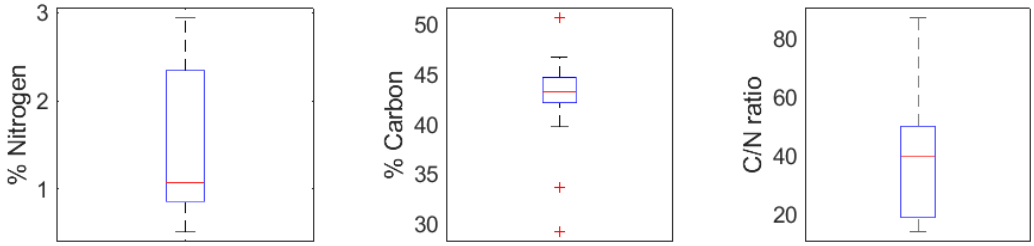

Figure 3.2. Boxplot of C concentration (a), N concentration (b) and C/N Ration in vegetation samples**.** The boxes edges represent 25th and 75th percentiles and the horizonal red line indicates the median value. Whiskers show the full range of the data (excluding outliers, which are plotted as red crosses).

3.2.2 Spatial distribution of nitrogen concentrations

Concentrations of N did not exhibit strong variability in either surface or depth samples (Figure 3.3). Values ranged from ~0.05 to 0.5% across all surface samples. Despite some scatter, the N content of surface samples, increases towards the forest interior (observed in 10 out of 12 of the cross-shore transects, Figure 3.3a). In general, the largest observed values were closer to the Piako River (transects G to J) towards the rear of the forest. Concentrations further out into the Firth were smaller with a cluster of low values at, and to the west of, the Piako River mouth. Concentrations were in general slightly smaller at depth (Figure 3.3b). In contrast to the surface distribution, the N percentages at depth do not show any clear trend. The range of variability in the depth samples for nitrogen is less broad than on the surface, and the values are concentrated around 0.2% and 0.3%. The largest N concentration is seen at the mouth of the Waihou River and transect G. On the other hand, the lowest values of N are observed in the northern part of transect A and at the Waihou River's bank (near Kopu). There was no relationship for the Nitrogen concentration in the surface and depth samples (r^2=0.009, p-val=0.379, Figure 3.4).

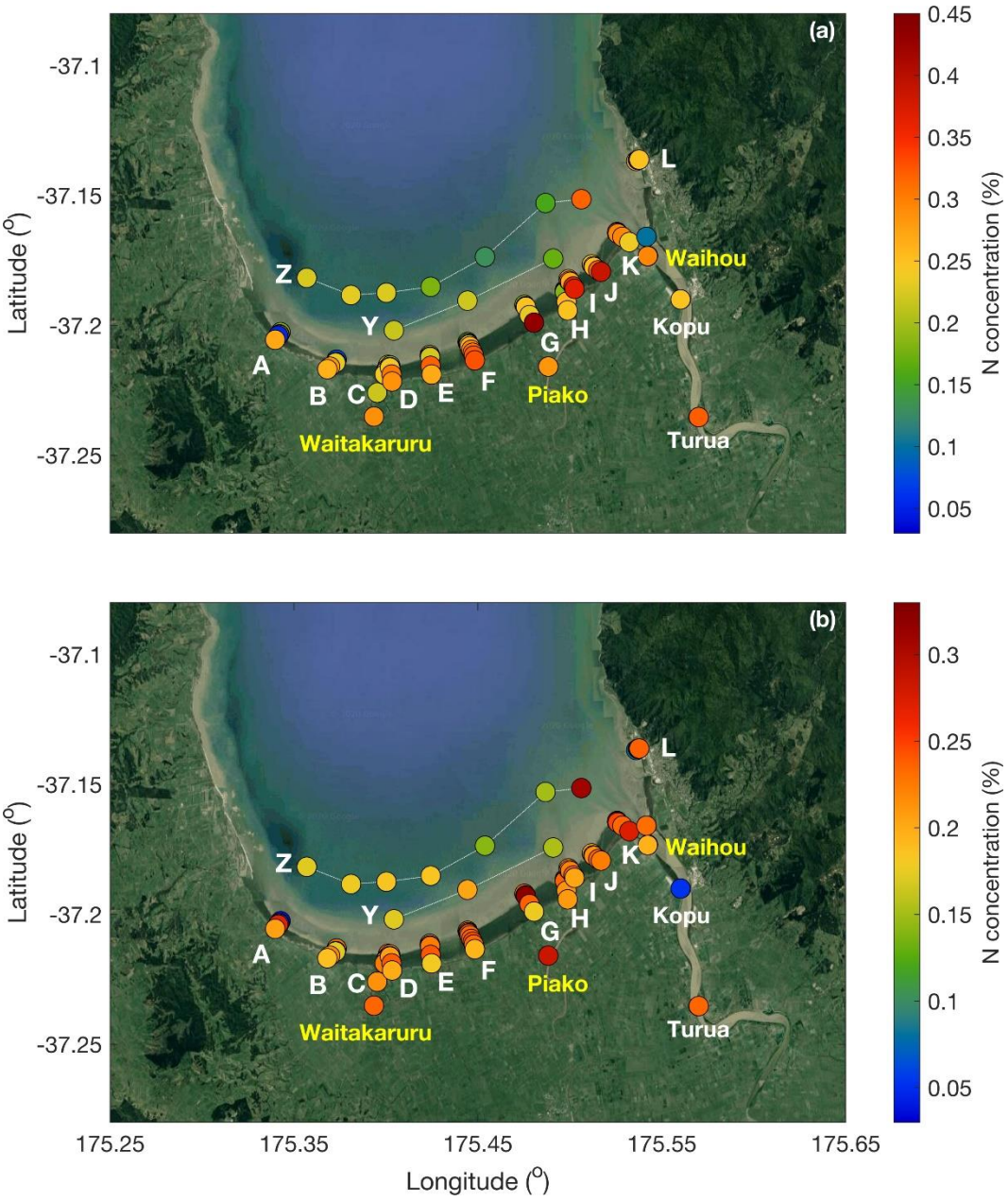

Figure 3.3. Spatial distribution of Nitrogen in surface (a) and depth (b) in sediment samples, Firth of Thames. Note the change in colour scale between (a) and (b).

To examine the distributions of N in the across-shore, we defined the sample 2 in the fringe as the origin for each transect and plotted concentrations as a function of distance, noting distances landward (into the forest) are positive distance and locations on the mudflat correspond to negative distances (Figure 3.5).

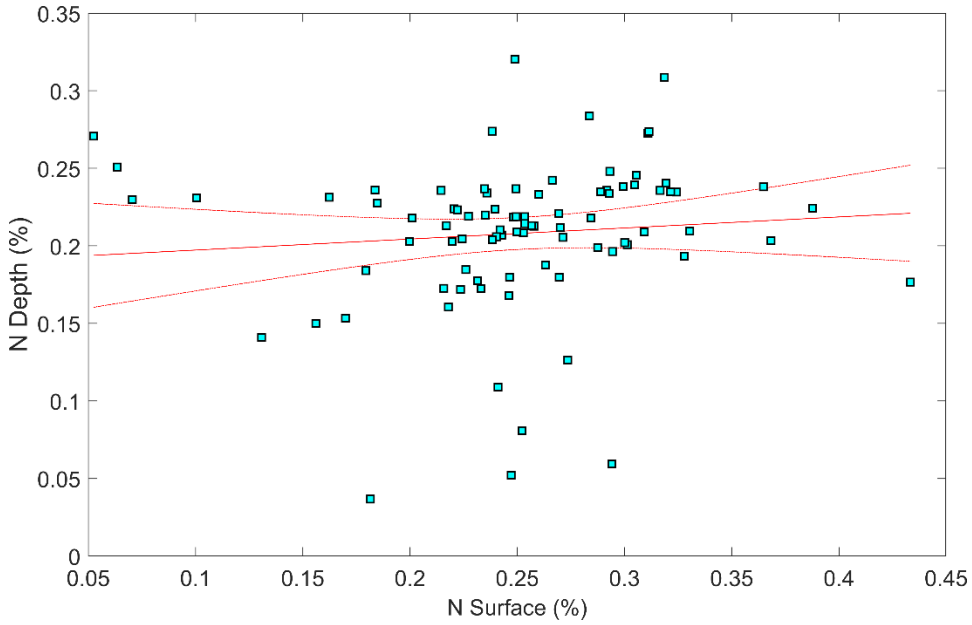

Figure 3.4. Relationship between Nitrogen content in surface and depth samples. The solid lines represent fitted linear regression lines and the dashed lines show 95% confidence intervals. r^2=0.0091, p-val=0.38

Figure 3.5. Representation of an across-shore transect. Distance is measured from station 2 defined as the origin) at the forest fringe.

Figure 3.6 shows the relationship between Nitrogen and the distance of the 12 across-shore transects in the FoT. A slight increase in the Nitrogen content with across-shore distance is notable in the surface samples (Figure 3.6a), while, despite some scatter, the depth samples tend to have more constant values (Figure 3.6b). The C, H and K transects, which were sampled on the riverbanks, show approximately constant values in surface and depth samples. In general, patterns are inversely related between surface and depth, that is, increases in content at the surface correspond to decreases in N content at depth. An exception to this is

transect L, where the same across-shore trends are observed at both surface and depth.

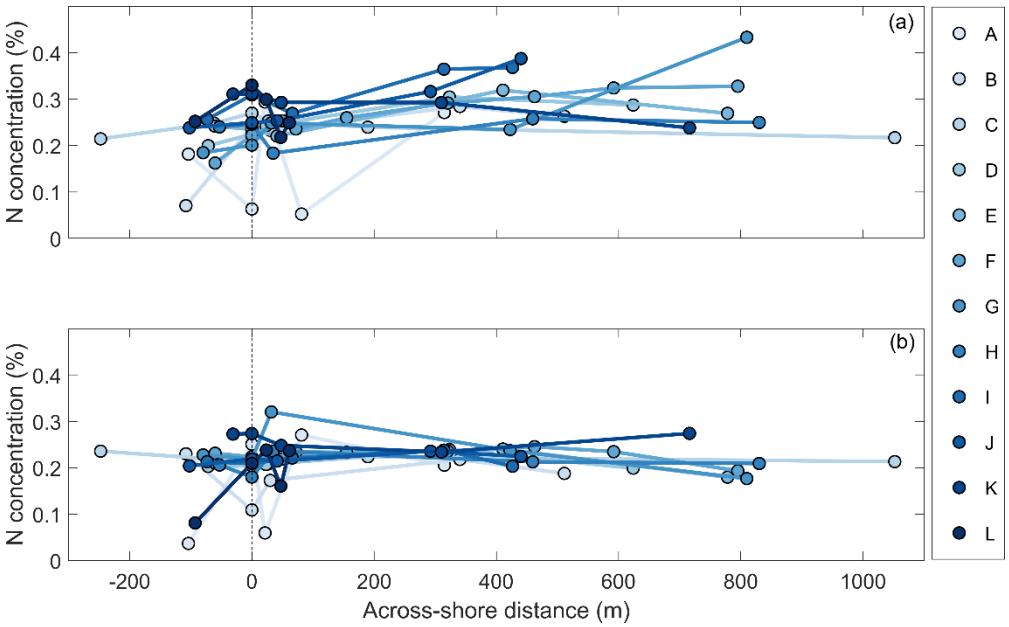

Figure 3.6. Relationship between distance within the across-shore transects and Nitrogen concentration in surface (a) and depth (b) samples. Colours represent different transects.

To test if rivers are a potential source of TN in the sediments, the N content in surface samples was plotted against the longitudinal distance to rivers (Figure 3.7). Distances from the Waihou River were compared to results from all the transects. The Piako River was analysed with transects F, G, H, I and J plus stations Y2, Y3, Z4, Z5, Z6. Finally, Waitakaruru River distances were plotted against N concentrations from the western stations Z1, Z2, Z3, Y1 and Y2, plus those from transects A, B, C, D and E.

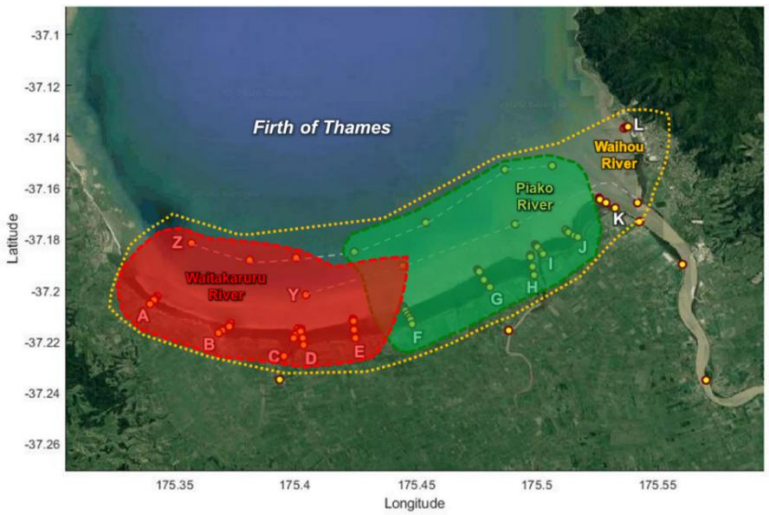

Figure 3.7. Map showing areas used to examine the influence of the rivers: Waihou (area with dotted orange line), Piako (green polygon) and Waitakaruru (red polygon).

Results are shown in Figure 3.8: Nitrogen concentration did not exhibit any clear trends when compared against the proximity of sampling sites to the rivers, neither when all data was considered together nor when grouped by across-transect positions (different symbols in Figure 3.8).

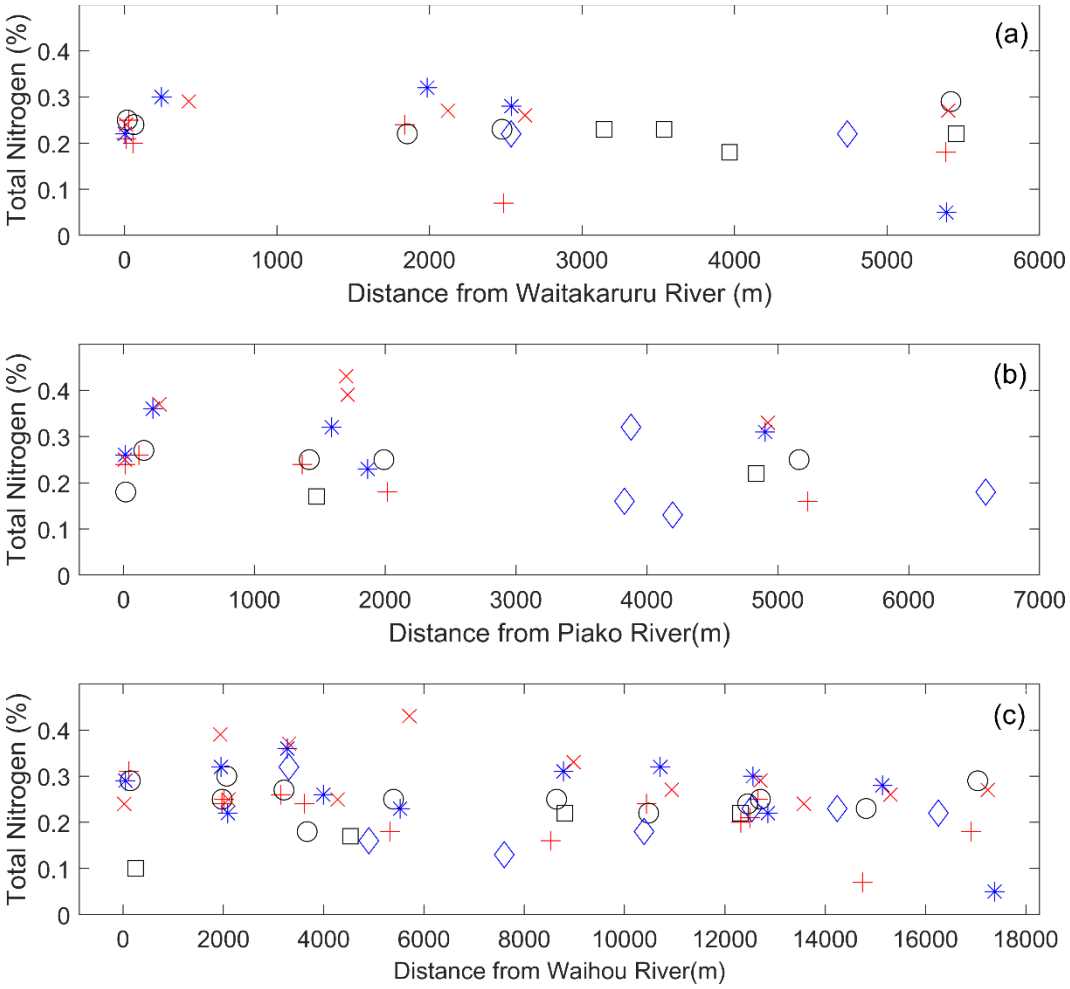

Figure 3.8. Relationship between distance from each main river in the FoT and the concentration of Nitrogen in surface samples. The areas plotted correspond to Outer mudflat (red plus signs), Middle mudflat (black circles), Inner mudflat (blue asterisks), Forest fringe (red crosses), Middle Forest (black squares) and Deep forest (blue diamonds).

3.2.3 Spatial distribution of carbon concentrations

For total carbon in surface samples (Figure 3.9a), the most notable pattern is a higher concentration in the mangrove forest in relation to the mudflat. In 11 of the 12 cross-shore transects, an increase in TC with distance landward is seen. The highest values of TC are in transects *G*, *I*, *J*, and *N*, while the lowest values were found in front of the Piako River mouth and towards the mudflat zone of transects *A* and *B*. For the depth samples (Figure 3.9b), a lower concentration of Carbon is observed, with values ranging from ~ 0.6 to 3%. In the vicinity of the Waihou River

a relatively higher concentration is observed compared to the western side of the Firth (transects A to F). The lowest values occurred in the mudflat of transects A and L, in addition to stations near Kopu. In transects *B*, *D*, *E*, *F* and *G*, the TC concentration decreases towards the forest interior. The mudflat in front of the mouth of the Piako River also has relatively low concentrations of TC. In Figure 3.10 the surface concentrations are plotted against concentrations at depth, and a linear fit reveals no correlation for these data (r^2= 0.0724, p-val= 0.0118).

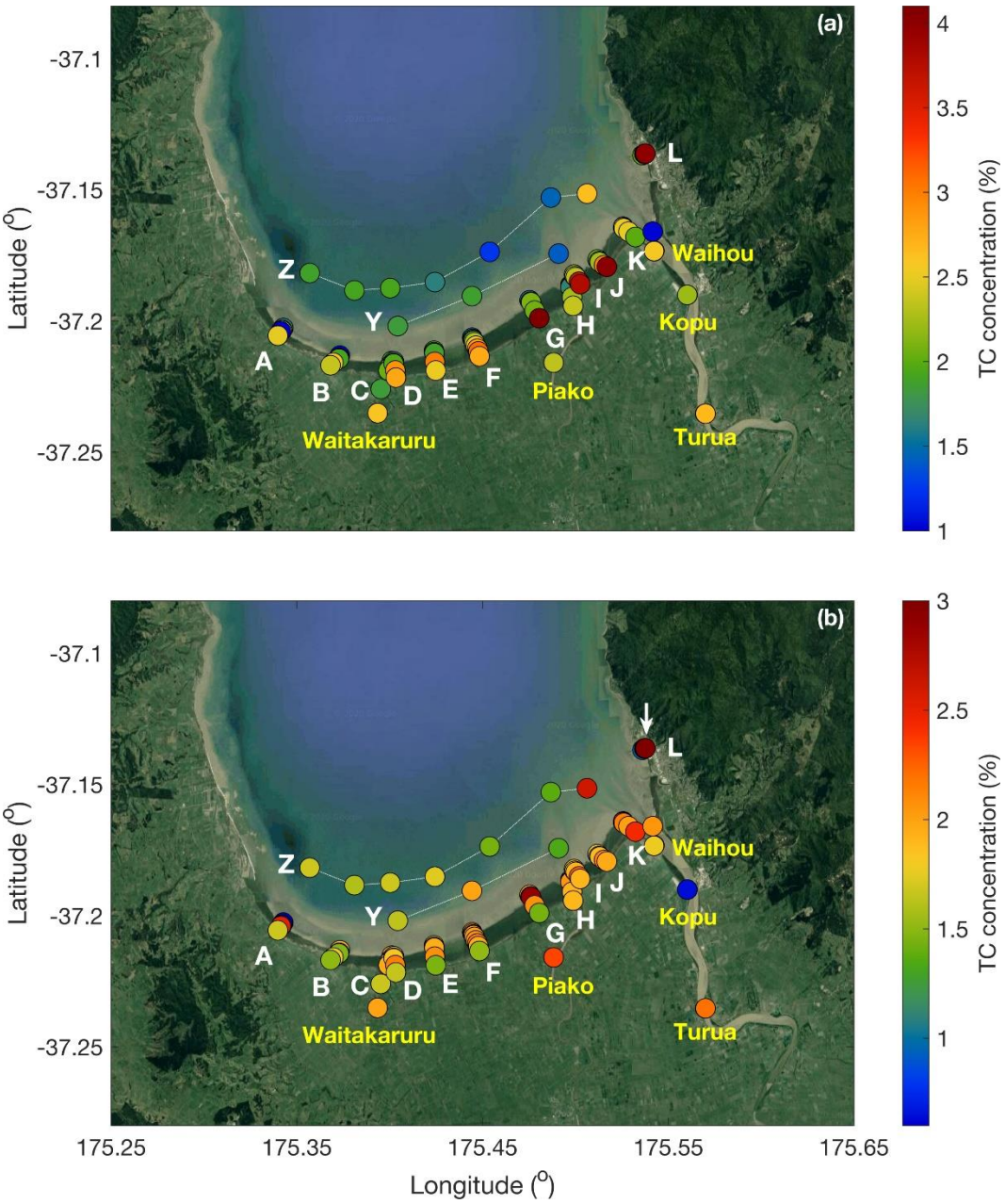

Figure 3.9. Spatial distribution of Total Carbon in surface (a) and depth (b) in sediment samples, Firth of Thames. Note the change in colour scale between (a) and (b). The white arrow in panel (b) indicates an outlier in station L5 which recorded a extreme high value of TC = 4.61%.

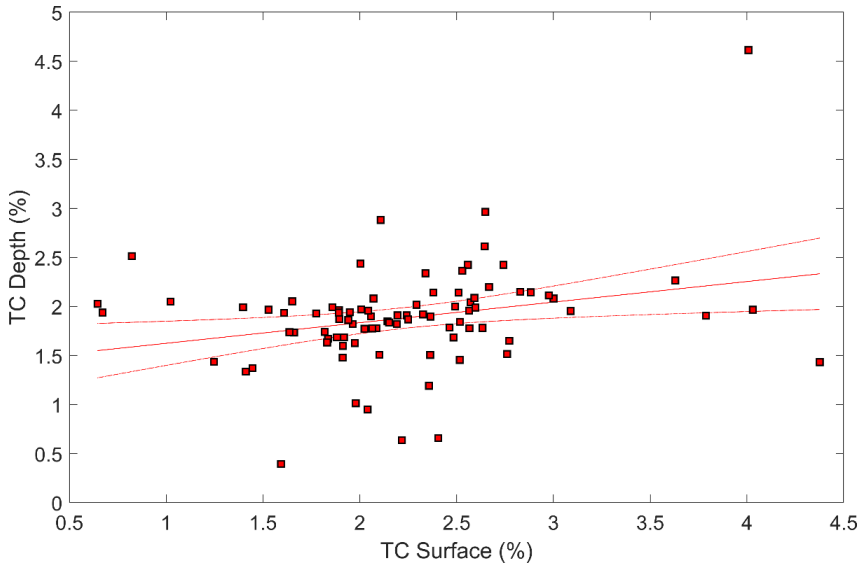

Figure 3.10. Relationship between Total Carbon content in surface and depth samples. The solid line is the fitted linear regression line and dashed lines show 95% C.I.s. r^2=0.072, p-val=0.012

The relationship between TC and the distance between each transect exhibited similar trends to those observed for Nitrogen content (Figure 3.11). In surface samples, an increase of TC percentage with distance is observed in most across-shore transects, however, transects C, H, and L show little cross-shore variation. The most pronounced increase in content is observed in the L transect both in surface and depth. On the other hand, results from depth samples reveal there is a slight decrease in the concentration of C landwards.

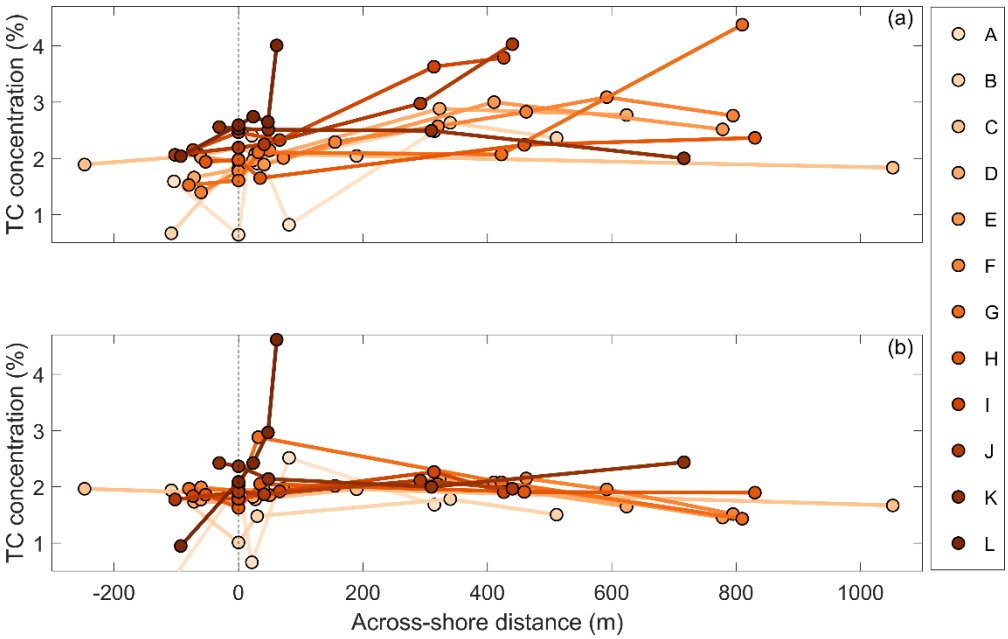

Figure 3.11. Relationship between distance within across-shore transects and Total Carbon concentration in surface (a) and depth (b) samples. Colours show different transects.

The concentration of total carbon was also compared to the distance from the three FoT rivers (as shown in Figure 3.7). As with Nitrogen concentrations, no significant correlations with distances (either positive or negative) were obtained and the distribution of the values appeared to be quite irregular.

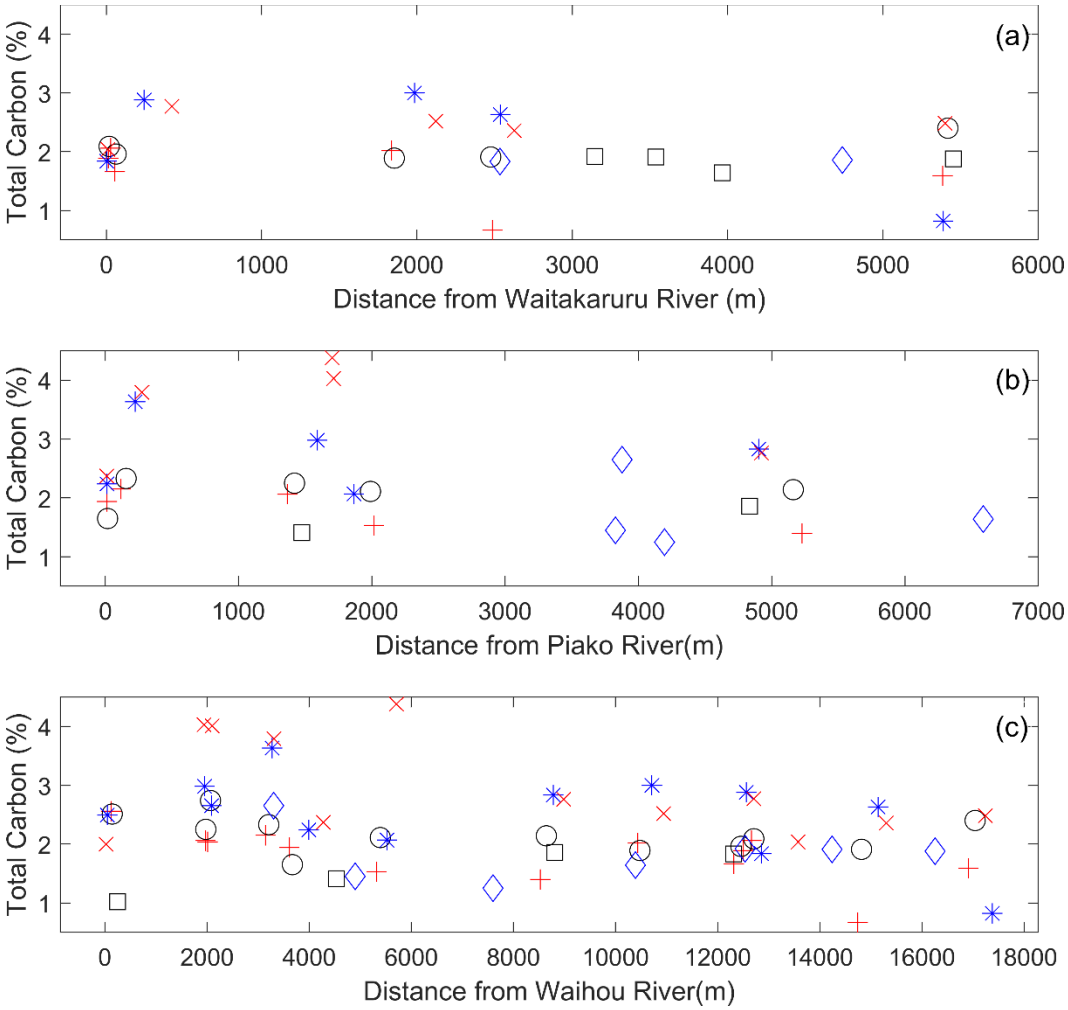

Figure 3.12. Relationship between distance from each main river in the FoT and the concentration of Total Carbon in surface samples. The areas plotted correspond to Outer mudflat (red plus signs), Middle mudflat (black circles), Inner mudflat (blue asterisks), Forest fringe (red crosses), Middle Forest (black squares) and Deep forest (blue diamonds).

3.2.4 Spatial distribution of organic carbon

As with total carbon, there is a larger concentration of organic carbon in the forest compared to mudflat and a broader range of values in surface compared to depth samples (Figure 3.13). In 10 of the 12 transects, the concentration increased landward. The G, I, J and N transects show the largest extreme values in OC while the A, B and G transects show the lowest values (Figure 3.13a). The distribution of OC within the forest is irregular in depth samples. The transects at the west side of

the Waihou River show similar concentrations (~1.6%), while very low values are found in the mouth of Waihou River and in transects A and G. A weak but significant correlation between surface and depth samples was found for Organic Carbon (r^2= 0.109, p-val= 0.0019, Figure 3.14).

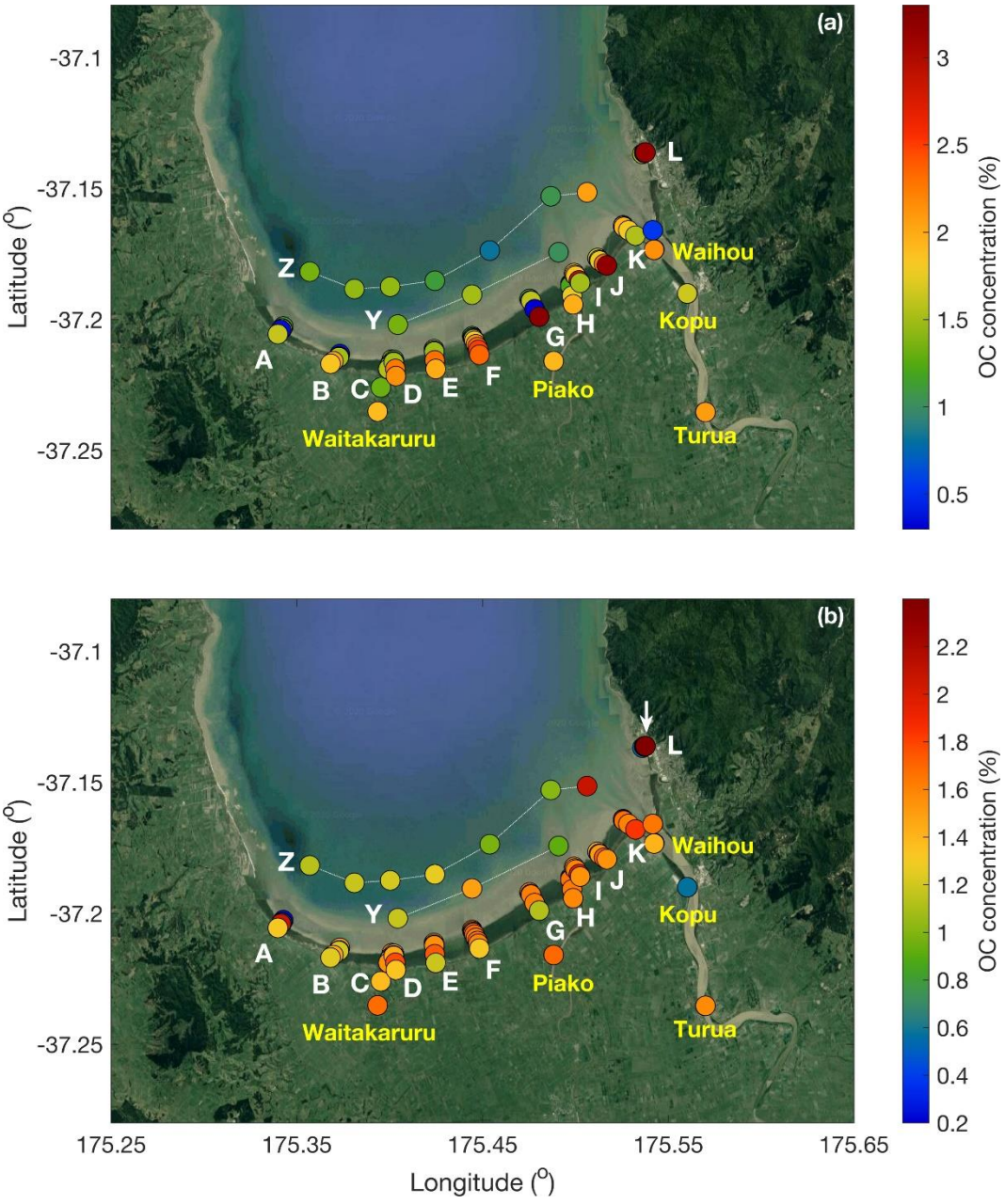

Figure 3.13. Spatial distribution of Organic Carbon in surface (a) and depth (b) in sediment samples, Firth of Thames. Note the change in colour scale between (a) and (b). The white arrow in panel (b) indicates an outlier in station L5 which recorded an extreme high value of TC = 3.33%.

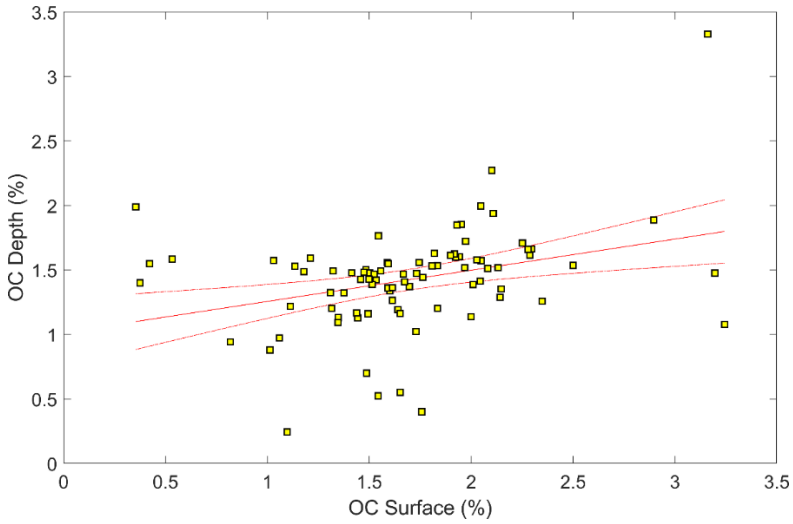

Figure 3.14. Relationship between Organic Carbon content in surface and depth samples. The solid line shows the linear fitted regression line and dashed lines show 95% C.I. r^2=0.11, p-val=0.0019.

The concentration of organic carbon is compared to the across-transect distance into the forest in Figure 3.15. Since much of the total carbon is from an organic source, the plots in Figure 3.11 (TC) and 3.15 follow similar patterns. Transects B, C, E, F, G, H, J and K, show an increase in OC with the distance for the surface samples. The most constant values continue to be in the transects C, H and K near the rivers in surface samples. The steep gradient in TC in the L transect is also reflected in the OC content. Although a decrease in OC towards the forest is not clearly observed in the distribution map, Figure 3.15b indicates that there is a slight reduction of this element with increasing distance.

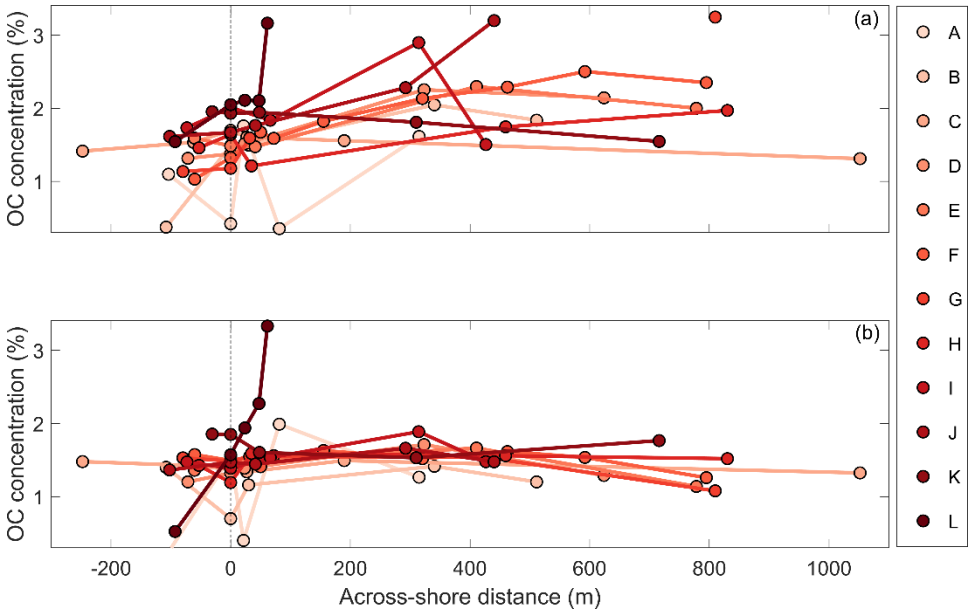

Figure 3.15. Relation between distance within across-shore transects and Organic Carbon concentration in surface (a) and depth (b) samples. Colours show different transects.

As with the other elements, there appeared to be little correlation between distance from the rivers and organic carbon concentrations.

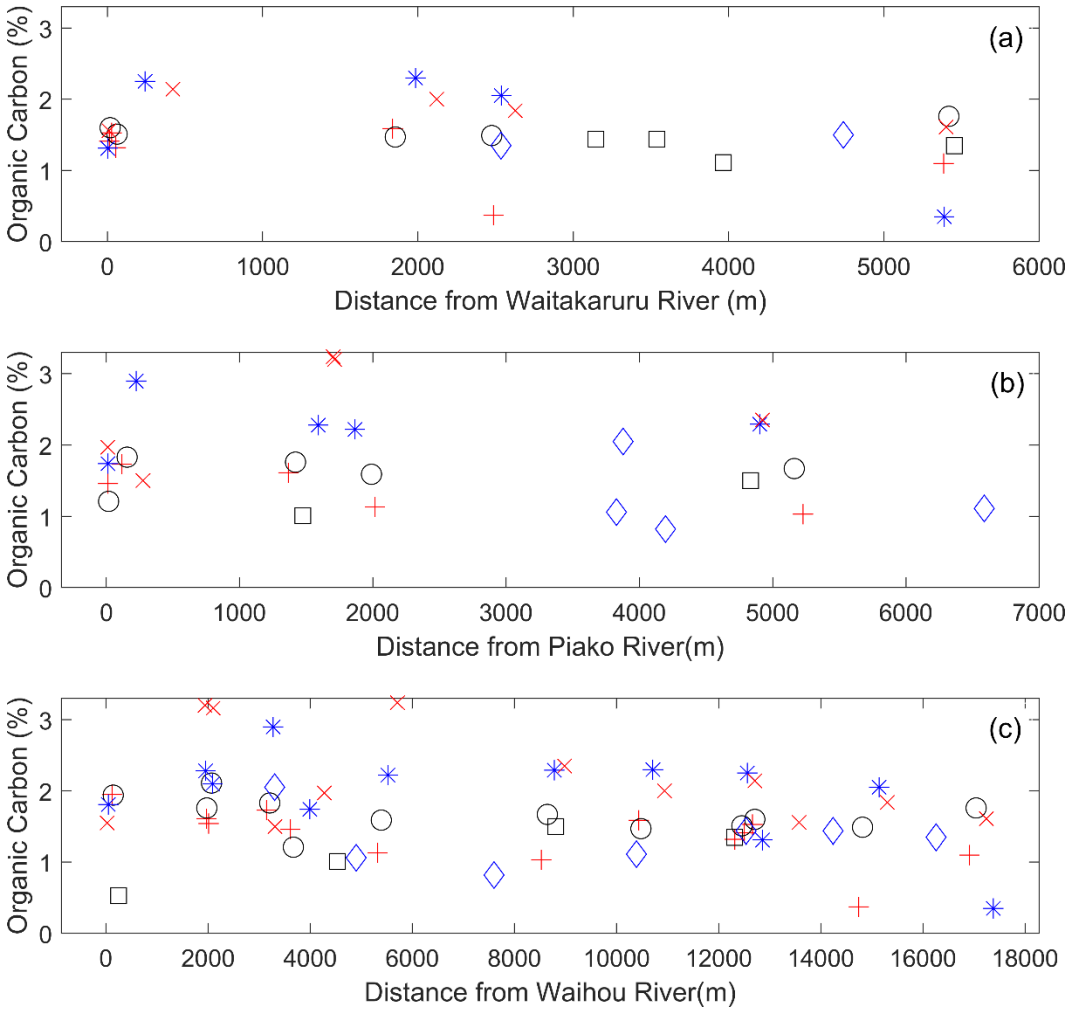

Figure 3.16. Relationship between distance from each main river in the FoT and the concentration of Total Carbon in surface samples. The areas plotted correspond to Outer mudflat (red plus signs), Middle mudflat (black circles), Inner mudflat (blue asterisks), Forest fringe (red crosses), Middle Forest (black squares) and Deep forest (blue diamonds).

3.2.5 Spatial distribution of inorganic carbon concentrations

The bulk of the samples show concentrations below 1% for inorganic carbon (Figure 3.17). In surface samples, an irregular distribution is seen (Figure 3.17a) with the largest values towards the southernmost stations of the cross-shore transects A G, I, J and L. On the other hand, in the depth samples (Figure 3.17b) the IC concentration is slightly higher in the mudflat relative to the mangrove forest. In 7 of the 12 cross-shore transects, a decrease in IC is visible landwards.

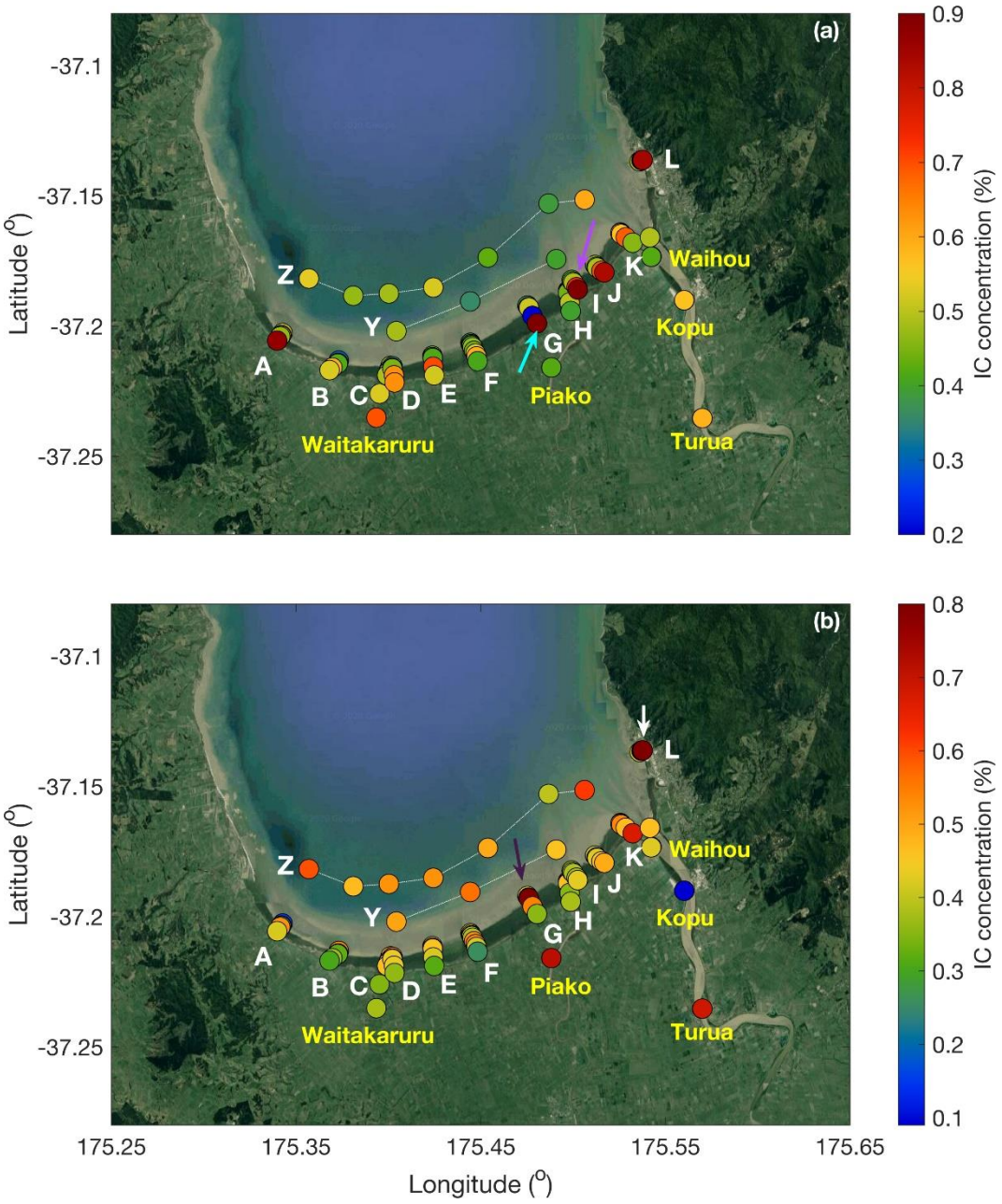

Figure 3.17. Spatial distribution of Inorganic Carbon in surface (a) and depth (b) in sediment samples, Firth of Thames. Note the change in colour scale between (a) and (b). The arrows indicate outliers in stations H5 surface =2.29% (purple), G5 surface =1.13% (cyan), G3 depth= 1.33% (dark purple) and L5 depth = 1.28 (white).

The correlation coefficient for the concentrations of surface and depth samples was the lowest recorded ($r^{2=}$ 0.00024, p-val = 0.887), thus no relationship exists (Figure 3.18). Unlike the other elements examined, concentrations of Inorganic Carbon do not show any clear trend with position in the forest, neither in surface nor in depth samples (Figure 3.19).

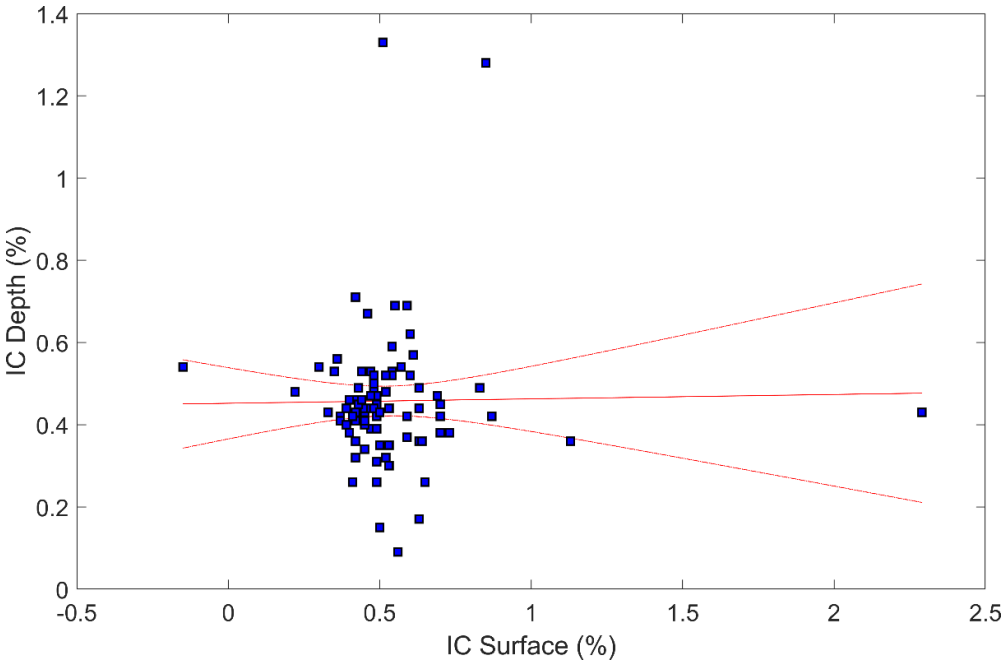

Figure 3.18. Relationship between Inorganic Carbon content in surface and depth samples. The solid lines represent fitted regression lines and dashed lines 95% C.I. . r^2=0.00024, p-val=0.89.

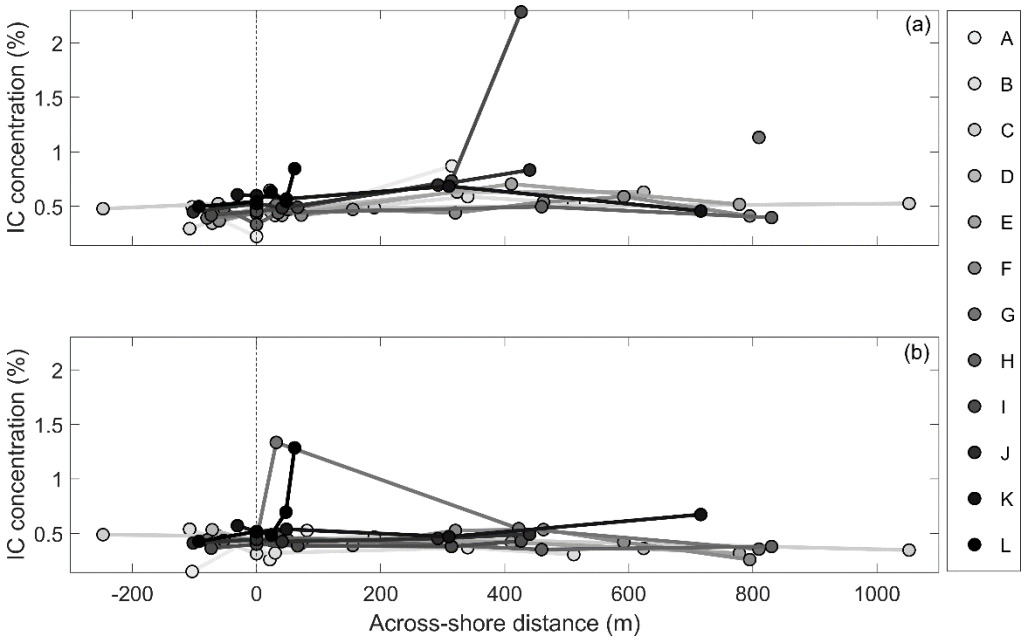

Figure 3.19 Relationship between distance within across-shore transects and Inorganic Carbon concentration in surface (a) and depth (b) samples. Colours show different transects.

3.2.6 Relationship between elements

There is no overall correlation between C and N content of the vegetation samples (Figure 3.20). In general N content is slightly larger in leaves (N> 2%), than woody sections (branches, pneumatphores and trunks), which have overlapping values. Similarly, the C concentration does not vary significantly between the different tree sections: 94.3% of the samples show C values between 40% and 50.6%.

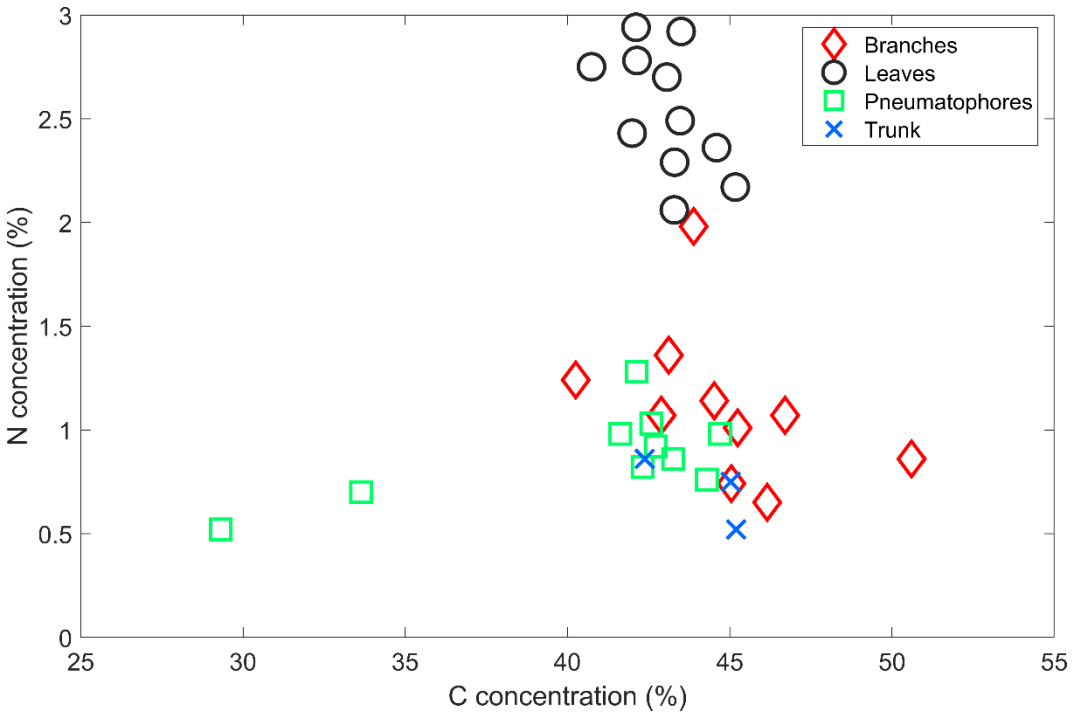

Figure 3.20. Carbon and Nitrogen concentrations in stems (red diamonds), leaves (black circles), pneumatophores (green squares) and trunks (blue crosses) of mangrove samples in the Firth of Thames.

3.2.7 Elemental along-shore distributions

To summarise the broad patterns in the distributions of elements, we group the stations into eight along-shore transects (Figure 3.21). The transects in the outer mudflat Y and Z remain the same and are denoted groups 1 and 2, respectively. The other samples were classified into groups based on cross-shore position; giving 5 groups throughout the mangrove forest and inner mudflat. The river stations were grouped in the southernmost transect called group 8.

Figure 3.21. Map showing the stations grouped from 1 (red) in the northern zone of FoT and 8 for southern locations (pink).

The data is presented in boxplots of surface and depth samples for the different groups (Figure 3.22), this graph summarizes the distribution pattern of elements across the Firth. The surface samples for N, TC and OC show a definite increase in concentration from group 1 in the north to group 7 in the south or deep forest (Figure 3.22a, c and e). The lowest values occur in group 2 for N, C and OC. The river stations show a slight decrease compared to the back of the forest in these same elements (group 8). In inorganic carbon for surface samples a slight increase towards the rear forest is observed with concentrations close to 0.5% (Figure 3.22g).

However, the behaviour of N, TC and OC values in depth samples do not follow similar patterns (Figure 3.22b, d and f). The median percentage of N in groups 1 and 2 is the lowest. No trend is apparent for values from the other groups, with concentrations which vary between 0.2 and 0.25% (Figure 3.22b). The percentage of TC shows roughly consistent from north to south (Figure 3.22d), while OC shows a slight increase in the groups associated with mangroves (groups 4 to 8). In the depth samples, the IC decreases from north to south (Figure 3.22h).

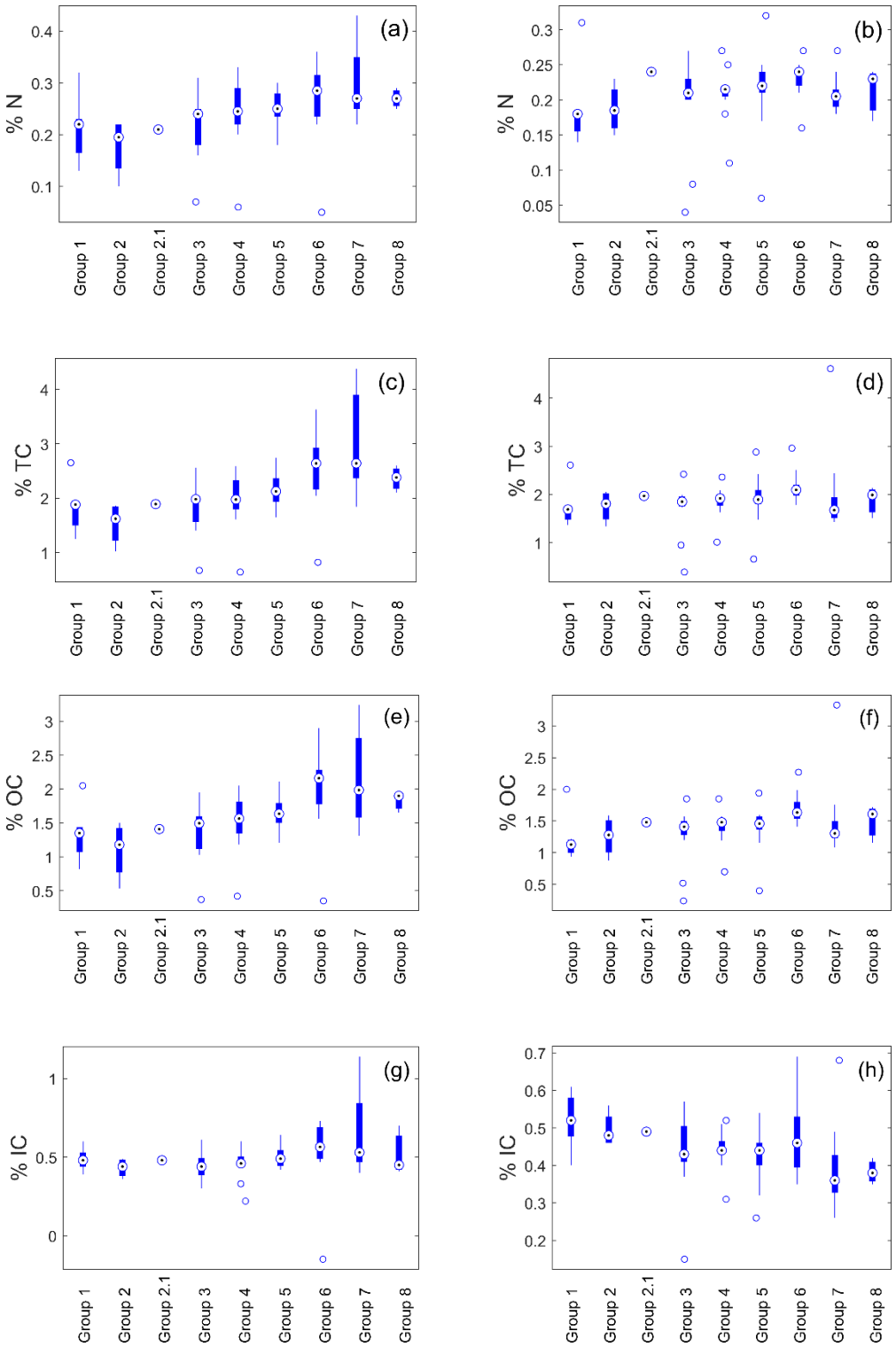

Figure 3.22. Along-shore groups boxplots. Nitrogen in surface (a) and depth (b), Total Carbon in surface (c) and depth samples (d). Organic Carbon in surface (e) and depth (f) and Inorganic Carbon in surface (g) and depth (h) samples. The boxes edges represent 25th and 75th percentiles and the black dot indicates the median value. Whiskers show the full range of the data (excluding outliers, which are plotted as blue circles.)

Figure 3.23 (a and b) shows a significant and strong positive linear relationship between N and OC content at both surface and depth with a stronger fit for the surface samples (r^2 = 0.786, p-val = $7.4x10^{-30}$) than the depth samples (r^2 = 0.583, p-val= $8.38x10^{-18}$). There are weak but still significant linear positive relationships between OC and IC, (Figure 3.22 c and d), with around 13 and 36 % of the variability in IC concentrations explained by the fit for surface and depth samples, respectively.

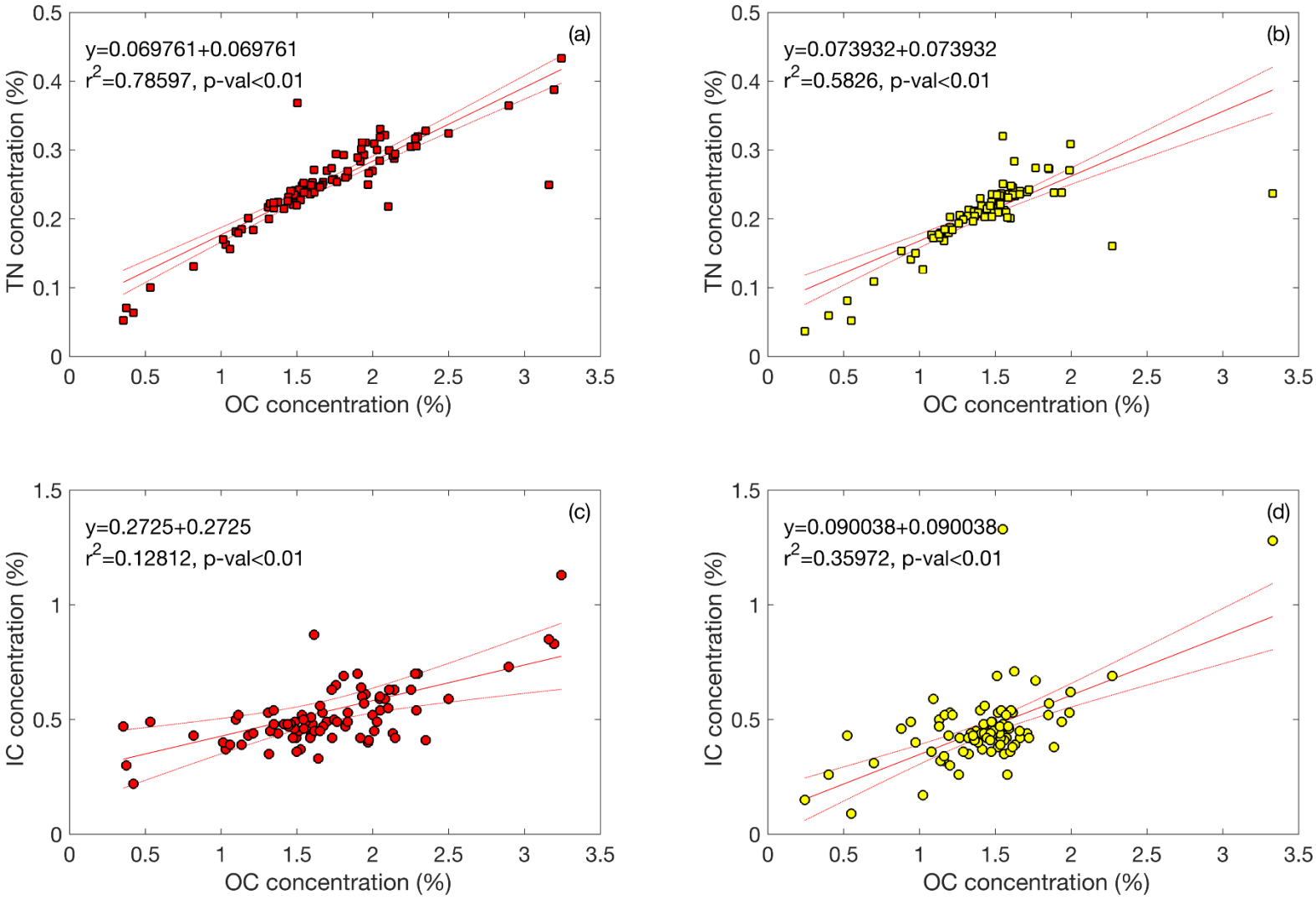

Figure 3.23. Relationships between Organic Carbon and Nitrogen in surface (a) and depth (b) samples and Organic Carbon vs Inorganic Carbon (c and d). The solid lines represent fitted regression lines and dashed lines 95% C.I. In panel (c), a single outlier at (1.5,2.3) has been cut off from the figure.

3.2.8 Depth profiles in cores

In the F across-shore transect towards the middle of the Firth, two cores were taken and sectioned into nine samples each to examine the element variations with depth in greater detail. The cores were extracted at station F3 in the fringe zone and station F7 in the middle of the forest (Figure 3.24).

Figure 3.24. Location of cores in the central transect F, Firth of Thames.

Figure 3.25 and Figure 3.26 show a similar profile for the curves of N, TC, and OC, with concentrations of these elements decreasing with depth (but not smoothly). These results show larger concentration of the elements in the middle forest compared with the samples extracted in the fringe zone. Also, for all elements the range of concentrations over depth is larger at site F7 than F3. N in the F3 site varies between 0.23 and 0.27%, while in F7 the values are between 0.24 and 0.33%. Similarly, the TC concentration is higher in position F7 compared to F3, where the average values are 2.70% and 2.11%, respectively. The OC range in the F3 core is 1.51-1.81%, and in core F7 it is 1.60-2.48%. The IC concentrations are much more variable with depth with no clear trend, in particular for the core F7.

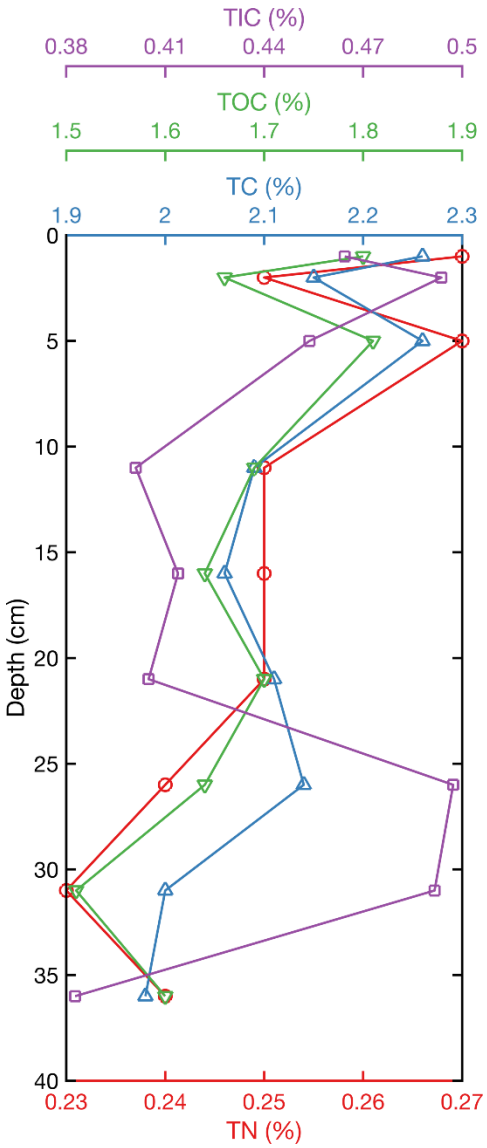

Figure 3.25. Depth profiles of concentrations of N, TC, OC and TIC core at location F3.

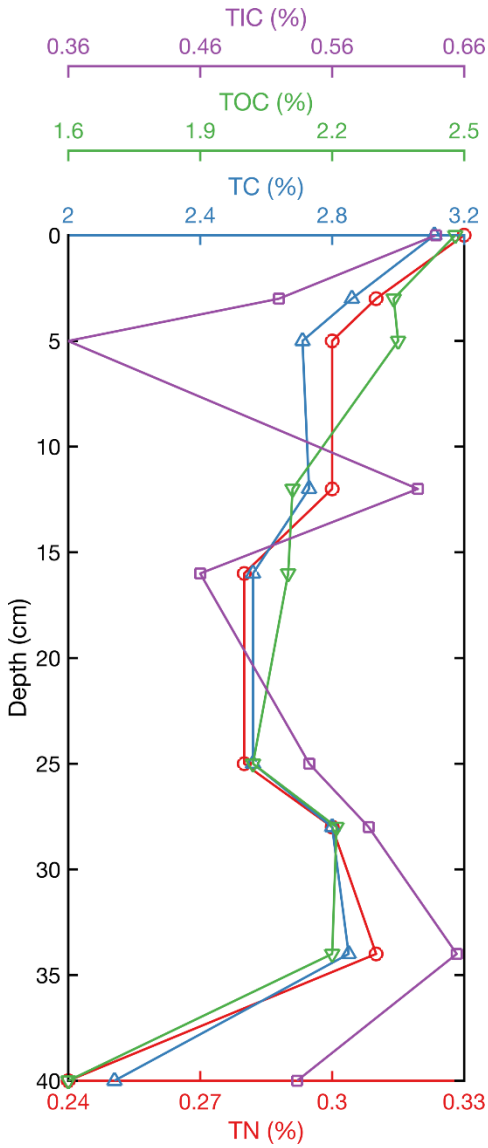

Figure 3.26 Depth profiles of concentrations of N, TC, OC and IC core at location F7.

3.3 Isotopic analysis

3.3.1 Summary statistics

The stable isotopic composition of sediments and mangrove samples is presented in this section (Table 3.3). The mean $\delta^{13}C$ values of the sediments are -23.04 ‰ and -22.98 ‰ in the surface and depth samples, respectively. The surface samples are slightly ^{15}N-enriched compared to depth samples. Three of four results of the isotopic sampling do not follow normal distributions as can be seen in the values of skewness. In the boxplot comparison (Figure 3.27), the median isotopic composition in sediment samples shows slight differences between surface and depth samples, (**Table 3.4**). The median $\delta^{13}C$ value for tree samples (-26.52 ‰) was isotopically lighter than that of the sediments (-23.04‰) (Figure 3.28). The median $\delta^{15}N$ composition of tree samples was 39.93‰ substantially different from the sediment value (8.27 ‰) (Figure 3.28). The values of $\delta^{15}N$ in the sediment exhibited a narrow range, compared to the vegetation samples which covered an interquartile range of ~30‰.

Table 3.3. Main descriptive statistics are shown for Isotopic results $\delta^{13}C$ and $\delta^{15}N$ for surface and depth samples.

	$\delta^{13}C$ (‰) Surface	**$\delta^{13}C$ (‰) Depth**	**$\delta^{15}N$ (‰) Surface**	**$\delta^{15}N$ (‰) Depth**
Mean	-23.04	-22.98	8.27	8.06
Variance	0.78	0.89	0.25	0.64
Skewness	-0.77	-2.19	-1.76	-3.57
Confidence level (95%)	0.19	0.20	0.11	0.17
Min	-26.36	-27.61	5.82	3.21
Max	-21.32	-21.25	9.10	9.21
n	86	87	87	87

Table 3.4. Mean difference in surface and depth samples of $\delta^{13}C$ and $\delta^{15}N$ values.

	$\delta^{13}C$ (‰)	**$\delta^{15}N$ (‰)**
Mean Diference	-0.065	0.205
Variance	0.852	0.359

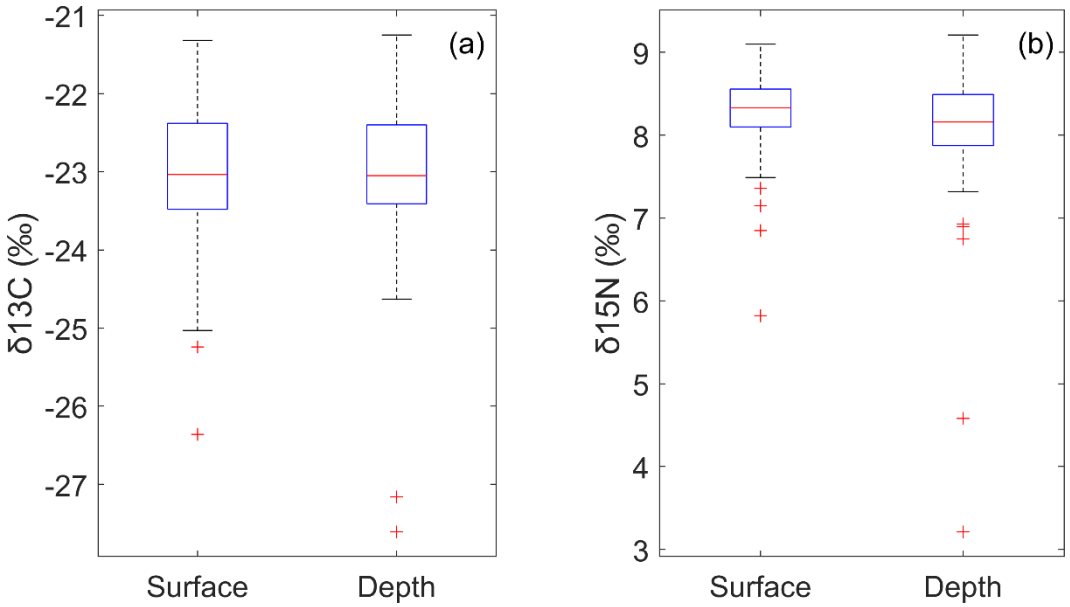

Figure 3.27. Boxplots showing $\delta^{13}C$ and $\delta^{15}N$ values in the sediment in surface (a) and depth samples (b). The boxes edges represent 25th and 75th percentiles and the horizonal red line indicates the median value. Whiskers show the full range of the data (excluding outliers, which are plotted as red crosses).

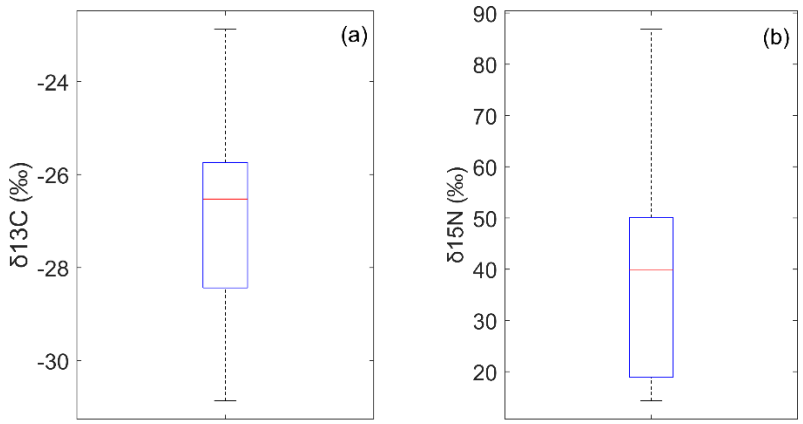

Figure 3.28. Boxplots of $\delta^{13}C$ and $\delta^{15}N$ values in mangrove tissues in the Firth of Thames. The boxes edges represent 25th and 75th percentiles and the horizonal red line indicates the median value. Whiskers show the full range of the data (excluding outliers, which are plotted as red crosses).

3.3.2 Spatial distribution of $\delta^{13}C$ and $\delta^{15}N$ isotopic compositions

The spatial distributions of carbon and nitrogen isotopic composition are shown in Figure 3.29 and Figure 3.30. One notable feature in the surface samples is that $\delta^{13}C$ is becomes more negative (isotopically lighter) with distance into the forest in all transects except I and K; additionally, a cluster of high $\delta^{13}C$ values in the outflow region of the Waitakaruru River is shown on the map (Figure 3.29a). The presence of two outliers in transect L (large negative values, Figure 3.27a) is noted. However, in the depth samples, no pronounced trend could be discerned with most profiles

remaining relatively flat or slightly increasing with distance along the full transect (Figure 3.29b). The west side of the Firth shows a slight $\delta^{13}C$-enrichment compared to the east section between the Piako and Waihou Rivers. Sediments within and around the entrance of the Waihou River tend to have ^{13}C-depleted samples. As with the surface results, there is an outlier in the L transect.

The distribution of $\delta^{15}N$ in surface samples is more uniform with values above 7.5 ‰ (Figure 3.30). In 8 of the 12 cross-shore transects, a landward ^{15}N-enrichment is shown for surface samples (Figure 3.30a). Low extreme values are located in transects A and L, and the larger values occur towards the centre of the Firth in transect F. The depth map for variations in the ^{15}N isotope does not show a clear pattern in spatial distribution (Figure 3.30b). The samples in the Waihou River have low values close to 7‰; the F transect represents the most ^{15}N-enriched zone in the Firth and extreme low values are recorded in the deep forest of the L transect.

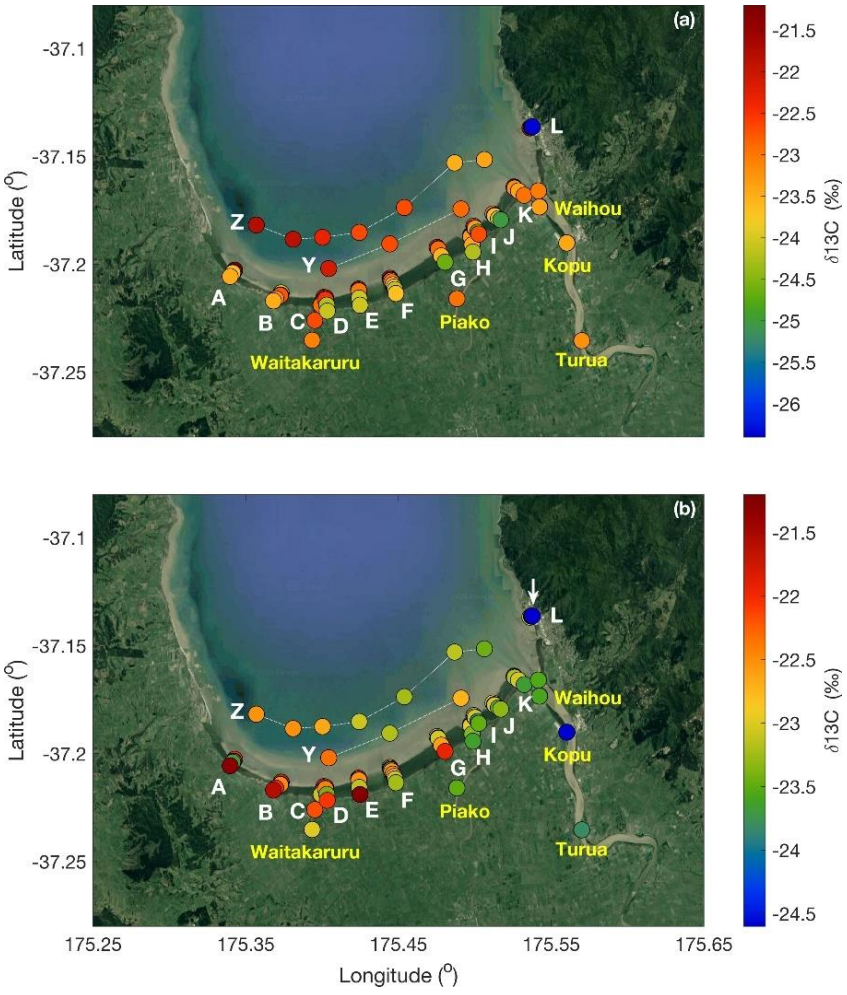

Figure 3.29. Spatial distribution of $\delta^{13}C$ in surface (a) and depth (b) in sediment samples, Firth of Thames. Note the change in colour scale between (a) and (b). The white arrows indicate outlier in stations L4 depth= -27.16‰ and L5 depth= -27.61‰.

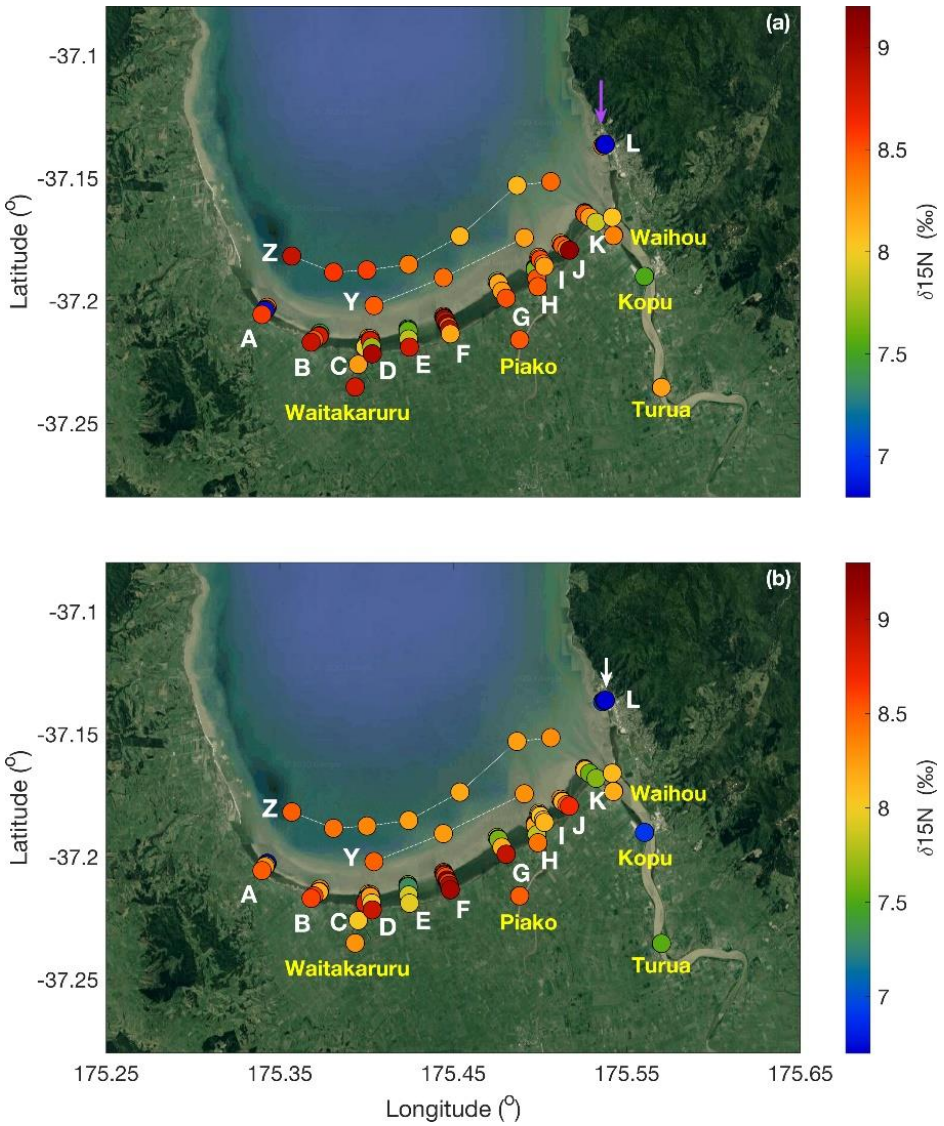

Figure 3.30. Spatial distribution of $\delta^{15}N$ in surface (a) and depth (b) in sediment samples, Firth of Thames. The arrows indicate outlier in stations L5 surface= 5.82‰ (purple), L4 depth= 4.58‰ and L5 depth= 3.21‰.

Figure 3.31 shows the relation between carbon isotopic composition in surface and depth samples: a weak but significant linear relationship is obtained (r^2=0.239, p-val=1.76x10^{-6}). In the same way, the $\delta^{15}N$ values show a significant relationship between sediments at the two different depths Figure 3.32 (r^2=0.442, p-val=2.17 x10^{-12})

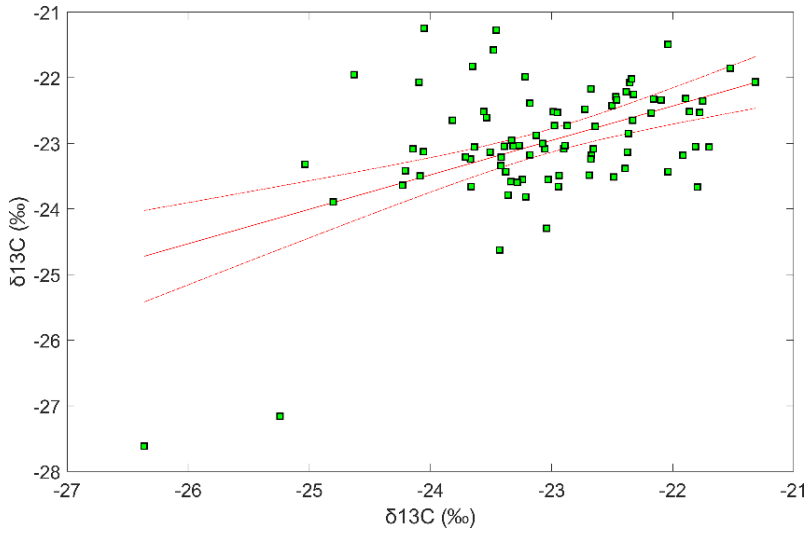

Figure 3.31. Relationship between $\delta^{13}C$ values in surface and depth samples. The solid line is the fitted linear regression line and dashed lines show 95% C.I.

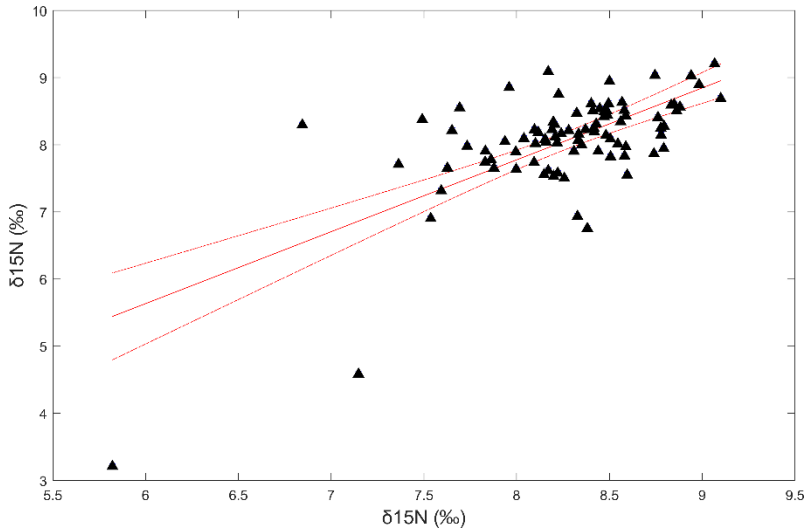

Figure 3.32. Relationship between $\delta^{15}N$ values in surface and depth samples. The solid line is the fitted linear regression line and dashed lines show 95% C.I.

The isotopic compositions were also contrasted with the distance from the forest fringe within across-shore transects. The $\delta^{13}C$ values have an evident enrichment towards the mudflat in 19 of the 24 curves (Figure 3.33). It is also notable that the highest data occurs near the fringe or zero point in most surface and depth samples. In the surface samples (Figure 3.33a), a ^{13}C depletion landwards is observed, while in depth samples (Figure 3.33b), low values are found towards the fringe zone, and then register a slight increase towards the forest rear. The most abrupt change in the Carbon isotope is observed in the L transect both in surface and depth.

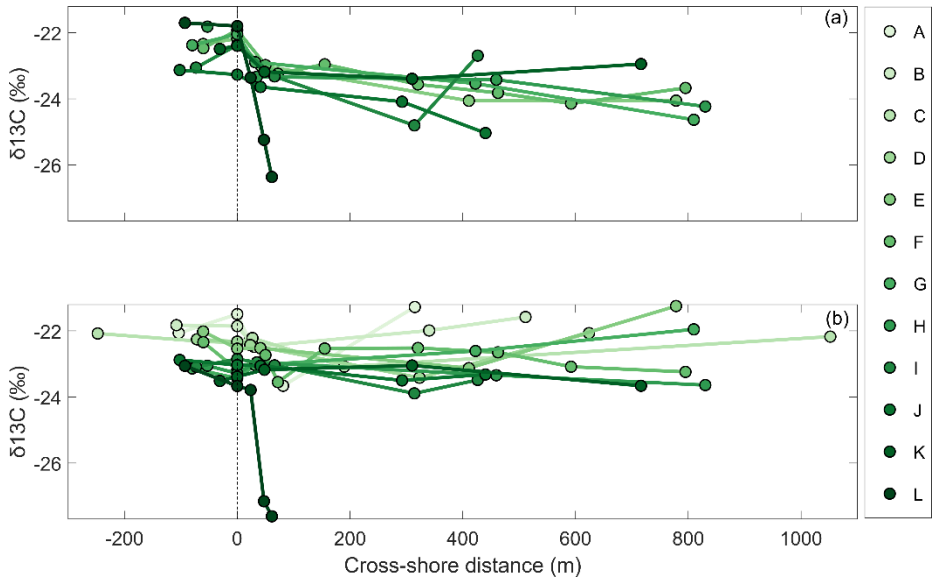

Figure 3.33. Relation between distance within across-shore transects and concentration $\delta^{13}C$ values in surface (a) and depth(b) samples. Colours show different transects.

Figure 3.34 shows the distance within each transect against the $\delta^{15}N$ value. A slight positive trend with distance is observed in 16 of the 24 curves. The transects C and K on the surface, plus the K in depth have stable values around 8%. The largest values are registered in the samples of the transect F towards the centre of the forest, which confirms the observations made using the map figures (Figure 3.30b). The isotopic signature of $\delta^{15}N$ drops quickly in the transect L at both depth levels.

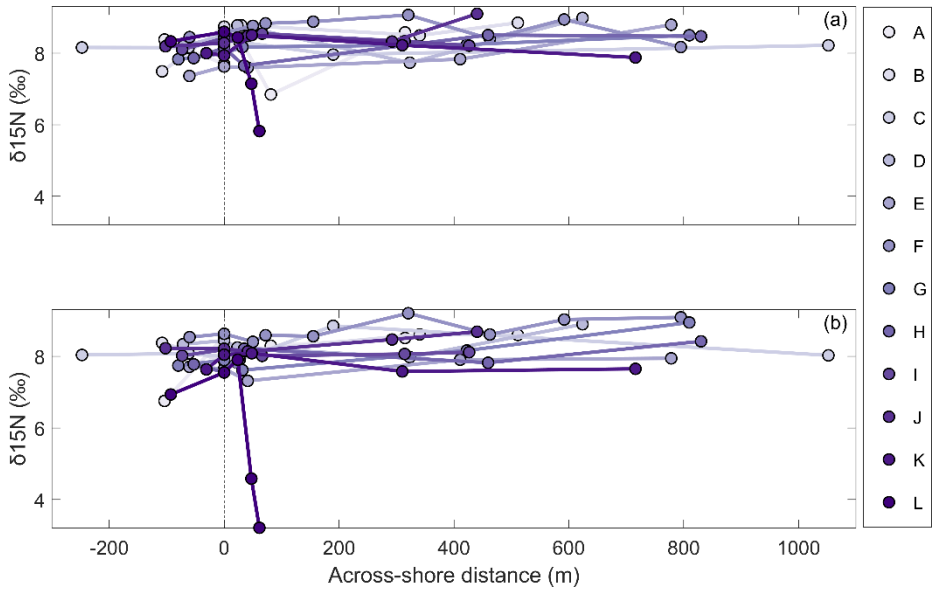

Figure 3.34. Relation between distance within across-shore transects and concentration $\delta^{13}C$ values in surface (a) and depth(b) samples. Colours show different transects.

3.3.3 Along-shore distributions of isotopic compositions

The pre-established along-shore transects (Figure 3.21) were also used to summarise the behaviour of ^{13}C and ^{15}N isotopes throughout the FoT (Figure 3.35). In the surface samples, an increase in the median value of $\delta^{13}C$ is visible from the mudflat outer (Group 1 = -22.59 ‰) to the fringe zone (Group 4 = -22.13 ‰), then there is a constant decrease until the deep forest (Group 7 = -23.94 ‰). Values at the river stations (group 8) fell between those of mudflat and forest (Figure 3.35a). However, the depth samples do not show a clear trend, there is a slight decrease from group 3 to 6, but group 7 increases again the average concentration of $\delta^{13}C$ (Figure 3.35b). The Nitrogen isotope composition has three trends in the surface samples. In the mudflat there is a decrease north-south (Group 1 to 3); from this point, an enrichment occurs in the fringe up to 8.49 ‰ dropping again in the middle forest to 8.23 ‰, then reaches 8.79‰ in the stations next to the rivers, this last median value is the highest obtained in sediment samples (Figure 3.35c). The depth samples show a low variability in the concentration of $\delta^{15}N$ (Figure 3.35d), ranging between 7.9 ‰ in the inner mudflat (Group 3) and 8.75 ‰ in the deep forest (Group 7).

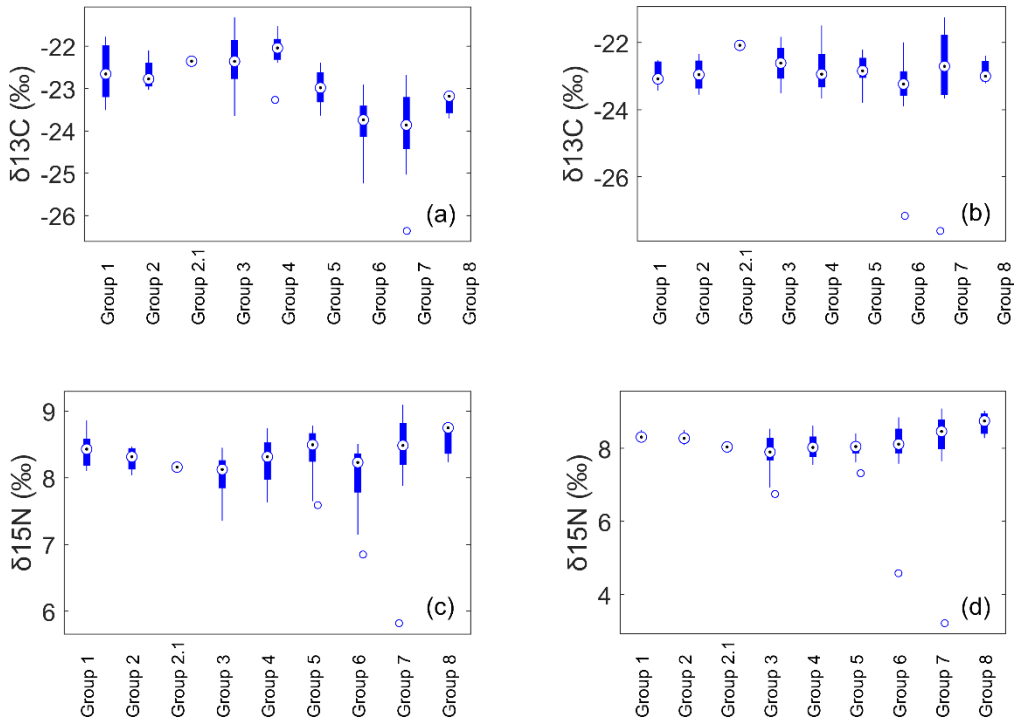

Figure 3.35. Along-shore groups boxplots. $\delta^{13}C$ values in surface (a) and depth (b) samples, $\delta^{15}N$ in surface (c) and depth samples (d). The boxes edges represent 25th and 75th percentiles and the black circle indicates the median value. Whiskers show the full range of the data (excluding outliers, which are plotted as empty circles).

3.3.4 Depth profiles in cores

The cores taken at F3 and F7 were also analysed to determine the isotopic fingerprint of $\delta^{15}N$ and $\delta^{13}C$ with depth (Figure 3.36 and Figure 3.37). The lowest value for $\delta^{13}C$ in core F3 occurs below the surface (-23.27‰) and the highest at the bottom of the core (-22.40‰), the curve shows a discontinuous increase in depth (Figure 3.36). The core from location F7 also shows an ^{13}C enrichment towards the bottom core but with a different trend – an abrupt increase occurs between -25 and -28 cm depth (Figure 3.37). The concentration in $\delta^{15}N$ values exhibit different behaviour between the two cores: on the one hand, $\delta^{15}N$ from the fringe core (F3) decreases irregularly in depth from 8.70 ‰ to 8.35 ‰ (with a slight increases to 8.52 ‰ at the core bottom depth) (Figure 3.36). On the other hand, the core extracted from the deep forest shows fluctuating $\delta^{15}N$ values, with an overall increase from 8.18 ‰ at the top to 8.67 ‰ near the bottom (Figure 3.37).

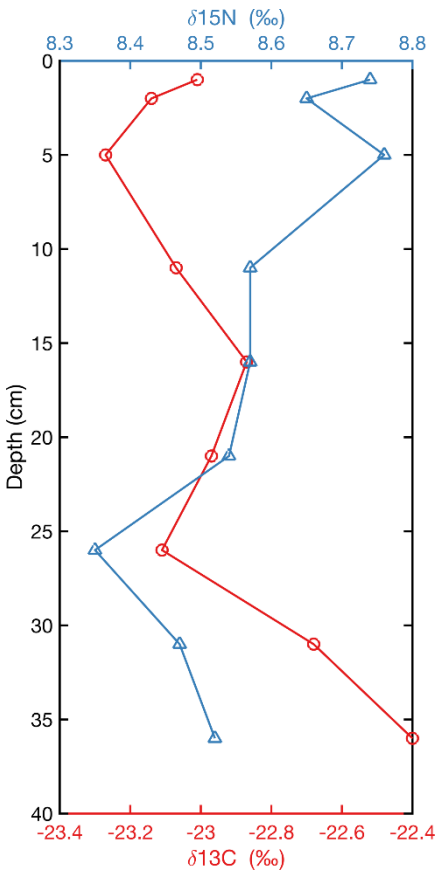

Figure 3.36. Isotopic analysis in core of Station F3

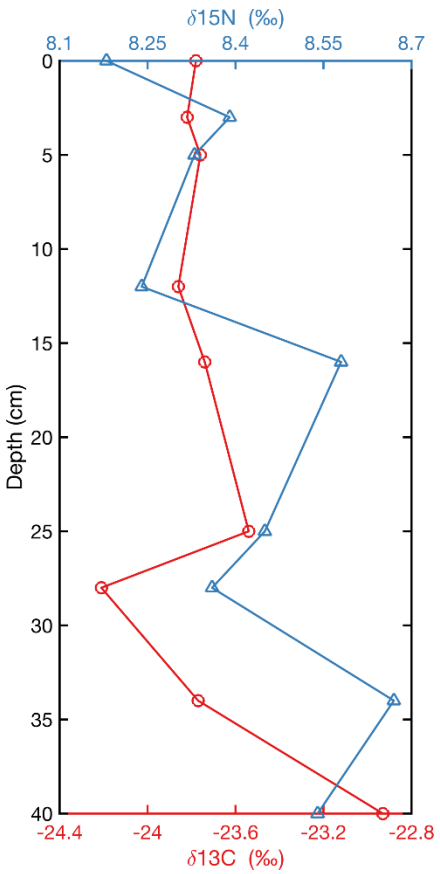

Figure 3.37. Isotopic analysis in core of Station F7

3.3.5 Relationship of between isotopic compositions

Values of $\delta^{13}C$ and $\delta^{15}N$ for both sediment and vegetation samples are shown in Figure 3.38. The mangrove samples are generally well separated from the sediment samples – with more negative values of $\delta^{13}C$, while the sediment sample with a high content of green algae is ^{13}C-enriched (-21.7 ‰). The isotopic relationship for the sediments focuses is a tight cluster between the vegetation samples and the sample rich in green algae, except for two outliers with low values of $\delta^{15}N$ and $\delta^{13}C$.

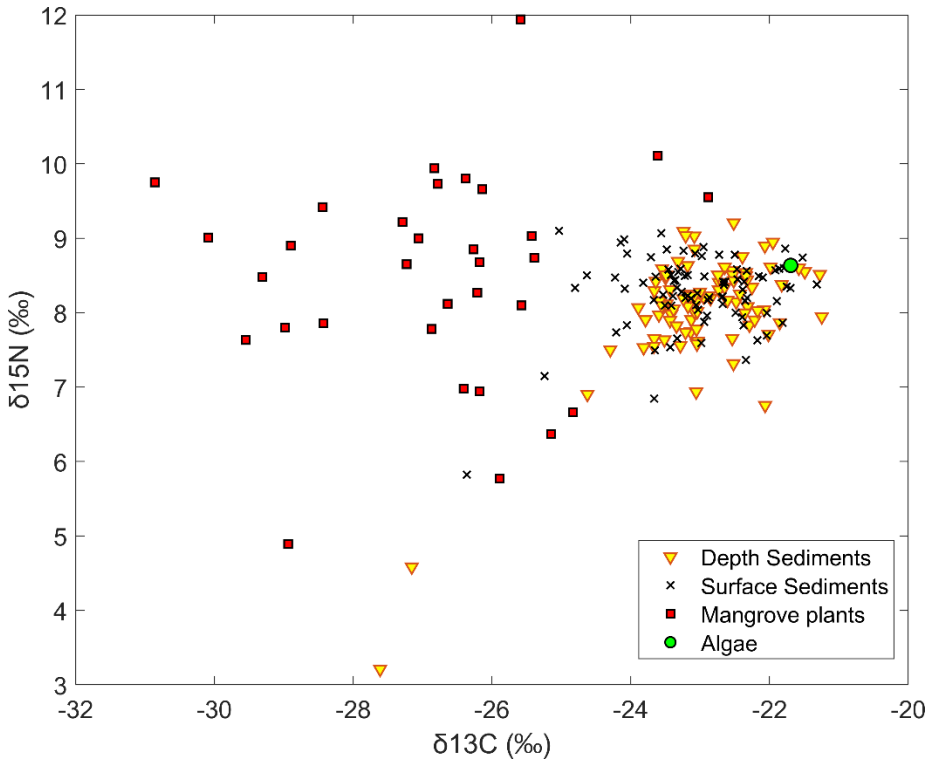

Figure 3.38. $\delta^{13}C$ and $\delta^{15}N$ relationship in sediment samples (yellow triangles for surface and black crosses for depth samples), mangrove samples (red squares) and algae sample (green circle).

Figure 3.39 shows a comparison of the concentration of N and C isotopes in the sediment and vegetation samples from transect F; ^{13}C-enrichment is evident in the superficial sediment samples, the samples in the fringe stations (2 and 3, red squares and green diamonds) have similar values, while the deep forest sample shows more enriched in the pneumatophores in relation to the sediments and has relatively high $\delta^{13}C$ values in all mangroves tissues. On the other hand, samples from stations 2 and 9 show $\delta^{15}N$-enrichment from the lowest values in the sediment to the maximum value in leaf tissues. Conversely, the $\delta^{15}N$ values from the fringe (red squares) show enrichment in the sediment and lower values in the tree samples.

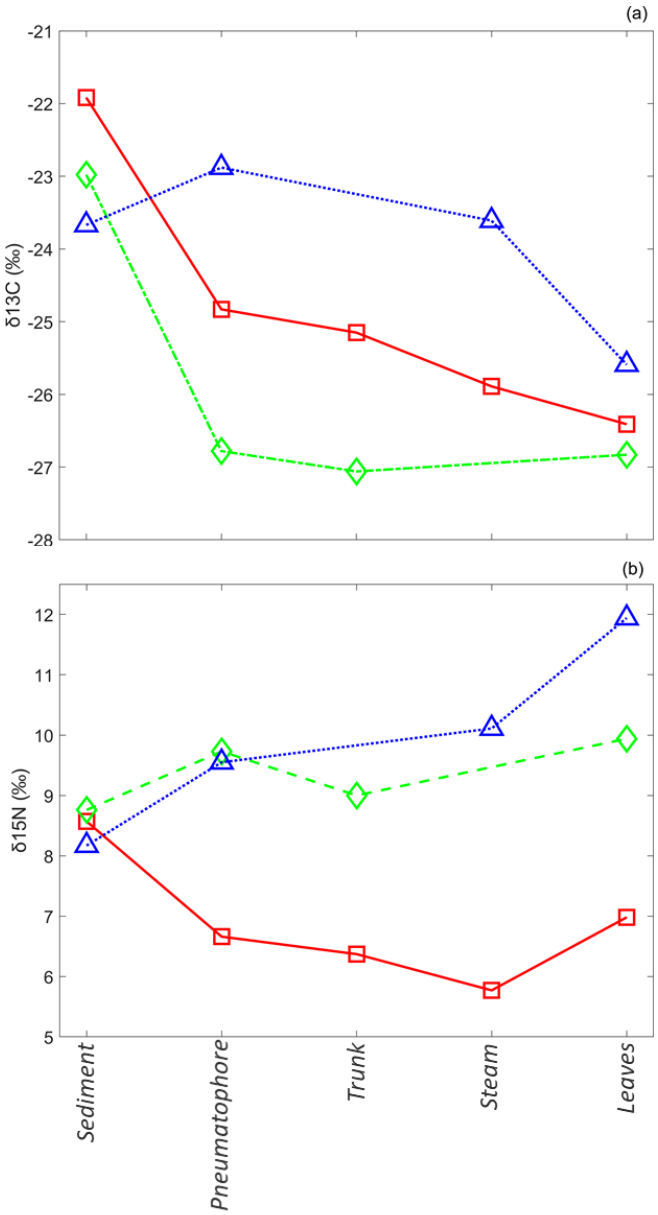

Figure 3.39. $\delta^{13}C$ concentrations (a) and $\delta^{15}N$ (b) in sediment and tissues samples from stations F2 (red squares), F3 (green diamonds) and F9 (blue triangles).

3.3.6 Relationship of isotopes and elements

When comparing the values of $\delta^{13}C$ and the percentage of organic carbon in the sediment samples, significant negative linear relations are obtained, so samples with lower organic carbon content had heavier isotopic compositions (for the surface samples $r^2 = 0.373$ and p-val <0.01, Figure 3.40a and for the depth samples $r^2 = 0.356$ and p-val <0.01, Figure 3.40b).

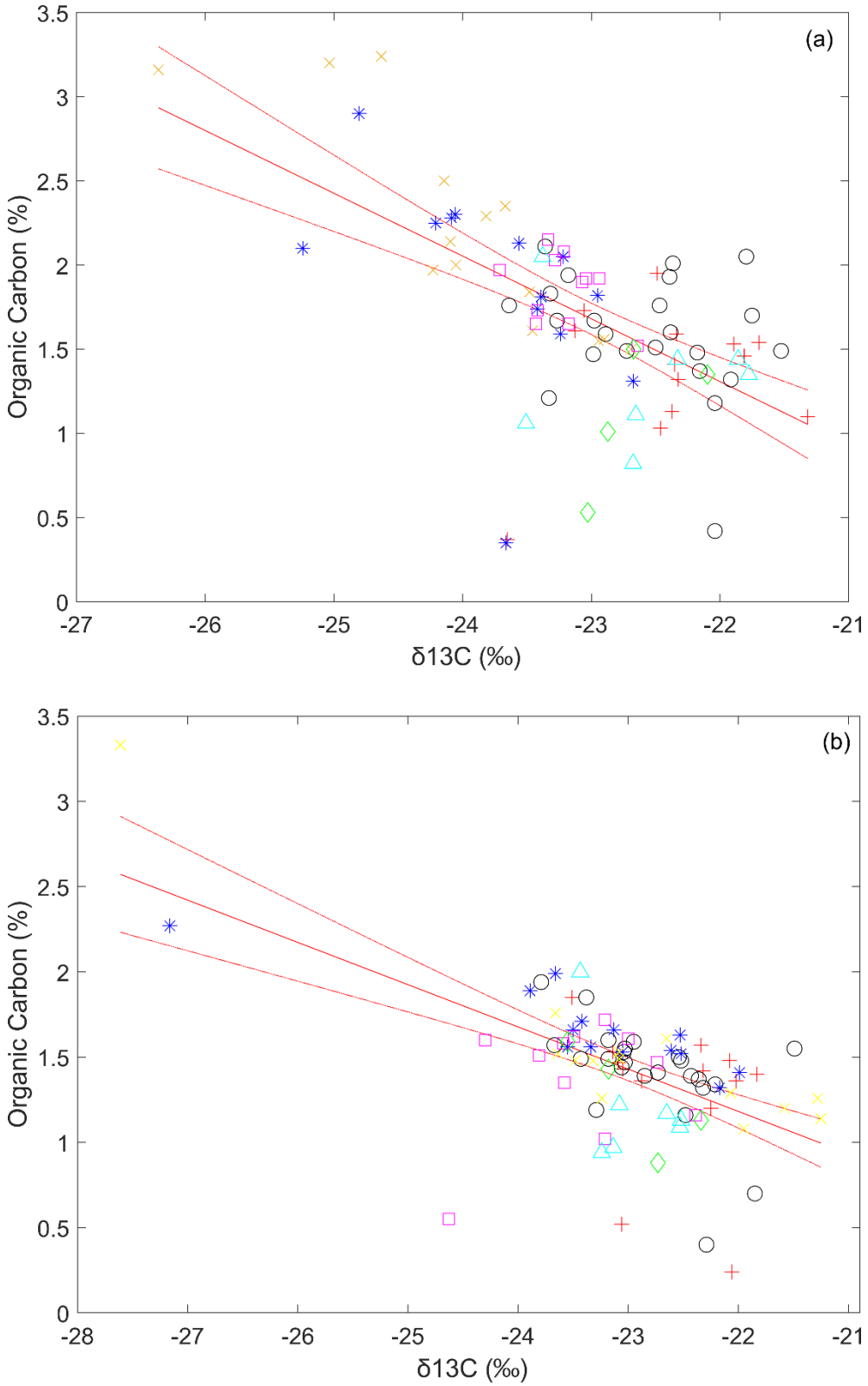

Figure 3.40. Relationship of $\delta^{13}C$ concentration and volume of Organic carbon in surface (a) and depth samples (b). Plots divided by the zones: Outer mudflat (cyan triangles), middle mudflat (green diamonds), inner mudflat (red plus signs), fringe (black circles), middle forest (blue asterisks) and deep forest (orange crosses).

3.3.7 δ ^{13}C and C/N ranges for organic inputs

Different sources of organic matter for coastal environments can be determined from $\delta^{13}C$ values and the C/N ratio as discussed and graphed in Lamb *et al.* (2006). The graphs below show nine possible sources from the relationship between C/N ratio and $\delta^{13}C$: C3 and C4 terrestrial plants, marine and freshwater dissolved organic carbon (DOC), marine and freshwater particulate organic carbon (POC), marine and freshwater algae and bacteria.

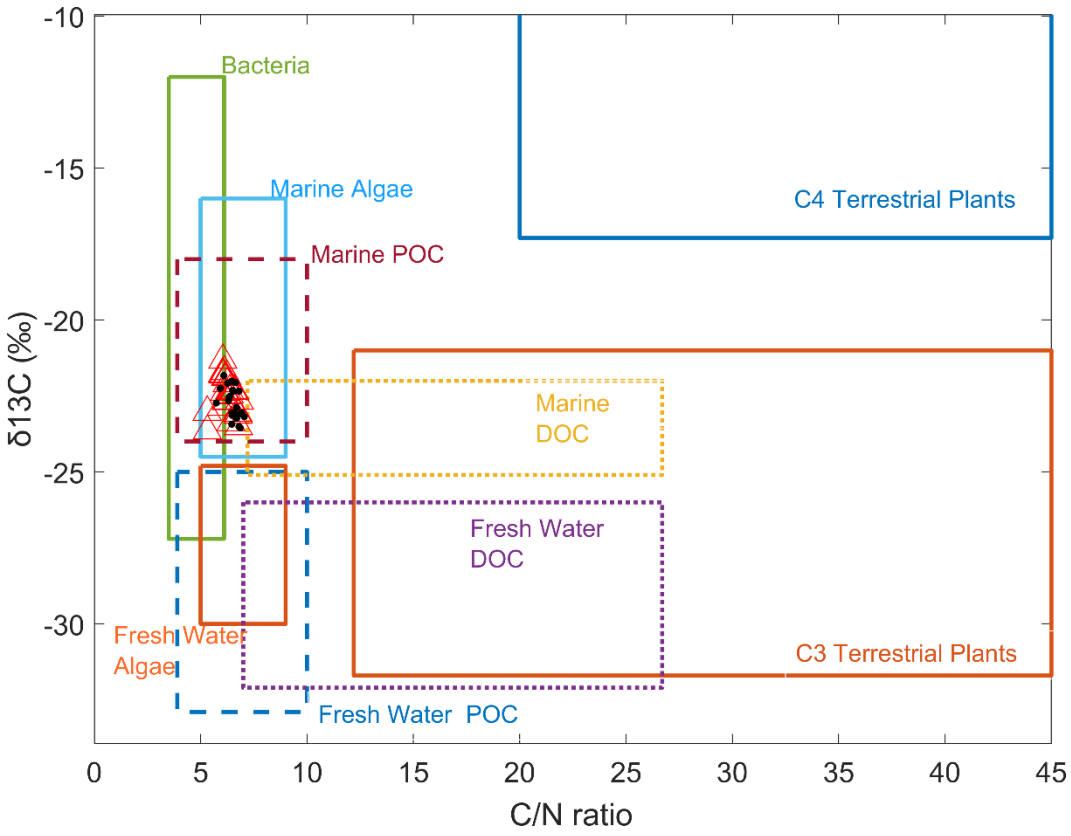

Figure 3.41. Relationship of C/N ratio and $\delta^{13}C$ in mudflat sediments. Values from the present study surface samples are shown as red triangles and black circles for surface and depth samples, respectively. Figure from Lamb *et al.* (2006) and references therein.

Our results from the Firth of Thames were separated into the different regions and graphed according to Lamb *et al.* (2006). The first zone corresponds to the mudflat area, which includes the samples of the Z, Y transects and stations 1 of each cross-shore transect (See Figure 2.2). Figure 3.41 shows that for surface and depth mudflat samples, the organic matter input is positioned to be a combination of marine algae, marine POC and bacteria (n= 48). In the front or fringe area of the mangrove forest (station 2 of transects A to L, n=24), the potential organic sources for sediments are the same as in the mudflat (Figure 3.42), plus a sample that may also belong to the marine DOC box. In general, the data cluster is very tight.

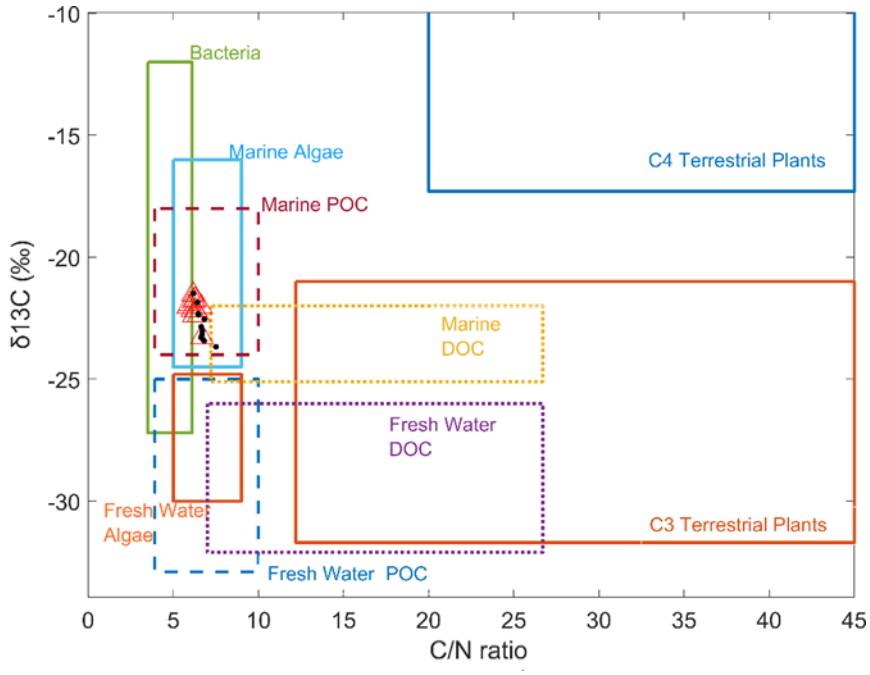

Figure 3.42. Relationship of C/N ratio and $\delta^{13}C$ in sediments at the fringe of the forest. Values from the present study surface samples are shown as red triangles and black circles for surface and depth samples, respectively. Figure from Lamb *et al.* (2006) and references therein.

Figure 3.43 show a wider dispersion of the data, the organic sources for the mangrove forest sediments (stations 3 to 5 in cross-shore transects) fall in areas classified as marine POC, marine algae and bacteria (n=98). The data, in this case, extends to the freshwater POC, DOC and algae boxes, and also for a few samples overlaps a source of C3 terrestrial plants.

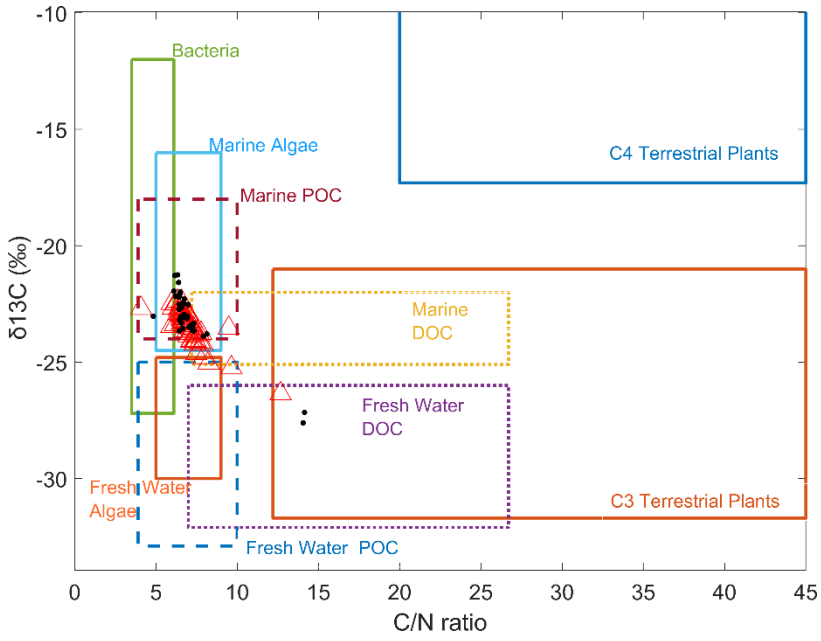

Figure 3.43. Relationship of C/N ratio and $\delta^{13}C$ in sediments at the forest. Values from the present study surface samples are shown as red triangles and black circles for surface and depth samples, respectively. Figure from Lamb *et al.* (2006) and references therein.

Similarly, the samples taken from the riverbanks are located within the boxes of marine POC, marine algae and bacteria, with two points also showing a possible marine DOC source (Figure 3.44). On the other hand, Figure 3.45 shows the vegetation samples, which include parts of pneumatophores, stems, branches and leaves taken in the F transect and the Piako River. All of these samples fit inside the C3 Terrestrial Plants box. The sediment sample with a high content of green algae is located inside the marine algae box. Figure 3.45 shows the extreme values found in the C/N ratio and $\delta^{13}C$.

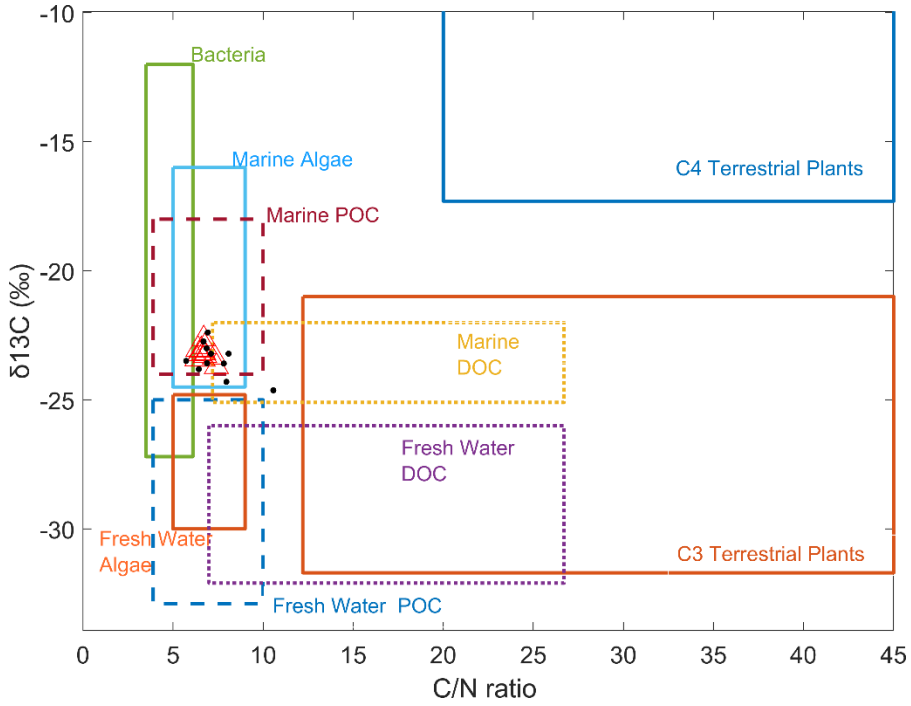

Figure 3.44. Relationship of C/N ratio and $\delta^{13}C$ in sediments of stations next to the rivers Waihou, Piako and Waitakaruru. Values from the present study surface samples are shown as red triangles and black circles for surface and depth samples, respectively. Figure from Lamb *et al.* (2006) and references therein.

Plotting all the sediment samples together with mangrove tissues in Figure 3.45 a clear predominance is given for sources from marine POC to marine algae in sediment samples with a slight dispersion towards the C3 terrestrial plants classification. The data for the different parts of mangrove plants naturally fall under this latter source classification.

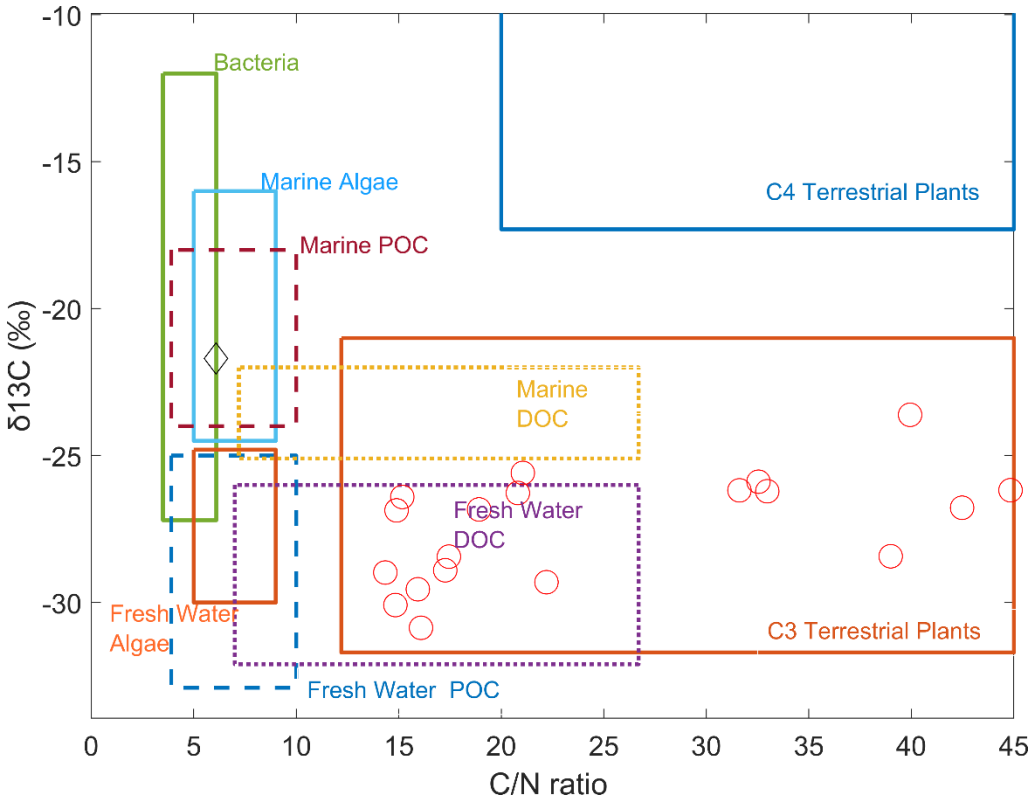

Figure 3.45. Relationship of C/N ratio and $\delta^{13}C$ in mangrove and algae samples. Values from the present study surface samples are shown as red triangles and black circles for surface and depth samples, respectively. Figure from Lamb *et al.* (2006) and references therein.

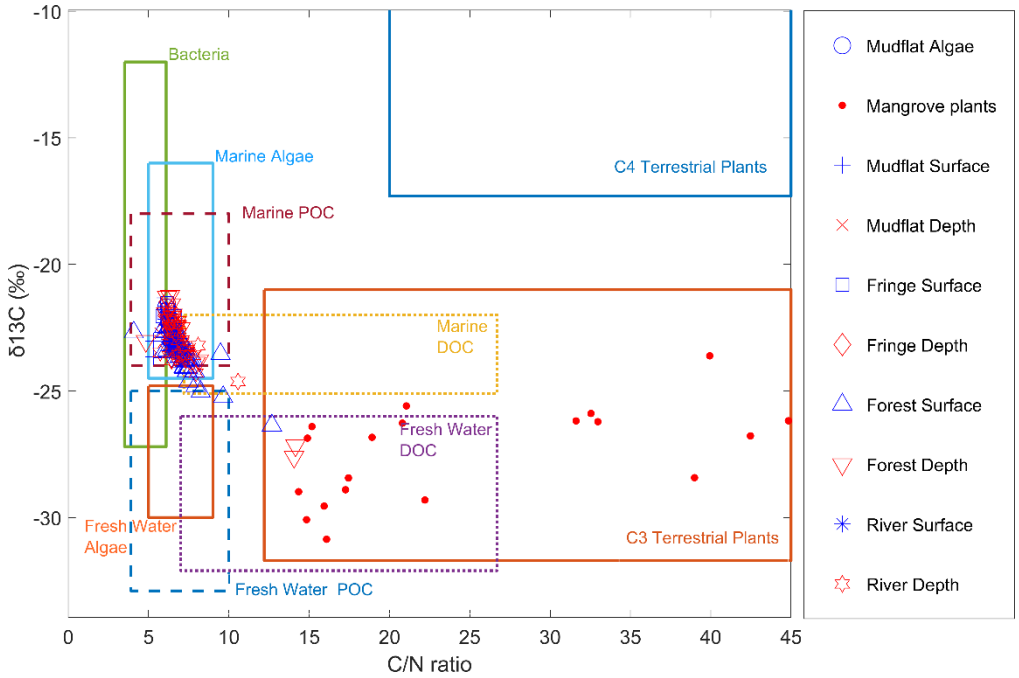

Figure 3.46. Relationship of C/N ratio and $\delta^{13}C$ in all sediment and mangrove samples. C/N ratio values over 45‰ are not displayed (13 samples). Figure from Lamb *et al.* (2006) and references therein.

3.4 Statistical analyses

In this section, we undertake statistical analysis to test the significance of the main trends described in the previous sections. The Shapiro-Wilk test was used to determine if differences in values between surface and depth were normally distributed. The normality condition was not found to hold for any variable. Therefore, we used a Wilcoxon signed rank test at the 5% significance level to examine if differences between surface and depth were significant. In each case, the null hypothesis was that the difference between surface and depth values of a variable comes from a distribution with a median equal to zero (i.e. a rejection of the null hypothesis indicates that values are significantly different).

Results comparing surface and depth values are shown in Table 3.5 and demonstrate that N, TC, OC, IC, and $\delta^{15}N$ differ significantly between depth and surface samples, only the C/N values did not exhibit a statistically significant difference. While the test for $\delta^{13}C$ produced a result to accept the null hypothesis the p-value indicates that results weren't significant, so firm conclusions for this parameter cannot be made.

Table 3.5. Results from a Wilcoxon signed rank test to assess differences between surface and depth samples.

Variable	z-statistic	rank	p-val	Reject or accept H_0	Additional information
N	5.4492	3136	<0.0001	Reject	
TC	4.6957	2961	<0.0001	Reject	
OC	5.0832	3051	<0.0001	Reject	
IC	3.1216	2484.5	0.0018	Reject	
C/N	-1.914	1426	0.0556	Accept	Significant at 10% level but not 5%
$\delta^{13}C$	-0.0153	1824	0.9878	Accept	
$\delta^{15}N$	3.5637	2756	<0.0001	Reject	

To compare differences between the forest and mudflat, the Shapiro-Wilk test was again used to determine if any variables were normally distributed, and no variables were found meet this condition (with a significant test result). Therefore, a Wilcoxon rank sum test (equivalent to the Mann-Whitney U-test) was used to examine if differences between areas were significant at the 5% level. The null hypothesis in each case was that the data from each location are samples from continuous distributions with equal medians. Results comparing surface samples on the mudflat to the forest are shown in Table 3.6 and all the variables except for $\delta^{15}N$ showed significant differences between both areas within the FoT. On the other hand, depth samples differ significantly between mudflat and forest only for concentrations of N, TC and OC (Table 3.7), whereas IC was not found to differ significantly. Tests for C/N, $\delta^{15}N$, and $\delta^{13}C$ did not produce statistically significant results, so for these variables we cannot definitively conclude there are no differences between areas.

Table 3.6. Results from a Wilcoxon signed rank test to assess differences in surface samples between the mudflat and forest zones.

Variable	z-statistic	rank	p-val	Reject or accept H_0	Additional information
N	-4.1058	550	<0.0001	Reject	
TC	-4.3443	529	<0.0001	Reject	
OC	-4.3898	525	<0.0001	Reject	
IC	-2.6543	678	0.0079	Reject	
C/N	-3.2313	627	0.0012	Reject	
$\delta^{13}C$	3.4583	1200	<0.0001	Reject	
$\delta^{15}N$	-1.7321	759	0.0833	Accept	Significant at 10% level but not 5%

Table 3.7. Results from a Wilcoxon signed rank test to assess differences in depth samples between the mudflat and forest zones.

Variable	z-statistic	rank	p-val	Reject or accept H_0	Additional information
N	-2.464	703	0.0137	Reject	
TC	-2.1847	728	0.0289	Reject	
OC	-2.7769	675	0.0055	Reject	
IC	1.8799	1092.5	0.0601	Accept	Significant at 10% level but not 5%
C/N	-1.503	789	0.1328	Accept	
$\delta^{13}C$	0.8605	1001.5	0.3895	Accept	
$\delta^{15}N$	-0.3632	891	0.7165	Accept	

3.5 Fluorometric data for Chlorophyll a

The estimated content of algae biomass was calculated by the method of fluorometric determination of chlorophyll *a* pigments. For this investigation, the surface samples have a mean value of 12.55 µg / g dw with substantial variability (values range from 2.25 to 52.43 µg / g dw), whereas depth samples exhibited little variability with an average of 1.50 µg / g dw and range from 0.13 to 9.63 µg / g dw. The largest value for the surface samples corresponds to the sample with high algae content (noted visually) taken from the mudflat in transect F (Figure 3.47).

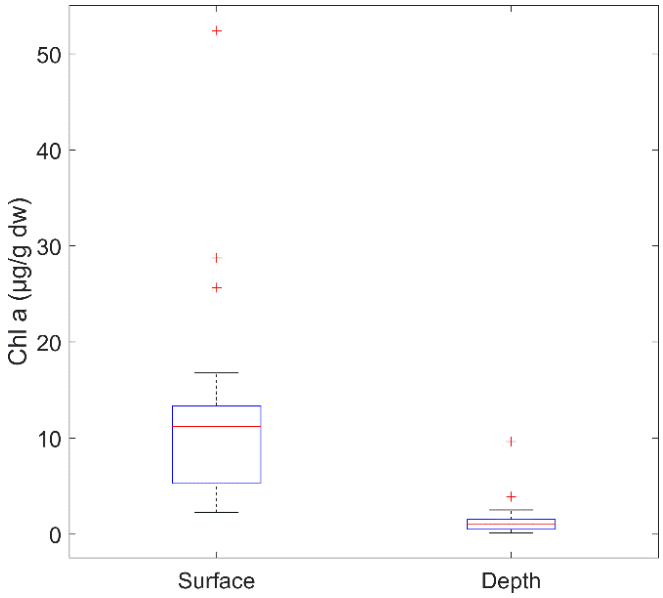

Figure 3.47. Boxplots of Chlorophyll *a* in sediment samples at the Firth of Thames. The boxes edges represent 25th and 75th percentiles and the horizonal red line indicates the median value. Whiskers show the full range of the data (excluding outliers, which are plotted as red crosses).

The maps in Figure 3.48 show the distribution of the chlorophyll *a* pigments concentration in the Firth of Thames. The highest values in *a* pigments in surface samples (> 20µg / g dw) were from transect L and the stations in Turua. Low values, were distributed throughout the Firth without an evident trend (~ 5 µg / g dw). In general, the depth samples had chlorophyll *a* values close to 1 µg / g dw except for the samples at the mouth of the Waihou River and west of this point in the K transect, with an overall average value of 2.59 µg / g dw.

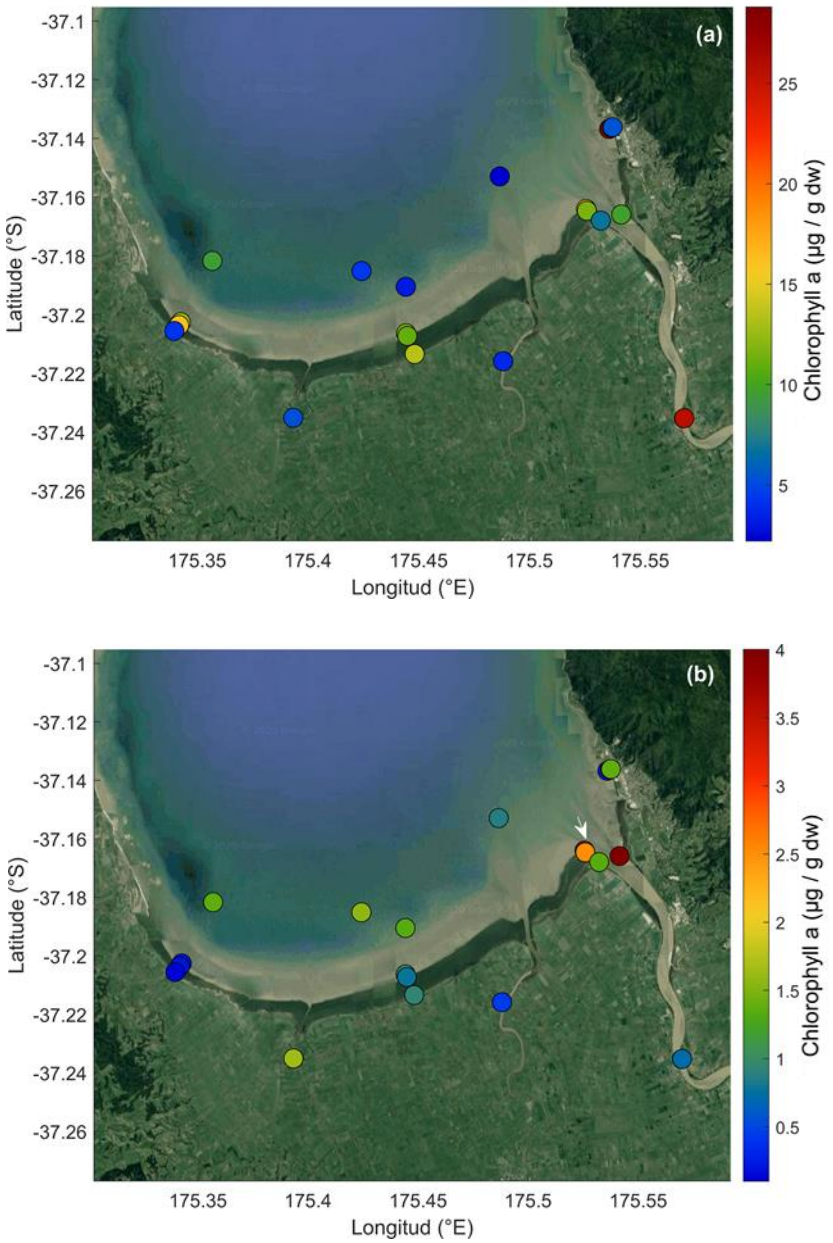

Figure 3.48. Spatial distribution of Chlorophyll *a* concentration in the Firth of Thames in surface(a) and depth (b) samples. The white arrow indicates an outlier in station Y4 with value 9.63 µg / g dw.

The relationships between estimated algal biomass and the concentrations of Nitrogen and Organic Carbon are shown in Figure 3.49. Depth samples consistently show close to zero Chl *a* content, irrespective of N or TOC concentrations. Surface samples show a much a larger range of Chl *a*, but values were not correlated with either N or TOC concentrations (r^2 = 0.0016 and r^2 = 0.002, respectively).

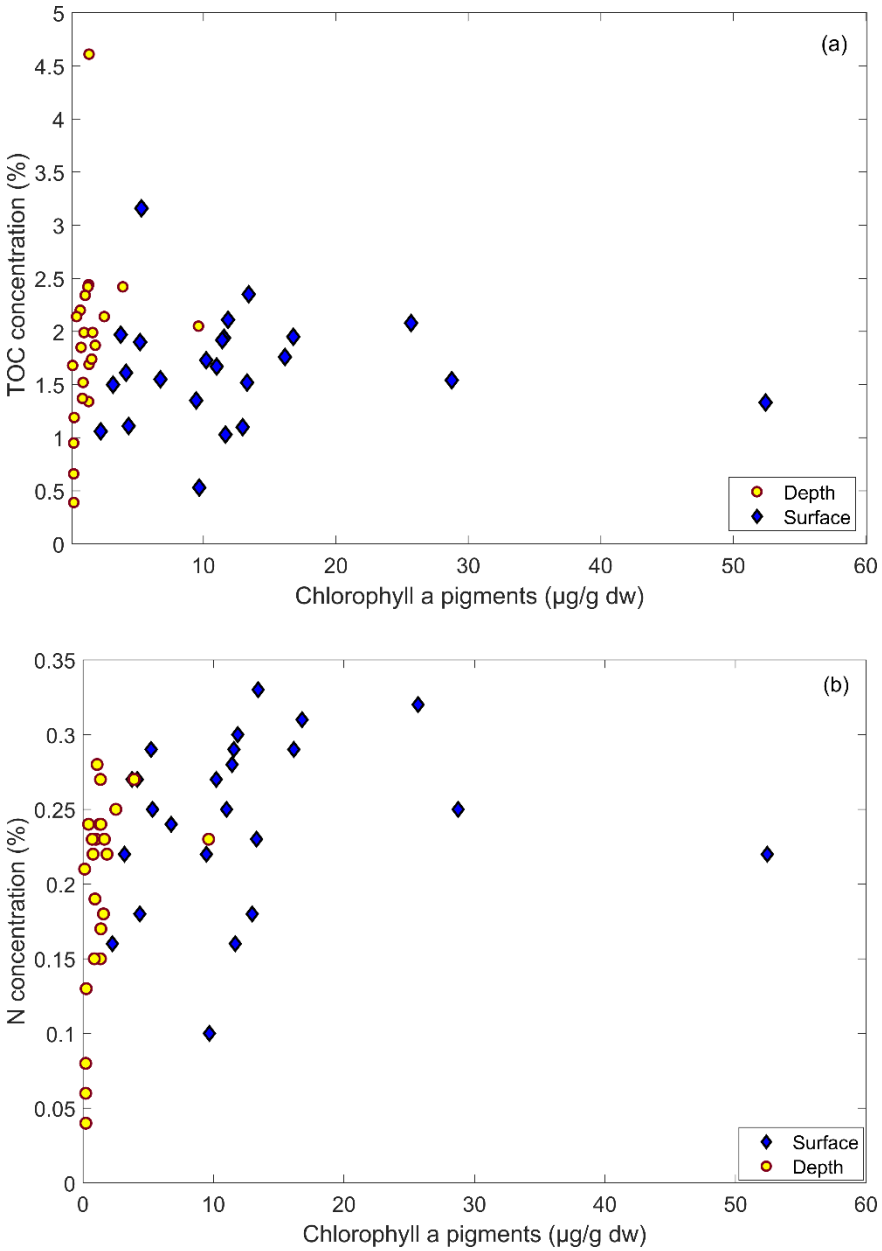

Figure 3.49. Chlorophyll *a* plotted against Organic Carbon (a) and Nitrogen concentration (b.)

3.6 Grain size results

The results of the grain size from the subset of sediment samples (n = 60) will be shown herein. Median grain sizes were similar for both surface (D50= 7.6 µm) and depth (D50= 8.78 µm) samples; although the depth samples exhibited more variability (Figure 3.50a). Similarly, the median (D90) values were 51.5 and 58.8 µm in surface and depth samples, respectively (Figure 3.50b).

When the total volume of all samples is combined and categorised by type of grain (Figure 3.50), the mean clay content is 29.94%, silt constitutes 53.88%, 14.56% is

fine sand (which includes very fine and fine sand of the Wentworth scale) and 1.60% is coarse sand (including medium, coarse and very coarse sand from the Wentworth scale).

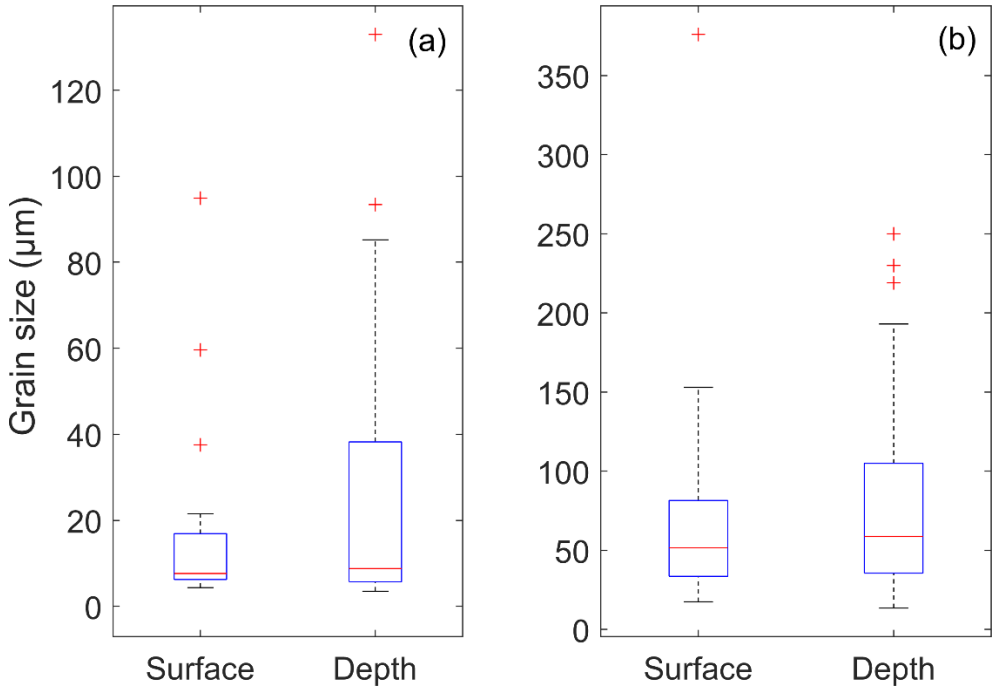

Figure 3.50. Boxplots of grain size in D50 (a) and D90 (b) in surface and depth samples. The boxes edges represent 25th and 75th percentiles and the horizonal red line indicates the median value. Whiskers show the full range of the data (excluding outliers, which are plotted as red crosses).

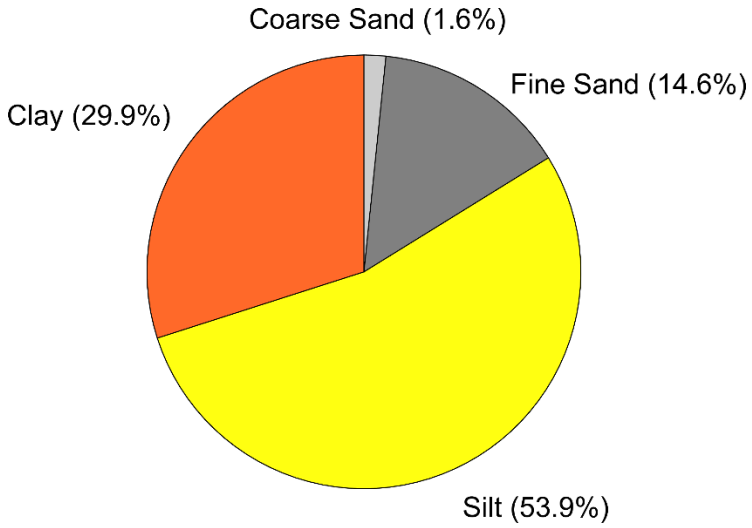

Figure 3.51. Pie chart of mean grain texture in the Firth of Thames. The ranges in grain size was defined as: Clay = 0.005-3.9µm, Silt= 7.8-63 µm, Fine sand= 74-250 µm and Coarse sand = 300-2000 µm.

The spatial distribution of the mean grain size shows that the sediments are predominantly mud (clay and silt) with D50 of 20.7 µm at both surface and depth

(Figure 3.52). The surface sediments are relatively uniformly distributed: Only a few samples had larger D50 of transects A, L and one sample from within the Waihou River mouth had a D50 value corresponding to fine sand (Figure 3.52a). Similarly, the median grain sizes of depth samples were around D50=17 µm, with a few samples with larger values in the transects A, C, and L (Figure 3.52b).

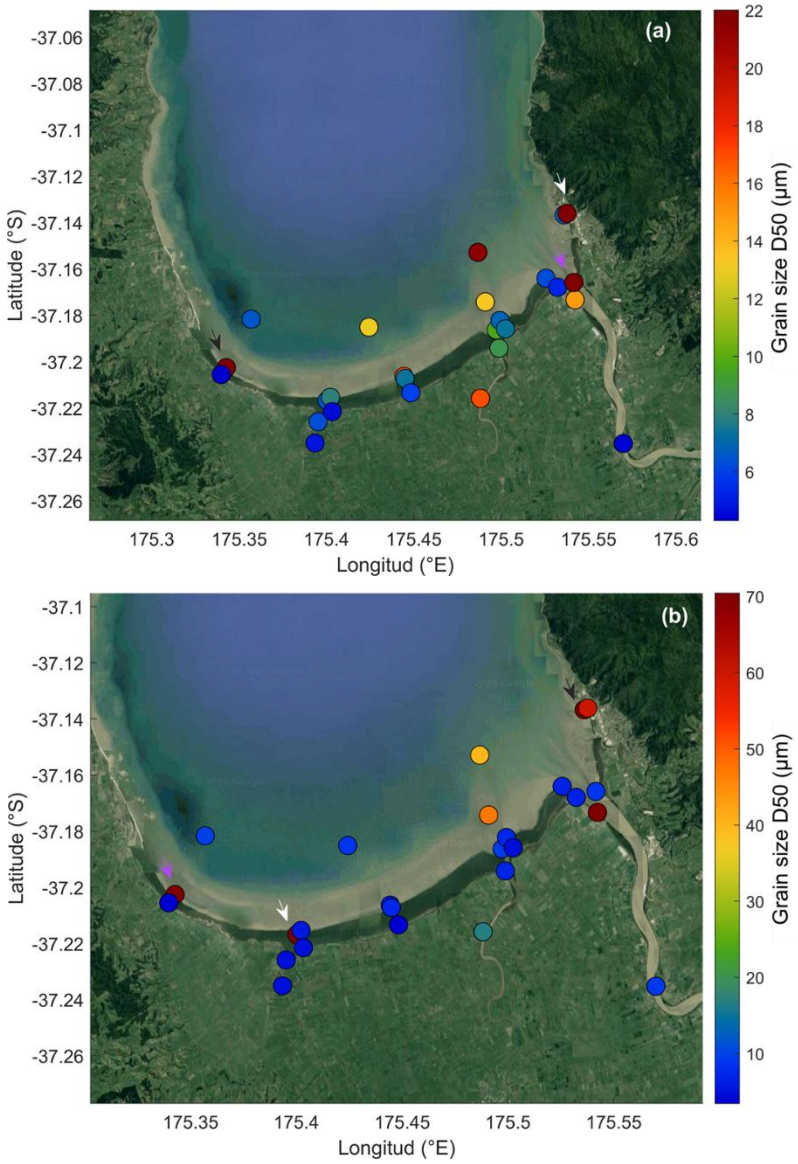

Figure 3.52. Distribution of D50 (median) grain size in surface (a) and depth (b) samples at the Firth of Thames. Arrows in panel (a) shows outliers in A1 surface =37.5 µm (black), N5 surface =59.6 µm (white) and 94.9 µm (black). Arrows in panel (a) shows outliers in A1 depth =93.4 µm (purple), N1 depth =85.2 µm (black) and 133 µm (white).

To examine relationships between grain size and OC content, the OC content was plotted against percentages of clay and silt in the samples (Figure 3.53). Linear model fits were not significant, explaining at most 5% of the variability in organic

carbon content (r^2 = 0.05, p-val = 0.215). Thus, the grain size is not a good indicator of the organic carbon content in the Firth of Thames.

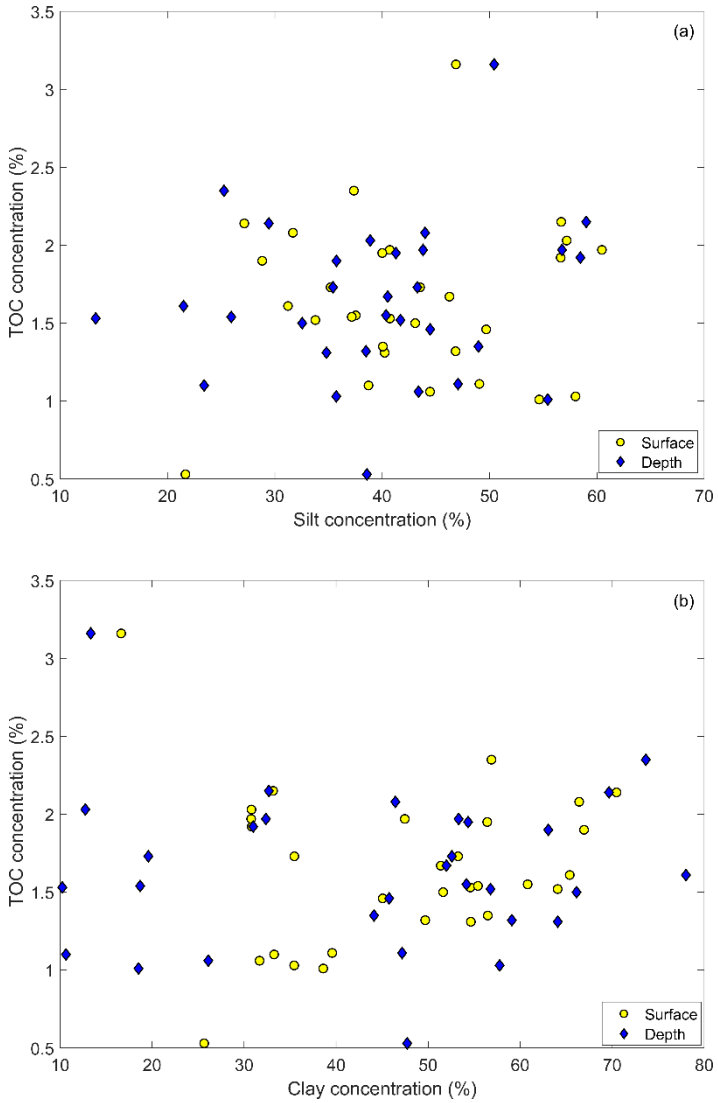

Figure 3.53. Relation between Silt concentration and Organic carbon (a), Clay concentration and Organic Carbon (b).

3.7 Loss on ignition results

124 sediment samples taken in the FoT were also analysed using the Loss on Ignition method to provide bulk estimates of organic material. For the surface samples, Soil Organic Matter (SOM) varied between 1.89 and 18.87 %, with a mean value of 11.62%. In agreement with the results from the isotope mass spectrometer , the depth samples have a slightly lower organic concentration; in this case, the average percentage is 10.92%, and the range of data is from 1.94% to 14.27% of SOM (Figure 3.54).

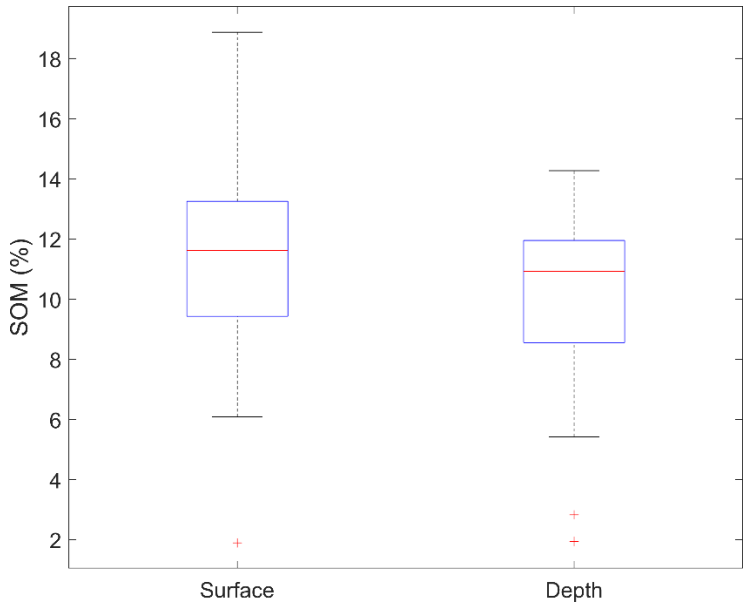

Figure 3.54. Boxplot of Soil Organic Matter volume in surface and depth samples. The boxes edges represent 25th and 75th percentiles and the horizonal red line indicates the median value. Whiskers show the full range of the data (excluding outliers, which are plotted as red crosses).

The relationship between SOM and Organic carbon concentrations in surface in depth samples is shown in Figure 3.55 and revealed a significant reasonable correlation (r^2= 0.52 with p-val <<0.01).

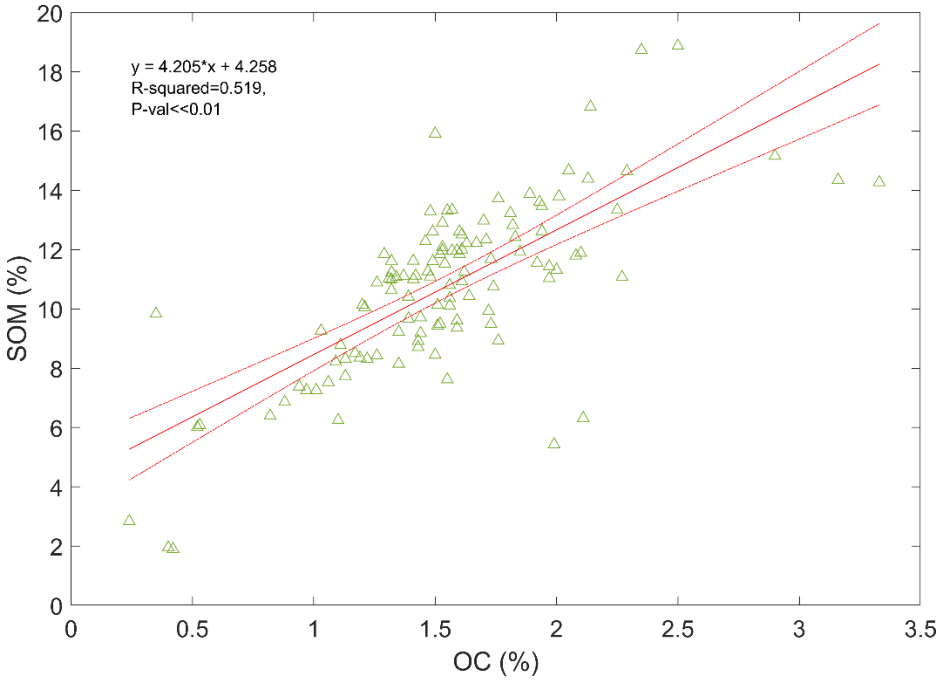

Figure 3.55. Relationship between results of elemental analysis and loss on ignition methods.

3.8 Summary

The results indicate a higher concentration of C, N and OC in the surface compared to depth samples. The IC content in surface and depth samples is low in the FoT sediments (Mean value = 0.49) and the C / N ratio is comparable for both depths (6.74 in surface and 6.90 in depth samples). The spatial distribution of C, N and OC shows higher percentages towards the interior of the mangrove forest in surface samples, while no clear pattern in depth samples could be discerned. In the mudflat in front of the Piako River, low values are repeated in all elements analysed in both surface and depth samples. A positive linear relationship was found between the concentrations of OC and N in sediments samples explaining 78 % of the variation (p-val<0.01), whereas no relationship was found with tree samples. Organic and inorganic carbon showed weak but significant linear correlations to each other (r^2=0,35, p-val<0.01 in surface; r^2=0.12, p-val<0.01 in depth samples).

The relationship between the concentration of elements and the distance within the transect showed that the values indeed increase towards the deep forest, while the transects sampled along the river banks tend to show constant concentrations and values. However, the relationship between the different concentrations and the distances to the rivers did not show any trend (Figure 3.8, Figure 3.12 & Figure 3.16). To corroborate a landward increase in N, C and OC, the stations were grouped as along-shore transects, to highlight the pattern in surface samples, whereby there is an enrichment of the elements towards the deep forest in contrast to low values in the mudflat (Figure 3.22).

The stable isotopes of C and N showed mean values of -23.01 ‰ in $\delta^{13}C$ and 8.16 in $\delta^{15}N$, while in plant tissues had average values of -26.52 ‰ and 39.93 ‰ in $\delta^{13}C$ and $\delta^{15}N$ respectively. The $\delta^{13}C$ spatial distribution in surface samples, and the relationship with the position within the transect shows an ^{13}C- enrichment in the mudflat compared to the mangrove forest. On the other hand, a ^{15}N-enrichment is observed landwards in surface samples. When both isotopes are compared, a cluster of mangrove tissues samples is clearly separated from the sediment samples (Figure 3.38). The relationship between $\delta^{13}C$ and OC showed a negative correlation (Figure 3.40). Our data were applied to results from Lamb *et al.* (2006) to determine sources of carbon and we observed that marine algae and marine POC are the main

organic inputs in the Firth. Finally, the concentration of Chlorophyll *a* pigments were not found to show a relationship with the OC concentration, nor was there a relationship between OC content and grain size. Bulk estimates of organic matter concentration using loss-on-ignition method corroborated the OC patterns observed. As expected, a positive correlation was obtained between SOM and OC, with an average ratio of 7:1.

4. Discussion

This research examines the spatial variability of elemental and isotopic concentrations of C and N in the sediments of a mangrove forest in New Zealand. The main goal of this chapter is to evaluate the organic spatial distribution in the Firth sediments in terms of the questions outlined in section 1.8, compare the results with previous studies from across the globe, thus setting the results into an international context, and to establish avenues for future research.

Firstly, it is worth noting that one key difference with most previous work is the high spatial resolution of our sampling covering 87 locations within an area of 82 Km^2. Most previous work has either considered many samples over a large region (e.g. Garcias-Bonet *et al.* (2019), who sampled 43 stations within the Red Sea – encompassing a 10 degree range in latitude, or Yu *et al.* (2018) whose sampling cover more than 20 km in front of The Yellow River Delta), or alternatively taken just a few samples over one local area e.g. Yang *et al.* (2018).

The concentrations of OC and N in the Firth sediments are strongly correlated as evidenced in Figure 3.23. This high correlation index (r^2=0.78) indicates that Nitrogen has an organic origin (Tue *et al.*, 2011). Such a positive relationship has also been observed from sediments in other experiments (Yu *et al.*, 2018; Garcias-Bonet *et al.*, 2019). Both OC and N content decrease with depth into the sediment in the Firth. Similarly, Castro - Rodríguez *et al.* (2018) reported observations from the Swamp of Mallorquin, Colombia in which the concentrations of N and C decreased with depth; although the mean percentage of TC was higher in Mallorquin than in FoT (3.9% and 2.7% respectively), and the mean Nitrogen concentration was the same (2.7%) in both forests. A steady decrease in OC with depth is also recorded in the mangrove forest of Vietnam (Tue *et al.*, 2018). This decrease in nutrients may be due to soil respiration. Although a decrease in both nutrients has been observed in depth, the correlation coefficient between concentrations in the surface and depth samples is very low (r^2 = 0.010 for C and r^2 = 0.009 for N); possibly implying variable respiration between locations.

Kristensen *et al.* (2008) reviewed a compilation of research from mangrove ecosystems, and found that in sediments, 44% of the data have an OC value of less than 2%, consistent with our results, while 28% of observations of OC

concentration fall in the range from 2 to 5%. In the Fujian province of China, Gao *et al.* (2019) reported that the content of soil organic carbon (SOC) in *A. Marina* cores among other mangrove species, remained below 2% up to more than 200 cm depth and indicating that *A. Marina* had lower values compared with other mangroves species. The authors attribute the low OC content to a plague which affected the mangrove for seven years. Another study performed on the Red Sea mangroves in Garcias-Bonet *et al.* (2019) found an average OC concentration in sediments equivalent to 1.85%. Our investigation showed that in FoT mangrove sediments, 61.8% of samples have a value of less than 2% in OC and 38.2% have a value equal to or greater than 2%, but less than 5%. These results show that our analyses are within the range reported by various authors for Organic Carbon in mangrove sediments, despite the relatively recent development of the mudflat (within the last 60 years).

Regarding the efficiency of nutrients burial in mangrove forests, a study in Matang Mangrove Reserve in Malaysia (Alongi *et al.*, 2004) where the species *Rhizophora apiculate* predominates, estimated that from the total carbon input to the ecosystem, the burial process only account up to 2%, whereas the 73% of C was lost in the breathing process (Figure 1.2, Table **1.1**). In contrast, N was efficiently buried in sediments (10-29%). Furthermore, they concluded that most carbon exchange occurred with the atmosphere and not with the estuary. Our results are in line with their conclusions, given the lack of evidence of carbon produced by mangrove trees in the mudflat samples, indicating little exchange of organic material with estuarine waters.

The C/N (OC/N) ratio is an essential component to establish the organic source in sediment analysis. Kristensen *et al.* (2008) estimate that 96% of mangroves have C/N ratios higher than 10 (measured as POC in their paper and equivalent to OC in this research). This statistic is higher than the values for the ratio observed in the Firth, where the mean value is 6.9 for all sediment samples in the mangrove forest. One possible explanation for lower C/N ratios is that when mangrove leaves decompose, a significant amount of organic material is used by bacteria which colonise the decaying leaves (addition of biomass to plant debris) and the addition of Nitrogen produced by bacteria in humidification processes (Cifuentes *et al.*, 1996).

The relationship between organic and inorganic carbon depends the hydrodynamic environment which predominates in an estuary (Yu *et al.*, 2018). In the Yellow River in China, concentrations of IC were about four times greater than OC (Yu *et al.*, 2018). However, the opposite trend was observed in the Firth, where the inorganic carbon content in sediments is relatively low (IC mean = 0.53%) compared to the overall mean OC value (1.73%). Our results may indicate a predominance of marine organic input over freshwater sources for the Firth of Thames. Additionally, the samples from the banks of the rivers flowing into the FoT do not show predominance in the IC values; on the contrary, it is the outer mudflat sediments which have relative larger IC content in the depth samples (Figure 3.17b). Moreover, the IC presence in the Firth is likely due to calcareous remains from fauna that inhabit the mangrove sediments, which is consistent with high values near the A transect were an extensive shell lag was found in the field. Another point of difference with the observations made by Yu *et al.* (2018) is that their results show a well-established positive correlation (r^2=0.945) between inorganic and organic carbon in the Yellow River; whereas in the Firth, the relationship is much weaker (r^2 =0.36, for surface and depth samples). The differences in the results could be explained by the difference in the number of samples; our research has 175 sediment samples compared to 15 samples used by Yu *et al.* (2018). Additionally, the carbon concentrations and likely sources differ between locations, which leads to different relationships.

One of our goals was to understand which dynamic or morphological aspects affect the content of organic carbon and nitrogen in FoT. For example, whether the rivers influence the isotopic and elemental composition of sediments. The Waihou River discharge 160,000 t yr^{-1} and Piako River 30,000 t yr^{-1} into the Firth of Thames (Hicks *et al.*, 2011) and these volumes of sediments may contain a considerable contribution of particulate organic carbon (POC) into the estuary as has been observed in other mangrove forests which receive freshwater from large catchments (Kuramoto & Minagawa, 2001). Within our experiments, the distance between rivers and the sampling points did not show an apparent relationship with the content of OC across the Firth or any other element analysed in the investigation (Figure 3.8, Figure 3.12, Figure 3.16). However, one notable result was that transects adjacent to rivers (C, H and K) exhibited the lowest variability in the concentrations of elements and isotopes compared to the other cross-shore

transects. This observation suggests that the organic matter carried by the three rivers only influences the riverbanks and their near surroundings with no influence further afield. This result is supported by a hydrodynamic study showing relatively little lateral penetration of river plumes into the surrounding forest (Vundavilli *et al.*, 2019). These conclusions could be strengthened by future measurements examining the concentrations of POC from water samples from the rivers.

Assessing the full spatial distribution of the different types of C and N within the mangrove forest was also a key aim of our research. The distribution maps (Figure 3.3, Figure 3.9, Figure 3.13, Figure 3.17) show that C, N and OC in surface samples are enriched landwards. This trend is also seen in the alongshore transects (Figure 3.22). The stations located in the deep forest (group 7) have the highest mean values for nutrient concentrations; when comparing these concentrations with the lowest values recorded in the middle mudflat (group 2), the mean values decrease by 40% in nitrogen, 48% in total carbon, and 49% in organic carbon. Our findings are in line with the field observations made by Norris *et al.* (2017) in the Mekong Delta, Vietnam; within their conclusions, they argue that high turbulent energy in the mangrove fringe can suspend fine sediments in the water column which may deposit further into the forest. The organic matter in suspension likely behaves as fine particles that are preferentially deposited towards the interior of the mangrove forest. This result is in-line with the hydrodynamic regime within the Firth of Thames: Under certain strong wind conditions, waves with significant velocities at the forest fringe interact with mangrove roots generating turbulence to prevent sediment settling (Lovett, 2017).

4.1 Mangrove isotopic comparisons

The $\delta^{13}C$ composition in the FoT plant samples showed that the pneumatophores and trunks are more enriched (mean = -26.14‰ and -25.39‰ respectively), whereas the leaves have lower $\delta\ ^{13}C$ values (mean = -27.65‰). Results for all tissues of mangrove samples were found between -30.86 and -22.88‰. A similar wide variability in $\delta^{13}C$ values in *A. marina* tissues was also observed by Kelleway *et al.* (2018) in the southwest of Australia, whose data ranged from -31.1 to -24.5‰. The authors of this research highlight this substantial variation to be incorporated in organic input studies since $\delta^{13}C$ fluctuations between different parts of

mangroves could be interpreted as the incorporation of other non-mangrove and ^{13}C-enriched sources.

An estuarine vegetation survey in the Firth of Thames (Graeme, 2006) studied the vegetation communities that live together with mangrove trees. The most notable findings are the absence of seagrass and the extensive presence of saltmarsh ribbonwood (*Plagianthus divaricatus*), a considerable number of large patches of *spartina sp*. and the presence of saltwater paspalum or *Paspalum vaginatum* (weeds) and Maori musk or sea meadow (*Mimulus repens*). All these communities represent organic inputs with different elemental and isotopic compositions which likely modify the values obtained in the mangrove sediments.

The study of Miao *et al.* (2016) showed results of five plant types, including two native mangrove species in the Pearl River estuary in China. When comparing the $\delta^{13}C$ composition in sediments and plants, their results are very similar to ours (Figure 3.39). Leaf tissues are more depleted in this isotope than the pneumatophore tissues and the sediments are the most enriched, and this behaviour is attributed to fractionation of $\delta^{13}C$ by plant physiological activities. The results obtained for $\delta^{15}N$ in the FoT show that trees use and preserve $\delta^{15}N$ in heterogeneous ways, which is not conditioned by the position in the forest (different results for trees in the fringe and middle forest) but by own and individual mechanisms of the plant. Further investigation and a wider sampling regime of the trees would be required to understand the $\delta^{15}N$ incorporation or assimilation pathways in this type of mangrove.

4.2 Sources of organic carbon in the inner Firth of Thames

Kristensen *et al.* (2008) provide a review of carbon dynamics in mangroves. Their data show that 58% of the samples have mean values lower than -25‰ in $\delta^{13}C$ and that relatively high values of $\delta^{13}C$, between -17 and -23‰, indicate a large contribution of carbon from different sources (such as seagrasses, phytoplankton and microphytobenthos). Additionally, Marchand *et al.* (2003) demonstrated that during the early growth phase of a mangrove forest, carbon from algae represents a high percentage of Carbon buried in the ecosystem. Our observations indicate that the Carbon isotope composition in the FoT is below the mean value shown by

Kristensen *et al.* (2008). Both surface and depth samples (-23.28 ‰ mean for both types of samples) indicate a significant OC input from other sources.

Gao *et al.* (2019) described negative correlations between $\delta^{13}C$ and soil organic carbon in five mangrove forest of China; and similar relationships were found by (Bouillon *et al.*, 2003) based on sediments from three mangrove ecosystems in the Godavari Delta in India and Sri Lanka (Galle and Pambala). Our data show this same behaviour for FoT sediments (Figure 3.40). The surface samples show a relatively segmented distribution depending on the type of area within the Firth: in the deep and middle forest there is a higher concentration of OC and more negative values of $\delta^{13}C$, whereas the outer and middle mudflat represent sediments with a higher enrichment in $\delta^{13}C$ and lower organic concentration. However, the depth samples do not reflect any differentiation by the area occupied within the estuary. These results imply that the samples in the inner forest have a higher organic input from the mangrove plants, whereas the mudflat contains OC from other marine sources such as marine phytoplankton (Bao *et al.*, 2013). The relationship between surface and depth samples for each isotope showed a weak to significant correlation (r^2 =0.24 for $\delta^{13}C$ and r^2 = 0.44 for $\delta^{15}N$, Figures 3.31 and 3.32). This result is likely due that sediments preserved at both depths received organic matter from the same sources.

Yang *et al.* (2013) evaluated the organic characteristics of sediments in a mangrove forest at Waitemata, Harbor in New Zealand. Their observations in across-shore transect showed in the forest fringe high values in $\delta^{13}C$ (-23.3‰) and low C:N ratios (13.1), which suggests input from marine organic material. In contrast, the forest interior recorded ^{13}C-depleted samples (-25 ‰), values close to carbon isotopic compositions in mangrove leaves. The N and OC values increased landwards, from 0.21 to 0.32%. Their study suggests that organic marine material is trapped in the fringe zone, and mangrove-derived carbon is sequestered in the back of the forest. Our results support the observations of Yang *et al.* (2013), with similar increases in OC and N concentrations and decreasing $\delta^{13}C$ values landwards. However, the values inside the forest interior vary considerably in both sites; they found average values above 0.03% in nitrogen, 2.62% in carbon and less 0.29‰ in $\delta^{13}C$. These differences likely indicate, that for the FoT, although an increase is seen in the mangrove-derived source in the forest interior, the main organic input is from a marine source. Both studies are carried out in *Avicennia marina* sediments in New

Zealand and have different elemental and isotopic concentrations; which suggests that, beyond the mangrove species, other local factors such as tidal and swell regimes, modify the organic concentration and source in mangrove sediments.

An investigation into lagoon ecosystems in Mexico (Gonneea *et al.*, 2004) described potential sources of OC in mangrove sediments. Ternary mixing diagrams are used to represent the combination of mangrove, seagrass and phytoplankton organic input. In some locations within their study, the contribution of phytoplankton reached 40% of sedimentary OC, while mangrove detritus contributed between 30-80% in fringe zones. Additionally, a recent study from the Red Sea (Garcias-Bonet *et al.*, 2019) sampled macroalgae blades, seagrass leaves, halophyte leaves and mangrove leaves as potential sources in seagrass and mangrove sediments. The $\delta^{15}N$ and $\delta^{13}C$ values of these tissues allowed them to estimate the percentage contribution of each primary producer to the sediments using the Bayesian mixing model. The results showed that in mangrove sediments mangrove leaves were the major contributor (56%), and the seagrass leaves contributed 43% in seagrass sediment. Unfortunately, as our investigation was strictly focussed on the Firth of Thames, we did not sample a wide range of other potential sources nor a significant number of marine algae. To better constrain the origin of the organic carbon origin in the FoT, further research and sampling of other plants and primary producers should be undertaken.

A study evaluated the importance of seagrass (*Zostera muelleri*) in the trophic chains of the Raglan, Tauranga and Whangapoua estuaries in New Zealand (Hailes, 2006). Carbon and nitrogen stable isotopes were used to asses potential food sources including seagrass live blades and detritus, plus phytoplankton and microphytobenthos (including green algae). The distinctive values found for phytoplankton were -23 and 7‰ in $\delta^{13}C$ and $\delta^{15}N$, respectively, while in the microphytobenthos samples, the values were -20 and 5‰, respectively. In figure Figure 4.1 below Hailes (2006) link the mean values of $\delta^{15}N$ and $\delta^{13}C$ of potential food sources. When comparing their results with our findings, there is an overlap between the sediment cluster of the Figure 3.38 and some of the microphytobenthos and phytoplankton isotopic signatures, more specifically between -26 and -21 ‰ in $\delta^{13}C$ and 6 and 10 ‰ in $\delta^{15}N$ values. The seagrass samples in the Hailes (2006) research have $\delta^{13}C$ compositions above -13‰; within our analyses, no ^{13}C-enriched samples were found as observed by them, which proves the absence of seagrasses

in the Firth, as indicated in the Environment Waikato report (Graeme, 2006). Although the data from Hailes (2006) does not include the FoT mangrove, their data may provide a reasonable idea of the phytoplankton and microphytobenthos communities that thrive in our study area; thus, the overlap that exists between the isotopic findings of both studies reflects the significant marine input to the inner Firth of Thames sediments.

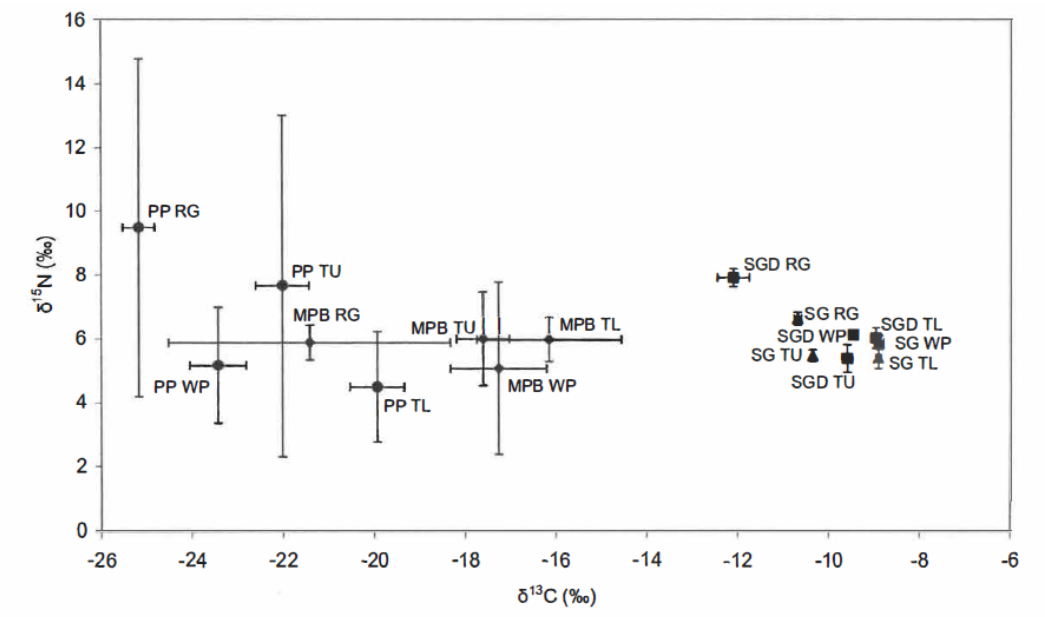

Figure 4.1. Mean (±1SD) $\delta^{13}C$ and $\delta^{15}N$ values of potential food sources in Hailes (2006) research. Study harbours: RG= Raglan, WP= Whangapoua, TU= Tauranga Upper and TL= Tauranga lower. Samples from SG= Seagrass blades, SGD = Seagrass detritus, PP= phytoplankton and MPB= microphytobenthos. Figure taken from Hailes (2006).

4.3 Other likely indicators for organic carbon in FoT sediments

The results obtained in the grain size analysis agree with the observations made in the FoT by Swales *et al.* (2015), while they observed a mean grain size of 20 µm in the superficial sediments, we obtained a predominance of grain size of less than 25 µm (Figure 3.50). The core sediments in our investigation likely correspond to the facies described by Swales *et al.* (2015): Nodular bioturbated muds with abundant mangrove roots and precipitates at stations 4 and 5 of the cross-shore transects (deep and middle forest), partially bioturbated muds with mangrove roots in the fringe zone (stations 2 and 3) and partially bioturbated muds in the inner mudflat area (stations 1).

Various studies demonstrate the correlation between grain size and organic content in marine sediments (Tyson, 1995; Ergin & Bodur, 1998; De Falco *et al.*, 2004; Dahl *et al.*, 2016); a high mud volume is related to high concentrations of organic matter. In contrast, our laboratory results do not show a significant relationship between grain size and OC percentage. However, the mean concentration of mud (clay and silt) represents 83% of the textural percentage, and a large majority of the samples showed a high dispersion in the grain size distribution (values between 0.4 and 200 μm), which shows the sediment heterogeneity. Thus, the textural properties of sediments are not a useful indicator of organic carbon concentration in the Firth of Thames.

Alongi (1988) examined the seasonality of microbial biomass in Australian mangroves and found low algal biomass (mean value 1.6 μg /g dw) due to the low light intensity in the dense mangrove canopy. The values of chlorophyll *a* pigments varied according to the season, with winter and spring being the most concentrated in green algae. The results obtained herein do not show a spatial relationship with the algal biomass; low values are not repeated in the deep or middle forest stations. Additionally, the mean value of chlorophyll *a* pigments was 11.21 μg / g dw, well above those found by (Alongi, 1988) in tropical mangroves. Figure 3.49 shows the relationship between the nitrogen and carbon concentrations versus the algae biomass; none showed a significant correlation. This result, which could have indicated a large input of marine algae to the FoT sediments, shows the need for further detailed studies establishing which type of phytoplankton and microphytobenthos communities predominate in the OC burial of the Firth.

Few studies have compared the Loss on Ignition and Carbon Elemental analysis methods in mangroves. Our observations showed a positive correlation between both results with a $r^2 = 0.51$ (n = 114). When comparing the mean values for both methods, in surface samples, the SOM concentration is 6.8 and 7.6 times more than the percentage of OC for surface and depth samples, respectively. In Chaikaew and Chavanich (2017) the relationship between both methods was also reported in a mangrove forest in the Upper Gulf of Thailand, where they estimated a SOM mean value of 11.12% and an OC = 5.59% (n = 29), the correlation coefficient was lower than that obtained here ($r^2 = 0.25$) and a ratio SOM:OC of 2. Although a consistent relationship was obtained between the two methods, further research is required to understand the high percentage of organic matter in the sediments of the Firth of

Thames. The high SOM values found in our measurements may be overestimated by the exposure time in the furnace or by loss of water in clay minerals, volatile salts, or carbon associated to carbonates (Heiri *et al.*, 2001).

4.4 Gross estimations of carbon and nitrogen stock in FoT sediments

To estimate the C and N stock in the FoT, it is necessary to calculate the dry bulk density of the sediment. Bulk density was measured from 5 surface samples and 5 depth samples from within the forest along F transect (F2 to F9). Mean dry bulk density was 0.6 $g.cm^{-3}$ (with standard deviation 0.034 $g.cm^{-3}$ for n=10). These results are in agreement with those obtained by Swales *et al.* (2008) who estimated DBD profiles in mud cores of 200 cm in the central FoT, and found values were very uniform and close to 0.5 $g.cm^{-3}$. Taking this DBD value and using mean C and N values of 2.21% and 0.24% from within the forest (locations 2 to 9, surface and depth samples combined), a depth floor of 40 cm, yields estimated stocks of 53 t C ha^{-1}, 40.8 t OC ha^{-1} and 5.9 t N ha^{-1} within the top 40 cm, (or 13.26 t C ha^{-1} , 10.2 t OC ha^{-1} and 1.47 t N ha^{-1} for 10 cm depth increments). When comparing these gross estimations with the C and N stocks reported in Bulmer *et al.* (2016) for New Zealand mangroves, it is observed that our values are within the range they reported for different forests. The average obtained for their samples yielded values between 6 and 16 t C ha^{-1} for 10 cm intervals in a core of 100 cm, while their estimates of N stock varied between 1 and 2 t N ha^{-1}. Similarly, Garcias-Bonet *et al.* (2019) reported values of organic carbon stocks of 14.54 t C ha^{-1}within the top 10 cm of sediments in mangroves in the Red Sea (although their organic carbon values were much greater than those from the FoT). Furthermore, taking 1730 ha as an estimate for Firth of Thames (Figure 4.2) mangrove forest coverage leads to total buried stocks of 91,740 t of Carbon and 10,170 t of Nitrogen within the top 40 cm. Thus, our research reinforces the importance of mangroves in their role as C and N pools in estuarine environments.

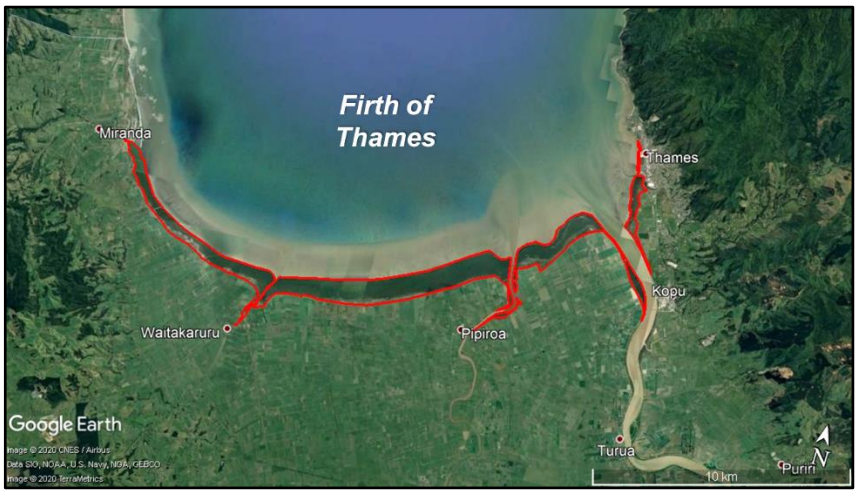

Figure 4.2. The red polygons delimit the mangrove forest area used in the Carbon and Nitrogen stocks estimations in the inner Firth of Thames.

5. Conclusions

This research investigated the content and elemental composition of carbon and nitrogen stored within the sediments of a relatively recently and rapidly established (within the 60 years) subtropical mangrove forest. The research analysed a large number of samples from across the forest and adjacent mudflat in the Firth of Thames, New Zealand, to explore if there exist spatial trends in concentration and composition of elements. The work here contributes to a broader understanding of the variability of, and controls on, carbon burial within vegetated environments. Such knowledge of the C and N retention capacity and distribution is required as the scientific basis to inform management decisions, for example on mangrove removal.

The major findings of the thesis are:

1. The concentrations of nitrogen, carbon and organic carbon are larger in the forest interior compared to the middle mudflat by approximately 40%, 48% and 49%, respectively. Such an increase occurs gradually in surface samples. On the other hand, depth samples tend to have steady or constant values across the forest.
2. The three main rivers that flow into the Firth of Thames do not appear to strongly influence the distributions of C, N, OC and IC concentrations on the large (forest-wide) scale. Rather the rivers appear to only affect concentrations within the immediate riverbanks (which exhibited different values from those inside the mangrove forest).
3. The concentration of Inorganic Carbon is much lower than that of Organic Carbon (approximately one third of carbon was inorganic) within the FoT sediments. Additionally, the weak correlation between both types of carbon may imply different settlement processes occur when they are buried in the mangrove sediments.
4. A relatively high mean value of $\delta^{13}C$ (-23.18‰) and a low C:N ratio (6.98) in surface and depth samples, reflect the predominance of an allochthonous marine source of carbon in the sediments of the Firth of Thames.
5. The comparison between $\delta^{13}C$ and OC concentration showed a negative relationship and a slight differentiation between the Firth areas; The samples

inside the forest have higher OC percentages and lower $\delta^{13}C$ values, indicating a higher organic contribution of mangroves to the sediments in this area of the Firth.

6. A rough estimate of Carbon and Nitrogen storage in the FoT showed for 10 cm depth increments stocks of approximately 13.26 t C ha^{-1}, 10.2 t OC ha^{-1} and 1.47 t N ha. Thus, in an area of 1,730 ha of mangrove forest, a total of 91,740 t and 10,170 t of Carbon and Nitrogen are estimated, respectively within the top 40 cm of sediment.
7. Other potential indicators of organic concentrations such as algal biomass or grain size were not found to be correlated with OC nor N content in the Firth of Thames sediments.
8. The OC concentration explains 52% of the Soil Organic Matter content. This relationship based on many (n=124) samples, implies that future research can use the more economical and straightforward (relative to isotope analysis) LOI method to provide an estimation of the concentration of Organic Carbon in sediments in the Firth of Thames.

5.1 Further Work

During this study, some questions arose that can only be answered through further research. Although a clear predominance of an organic marine source was established in the FoT sediments, additional sampling would be necessary to more precisely quantify the contributions from the phytoplankton and microphytobenthos communities. Combining results of such additional sampling with our research, would allow for formation of ternary mixing diagrams, and the percentage of Organic Carbon contributed by the various marine and mangrove sources could be clarified. Our work did not provide information on the concentrations of particulate organic carbon (POC) and dissolved organic carbon (DOC) which are supplied by the freshwater sources to the FOT, and thus allow for distinguishing their distribution in the inner and middle mudflat. Further experiments could focus on water sampling, over different temporal scales from individual tidal cycles to seasonal (high and low river flows). A further aspect, far outside the scope of this thesis is the mechanisms through which ^{15}N is incorporated into mangrove plants. Unlike $\delta^{13}C$, the values of $\delta^{15}N$ did not exhibit any pattern by tissue type or position in the forest.

References

Alongi, D. (1988). Bacterial productivity and microbial biomass in tropical mangrove sediments. *An International Journal, 15*(1), 59-79.

Alongi, D. (2002). Present state and future of the world's mangrove forests. *Environmental Conservation, 29*(3), 331-349.

Alongi, D. M. (2008). Mangrove forests: Resilience, protection from tsunamis, and responses to global climate change. *Estuarine, Coastal and Shelf Science, 76*(1), 1-13.

Alongi, D. M. (2014). Carbon Cycling and Storage in Mangrove Forests. *Annu. Rev. Mar. Sci., 6*(1), 195-219.

Alongi, D. M. (2018). *Blue Carbon Coastal Sequestration for Climate Change Mitigation*. (1st ed. 2018.. ed.). Cham : Springer International Publishing : Imprint: Springer.

Alongi, D. M., & Mukhopadhyay, S. K. (2015). Contribution of mangroves to coastal carbon cycling in low latitude seas. *Agricultural and Forest Meteorology, 213*, 266-272.

Alongi, D. M., Sasekumar, A., Chong, V. C., Pfitzner, J., Trott, L. A., Tirendi, F., Dixon, P., & Brunskill, G. J. (2004). Sediment accumulation and organic material flux in a managed mangrove ecosystem: Estimates of Land–ocean–atmosphere Exchange in Peninsular Malaysia. *Marine Geology, 208*(2), 383-402.

Balke, T., Swales, A., Lovelock, C. E., Herman, P. M. J., & Bouma, T. J. (2015). Limits to seaward expansion of mangroves: Translating physical disturbance mechanisms into seedling survival gradients. *Journal of Experimental Marine Biology and Ecology, 467*, 16-25.

Bao, H., Wu, Y., Tian, L., Zhang, J., & Zhang, G. (2013). Sources and distributions of terrigenous organic matter in a mangrove fringed small tropical estuary in South China. *Acta Oceanologica Sinica, 32*(4), 18-26.

Bouillon, S., Borges, A. V., Castañeda‐Moya, E., Diele, K., Dittmar, T., Duke, N. C., Kristensen, E., Lee, S. Y., Marchand, C., Middelburg, J. J., Rivera-Monroy, V. H., Smith, T. J., & Twilley, R. R. (2008). Mangrove production and carbon sinks: A revision of global budget estimates. *Global Biogeochemical Cycles, 22*(2), n/a-n/a.

Bouillon, S., Dahdouh-Guebas, F., Rao, A. V. V. S., Koedam, N., & Dehairs, F. (2003). Sources of organic carbon in mangrove sediments: variability and possible ecological implications. *The International Journal of Aquatic Sciences, 495*(1), 33-39.

Brodie, C. R., Leng, M. J., Casford, J. S. L., Kendrick, C. P., Lloyd, J. M., Yongqiang, Z., & Bird, M. I. (2011). Evidence for bias in C and N concentrations and Or 13C composition of terrestrial and aquatic organic

materials due to pre-analysis acid preparation methods. *Chemical Geology, 282*(3), 67-83.

Bulmer, R., Schwendenmann, L., & Lundquist, C. (2016). Carbon and Nitrogen Stocks and Below-Ground Allometry in Temperate Mangroves. *Frontiers in Marine Science, 3*.

Bulmer, R. H., Schwendenmann, L., Lohrer, A. M., & Lundquist, C. J. (2017). Sediment carbon and nutrient fluxes from cleared and intact temperate mangrove ecosystems and adjacent sandflats. *Science of the Total Environment, 599-600*, 1874-1884.

Castro - Rodríguez, E., León - Luna, I., & Pinedo - Hernández, J. (2018). Biogeochemistry of mangrove sediments in the Swamp of Mallorquin, Colombia. *Regional Studies in Marine Science, 17*, 38-46.

Chaikaew, P., & Chavanich, S. (2017). Spatial Variability and Relationship of Mangrove Soil Organic Matter to Organic Carbon. *Applied and Environmental Soil Science, 2017*, 4010381.

Cifuentes, L. A., Coffin, R. B., Solorzano, L., Cardenas, W., Espinoza, J., & Twilley, R. R. (1996). Isotopic and Elemental Variations of Carbon and Nitrogen in a Mangrove Estuary. *Estuarine, Coastal and Shelf Science, 43*(6), 781-800.

Costanza, R., Ralph, D. A., Rudolf De, G., Stephen, F., Monica, G., Bruce, H., Karin, L., Shahid, N., Robert, V. O. N., Jose, P., Robert, G. R., Paul, S., & Marjan Van Den, B. (1997). The value of the world's ecosystem services and natural capital. *Nature, 387*(6630), 253.

Dahl, M., Deyanova, D., Gütschow, S., Asplund, M., Lyimo, L., Karamfilov, V., Santos, R., Björk, M., & Gullström, M. (2016). Sediment Properties as Important Predictors of Carbon Storage in Zostera marina Meadows: A Comparison of Four European Areas. *PLoS One, 11*(12), e0167493.

Daniel, C. D., Kauffman, J. B., Daniel, M., Sofyan, K., Melanie, S., & Markku, K. (2011). Mangroves among the most carbon-rich forests in the tropics. *Nature Geoscience, 4*(5), 293.

Dawson, T. E., Siegwolf, R. T. W., & Siegwolf, R. (2007). *Stable Isotopes As Indicators of Ecological Change*. Amsterdam, UNITED STATES: Elsevier Science & Technology.

De Falco, G., Magni, P., Teräsvuori, L. M. H., & Matteucci, G. (2004). Sediment grain size and organic carbon distribution in the Cabras lagoon (Sardinia, Western Mediterranean). *Chemistry and Ecology, 20*(Supplement 1), 367-377.

Duke, N. C. (2017). Mangrove floristics and biogeography revisited: Further deductions from biodiversity hot spots, ancestral discontinuities, and common evolutionary processes. In V. H. Rivera-Monroy, *et al.* (Eds.), *Mangrove Ecosystems: A Global Biogeographic Perspective. Structure, Function, and Services.* (Chapter 2, pp. 17-53). Springer.

Ergin, M., & Bodur, M. (1998). Silt/clay fractionation in surficial Marmara sediments: implication for water movement and sediment transport paths in a semi-enclosed and two-layered flow system (northeastern Mediterranean Sea). *An International Journal of Marine Geology, 18*(3), 225-233.

Froelich, P. N. (1980). Analysis of organic carbon in marine sediments. *Limnology and Oceanography, 25*(3), 564-572.

Gao, Y., Zhou, J., Wang, L., Guo, J., Feng, J., Wu, H., & Lin, G. (2019). Distribution patterns and controlling factors for the soil organic carbon in four mangrove forests of China. *Global Ecology and Conservation, 17*.

Garcias-Bonet, N., Delgado-Huertas, A., Carrillo-de-Albornoz, P., Anton, A., Almahasheer, H., Marbà, N., Hendriks, I., Krause-Jensen, D., & Duarte, C. (2019). Carbon and Nitrogen Concentrations, Stocks, and Isotopic Compositions in Red Sea Seagrass and Mangrove Sediments. *Frontiers in Marine Science, 6*.

Giri, C., Ochieng, E., Tieszen, L. L., Zhu, Z., Singh, A., Loveland, T., Masek, J., & Duke, N. (2011). Status and distribution of mangrove forests of the world using earth observation satellite data. *Global Ecology and Biogeography, 20*(1), 154-159.

Gonneea, M. E., Paytan, A., & Herrera-Silveira, J. A. (2004). Tracing organic matter sources and carbon burial in mangrove sediments over the past 160 years. *Estuarine, Coastal and Shelf Science, 61*(2), 211-227.

Graeme, M. (2006). *Estuarine Vegetation Survey: Inner FIrth of Thames.* Waikato Regional Council, Hamilton, New Zealand. 37p. https://www.waikatoregion.govt.nz/assets/WRC/WRC-2019/tr06-40.pdf.

Hailes, S. (2006). *Contribution of seagrass (Zostera muelleri) to estuarine food webs revealed by carbon and nitrogen stable isotope analysis.* Masters Degree Theses thesis, University of Waikato Hamilton, New Zealand.

Harris, D., Horwáth, W. R., & Kessel, C. (2001). Acid fumigation of soils to remove carbonates prior to total organic carbon or carbon-13 analysis. *Soil Science Society of America Journal, 65*(6), 1853-1856.

Heiri, O., Lotter, A., & Lemcke, G. (2001). Loss on Ignition as a Method for Estimating Organic and Carbonate Content in Sediments: Reproducibility and Comparability of Results. *Journal of Paleolimnology, 25*.

Hicks, D., Shankar, U., McKerchar, A., Basher, L., Lynn, I., Page, M., & Jessen, M. (2011). Suspended sediment yields from New Zealand rivers. *Journal of Hydrology, 50*(1), 81-142.

Horstman, E. M., Lundquist, C. J., Bryan, K. R., Bulmer, R. H., Mullarney, J. C., & Stokes, D. J. (Compiler) (2018). *The dynamics of expanding mangroves in New Zealand*: Springer.

Huxham, M., Dencer-Brown, A., Diele, K., Kathiresan, K., Nagelkerken, I., & Wanjiru, C. (2017). *Mangroves and people: Local ecosystem services in a changing climate*.

Inglett, P. W., Rivera-Monroy, V. H., & Wozniak, J. R. (2011). Biogeochemistry of Nitrogen Across the Everglades Landscape. *Critical Reviews in Environmental Science and Technology, 41*(sup1), 187-216.

Kandasamy, K., & Bingham, B. (2001). Biology of Mangroves and Mangrove Ecosystems. *Advances in Marine Biology, 40*, 81-251.

Kelleway, J. J., Mazumder, D., Baldock, J. A., & Saintilan, N. (2018). Carbon isotope fractionation in the mangrove Avicennia marina has implications for food web and blue carbon research. *Estuarine, Coastal and Shelf Science, 205*, 68-74.

Kristensen, E., Bouillon, S., Dittmar, T., & Marchand, C. (2008). Organic carbon dynamics in mangrove ecosystems: A review. *Aquatic Botany, 89*(2), 201-219.

Kuramoto, T., & Minagawa, M. (2001). Stable Carbon and Nitrogen Isotopic Characterization of Organic Matter in a Mangrove Ecosystem on the Southwestern Coast of Thailand. *edited by The Oceanographic Society of Japan, 57*(4), 421-431.

Lamb, A. L., Wilson, G. P., & Leng, M. J. (2006). A review of coastal palaeoclimate and relative sea-level reconstructions using Or 13C and C/N ratios in organic material. *Earth Science Reviews, 75*(1), 29-57.

Lovelock, C., Sorrell, B., Hancock, N., Hua, Q., & Swales, A. (2010). Mangrove Forest and Soil Development on a Rapidly Accreting Shore in New Zealand. *Ecosystems, 13*(3), 437-451.

Lovett, N. (2017). *Sediment transport in the Firth of Thames mangrove forest, New Zealand.* . Master thesis, University of Waikato, Hamilton, New Zealand.

Lundquist, C. J., Morrisey, D. J., Gladstone-Gallagher, R. V., & Swales, A. (2014). *Managing mangrove habitat expansion in New Zealand*.

Manley, W., Foot, K., & Davis, A. (Compiler) (2019). *Nitrogen cycle*: Oxford University Press.

Marchand, C., Lallier-Vergès, E., & Baltzer, F. (2003). The composition of sedimentary organic matter in relation to the dynamic features of a mangrove-fringed coast in French Guiana. *Estuarine, Coastal and Shelf Science, 56*(1), 119-130.

Mazda, Y., Magi, M., Kogo, M., & Hong, P. (1997). Mangroves as a coastal protection from waves in the Tong King delta, Vietnam. *Mangroves and Salt Marshes, 1*(2), 127-135.

Miao, S. Y., Long, L. D., Tao, W. Q., Zeng, Q. C., Chen, J. H., Huang, J. L., Wu, Q. H., & Tang, Y. J. (2016). Composition of stable carbon and nitrogen

isotopes in five wetland plants and sediments from the Pearl River estuary, South China. *Chemistry and Ecology, 32*(7), 609-623.

Montoya, J. P. (2008). *Nitrogen Stable Isotopes in Marine Environments*.

Naish, T. R., Nelson, C. S., & Hodder, A. P. W. (1993). Evolution of Holocene sedimentary bentonite in a shallow-marine embayment, Firth of Thames, New Zealand. *Marine Geology, 109*(3), 267-278.

Norris, B. K., Mullarney, J. C., Bryan, K. R., & Henderson, S. M. (2017). The effect of pneumatophore density on turbulence: A field study in a Sonneratia-dominated mangrove forest, Vietnam. *Continental Shelf Research, 147*(C), 114-127.

Polidoro, B. A., Carpenter, K. E., Collins, L., Duke, N. C., Ellison, A. M., Ellison, J. C., Farnsworth, E. J., Fernando, E. S., Kathiresan, K., Koedam, N. E., Livingstone, S. R., Miyagi, T., Moore, G. E., Ngoc Nam, V., Ong, J. E., Primavera, J. H., Salmo, S. G., Sanciangco, J. C., Sukardjo, S., Wang, Y., & Yong, J. W. H. (2010). The Loss of Species: Mangrove Extinction Risk and Geographic Areas of Global Concern (Mangrove Extinction Risk). *PLoS ONE, 5*(4), e10095.

Reece, J. B., Urry, L. A., Cain, M. L., Wasserman, S. A., Minorsky, P. V., Jackson, R. B., & Campbell, N. A. (2014). *Campbell biology*.

Stein, L. Y., & Klotz, M. G. (2016). The nitrogen cycle. *Current Biology, 26*(3), R94-R98.

Stute, M. (2006). *Class notes for Isotope Hydrology EESC W 4886: Radiocarbon 14C*. Retrieved 21-02-2020, 2020, from https://www.ldeo.columbia.edu/~martins/isohydro/c_14.html.

Swales, A., Bell, R. G., Ovenden, R., Hart, C., Horrocks, m., Hermanspahn, N., & Smith, R. K. (2008). *Mangrove-habitat expansion in the southern Firth of Thames: sedimentation processes and coastalhazards mitigation.* . Environment Waikato, Hamilton, New Zealand https://www.waikatoregion.govt.nz/assets/WRC/WRC-2019/tr0813-1.pdf.

Swales, A., Bentley, S. J., & Lovelock, C. E. (2015). Mangrove-forest evolution in a sediment-rich estuarine system: opportunists or agents of geomorphic change? *Earth Surface Processes and Landforms, 40*(12), 1672-1687.

Swales, A., Waikato . Environment, W., National Institute of, W., & Atmospheric, R. (2007). *Mangrove-habitat expansion in the southern Firth of Thames : sedimentation processes and coastal-hazards mitigation*. Hamilton [N.Z.]: Hamilton N.Z. : Environment Waikato.

Thimdee, W., Deein, G., Sangrungruang, C., Nishioka, J., & Matsunaga, K. (2003). Sources and fate of organic matter in Khung Krabaen Bay (Thailand) as traced by Or 13 C and C/N atomic ratiosand C/N atomic ratios. *Wetlands, 23*(4), 729-738.

Tue, N., Hamaoka, H., Sogabe, A., Quy, T., Nhuan, M., & Omori, K. (2011). The application of Or 13 C and C/N ratios as indicators of organic carbon sources and paleoenvironmental change of the mangrove ecosystem from Ba Lat Estuary, Red River, Vietnam. *Environmental Earth Sciences, 64*(5), 1475-1486.

Tue, N. T., Nguyen, P. T., Quan, D. M., Dung, L. V., Quy, T. D., Nhuan, M. T., & Thai, N. D. (2018). Sedimentary composition and organic carbon sources in mangrove forests along the coast of northeast Vietnam. *Regional Studies in Marine Science, 17*, 87-94.

Twilley, R. R., Castañeda-Moya, E., Rivera-Monroy, V. H., & Rovai, A. (2017). Productivity and carbon dynamics in mangrove wetlands. In V. H. Rivera-Monroy, *et al.* (Eds.), *Mangrove Ecosystems: A Global Biogeographic Perspective. Structure, Function, and Services.* (Chapter 5, pp. 113-162). Springer.

Tyson, R. V. (1995). *Sedimentary organic matter : organic facies and palynofacies*. London: London : Chapman & Hall.

Vo-Luong, P., & Massel, S. (2008). Energy dissipation in non-uniform mangrove forests of arbitrary depth. *Journal of Marine Systems, 74*(1), 603-622.

Vundavilli, H., Mullarney, J. C., MacDonald, I., & Bryan, K. R. (2019). *Interaction of buoyant river plumes with vegetation and consequences for sediment transport and deposition* Presented at the 11th River, Costal and Estuarine Morphodynamics Symposium (RCEM 2019).

Yang, J., Gao, J., Cheung, A., Liu, B., Schwendenmann, L., & Costello, M. J. (2013). Vegetation and sediment characteristics in an expanding mangrove forest in New Zealand. *Estuarine, Coastal and Shelf Science, 134*(C), 11-18.

Yang, Z., Song, W., Zhao, Y., Zhou, J., Wang, Z., Luo, Y., Li, Y., & Lin, G. (2018). Differential responses of litter decomposition to regional excessive nitrogen input and global warming between two mangrove species. *Estuarine, Coastal and Shelf Science, 214*, 141-148.

Yu, Z., Wang, X., Han, G., Liu, X., & Zhang, E. (2018). Organic and inorganic carbon and their stable isotopes in surface sediments of the Yellow River Estuary. *Scientific Reports, 8*(1), <xocs:firstpage xmlns:xocs=""/>.